# *CD73: A Key Player in HIV Persistence*

Inaugural-Dissertation

to obtain the academic degree

Doctor rerum naturalium (Dr. rer. nat.)

submitted to the Department of Biology, Chemistry, Pharmacy

of Freie Universität Berlin

by

HANNAH SABETH SPERBER

2021

Die Dissertation wurde unter Anleitung von Satish K. Pillai im Zeitraum von Juni 2017 – Februar 2021 am Vitalant Research Institute, San Francisco, CA, USA angefertigt.

1. Gutachter*in: Prof. Dr. Satish K. Pillai

2. Gutachter*in: Prof. Dr. Florian Heyd

Disputation am 22.06.2021

# Table of Contents

# Zusammenfassung

Antiretroviral Therapie (ART) kann heutzutage die Replikation des humanen Immundefizienz-Virus (HIV) so wirksam hemmen, dass im Blut infizierter Personen keine Viren mehr nachgewiesen werden können. Aufgrund der Persistenz latent infizierter Zellen gibt es derzeit jedoch keine Behandlungsmethode die HIV vollständig heilen kann. Latente Zellen formen die sogenannten Virusreservoire, die sich sehr früh während der Infektion etablieren, vom Immunsystem des Wirts unerkannt bleiben und im Körper trotz jahrzehntelanger Therapie verweilen. Ein besseres Verständnis der HIV-Persistenz und eine zuverlässige Identifizierung latent infizierter Zellen sind erforderlich, um effektive Heilungsstrategien zu entwickeln. Um dieses Problem zu adressieren, wurden primäre CD4+ T-Zellen mit einem HIV-Reportervirus infiziert, dass die Isolation von nicht-infizierten, produktiv-infizierten und latent-infizierten Zellen ermöglicht. Anschließende NanoString- und differentielle Genexpressionsanalyse haben spezifische Eigenschaften latent infizierter Zellen aufgedeckt, mit dem Oberflächenprotein CD73 als zentrales Element. Nachfolgende Experimente haben dann einen signifikanten Zusammenhang zwischen latenter Infektion und erhöhter CD73 Expression nachgewiesen, sowohl *in vitro* als auch *in vivo*, und umgekehrt gezeigt, dass CD73+ Zellen latentes Virus anreichern. Hypoxische Kulturbedingungen, die die lymphoide Mikroumgebung *in vivo* widerspiegeln, erhöhten deutlich den Prozentsatz an CD73+ T-Zellen und folglich die Gesamthäufigkeit latenter Infektionen, während die phänotypische Charakterisierung von CD73+ CD4+ T-Zellen zelluläre Merkmale offengelegt hat, die eine latente Infektion begünstigen. Darüber hinaus habe ich eindeutige Beweise gefunden, dass dieses Zellkompartiment ein intaktes HIV-Reservoir beherbergen und damit zur Ausbreitung

einer neuentfachten Infektion beitragen kann. Schließlich habe ich entdeckt, dass die enzymatische Aktivität von CD73 an HIV-Latenz beteiligt sein könnte, was auf einen faszinierenden Mechanismus hinweist, der die Hypoxie-induzierte CD73 Expression und die nachgeschaltete Adenosin-Signalübertragung mit der Etablierung der HIV-Latenz und dem langfristigen Überleben infizierter Zellen *in vivo* verbindet.

Meine Ergebnisse zeigen zum ersten Mal eine kohärente, direkte Korrelation zwischen der HIV-Latenz und CD73 Expression sowie dessen Regulation und Funktion. Meine Entdeckung liefert nicht nur neue Einblicke in die Biologie der Viruspersistenz, sondern enthüllt auch innovative phänotypische und mechanistische Angriffspunkte für HIV-Heilungsansätze.

# Abstract

Replication of human immunodeficiency virus (HIV) is suppressed to undetectable levels by effective antiretroviral therapy (ART). However, current therapeutic regimens fail to completely eradicate HIV due to the persistence of latently-infected cells. These viral reservoirs are established very early during infection, remain invisible to the host's immune system, and persevere for decades despite ART. A better understanding of viral persistence and identification of unique features of latently-infected cells are needed to inform HIV cure strategies. To address this gap, I utilized blood-derived, primary CD4+ T cells, which were infected with an HIV dual reporter virus allowing for isolation of uninfected, productively-infected and latently-infected cells. NanoString profiling and differential gene expression analysis uncovered distinct signatures of latently-infected cells and the surface protein CD73 as a key marker of latent infection. Subsequent experiments showed a significant association between latent infection and increased CD73 expression, both *in vitro* and *in vivo*, and demonstrated vice versa that CD73+ cells are significantly enriched for latent virus. Hypoxic conditioning, reflecting the lymphoid microenvironment *in vivo*, drastically increased the percentage of CD73+ T cells and consequently the overall frequency of latent infections, while phenotypic characterization of CD73+ CD4+ T cells revealed cellular features favorable for latent infection. In addition, I found clear evidence that this compartment can harbor a functional HIV reservoir and reinitiate spreading infection. Finally, I discovered that the enzymatic activity of CD73 may be involved in viral quiescence, suggesting an intriguing mechanism linking hypoxia-induced CD73 expression and downstream adenosine signaling to the establishment of HIV latency and the long-term survival of infected cells *in vivo*.

My results present for the first time a coherent, direct correlation between HIV latency and CD73 expression, as well as its regulation and function. My discovery does not only provide new insights into the biology of viral persistence but also reveals novel encouraging phenotypic and mechanistic target sites for HIV cure approaches.

# Abbreviations

| | |
|---|---|
| **AIDS** | Acquired Immunodeficiency Syndrome |
| **ART** | Antiretroviral therapy |
| **ATI** | Antiretroviral treatment interruption |
| **BSA** | Bovine serum albumin |
| **CA** | Capsid |
| **cART** | Combination of ART |
| **cDNA** | Complementary DNA |
| **DMOG** | Dimethyloxalylglycine |
| **DMSO** | Dimethyl sulfoxide |
| **DNA** | Deoxyribonucleic acid |
| **eGFP** | Enhanced green fluorescent protein |
| **Env** | Envelope protein |
| **FACS** | Fluorescence-activated cell sorting |
| **FBS** | Fetal bovine serum |
| **gp120** | Glycoprotein 120 |
| **gp41** | Glycoprotein 41 |
| **HAART** | Highly active ART |
| **HIF** | Hypoxia-inducible factor |
| **HIV** | Human immunodeficiency virus |
| **HRE** | Hypoxia-response element |
| **I** | Ionomycin |
| **IN** | Integrase |
| **LTR** | Long terminal repeat |
| **MA** | Matrix protein |
| **MFI** | Mean fluorescence intensity |
| **mKO2** | mKusabira-Orange2 |
| **mRNA** | Messenger RNA |
| **NC** | Nucleocapsid protein |
| **Nef** | Negative regulatory factor |
| **NFAT** | Nuclear factor of activated T-cells |
| **NF-κB** | Nuclear Factor-κ B |

| | |
|---|---|
| **PBMC** | Peripheral blood mononuclear cell |
| **PBS** | Phosphate buffered saline |
| **PEI** | Polyethylenimine |
| **PKA** | Protein kinase A |
| **PLWH** | People living with HIV |
| **PR** | Protease |
| **Rev** | Regulator of expression |
| **RNA** | Ribonucleic acid |
| **RT** | Room temperature |
| **RTr** | Reverse transcriptase |
| **SD** | Standard deviation |
| **SEM** | Standard error of the mean |
| **SU** | Surface subunit |
| **TAT** | Transactivvator of transcription |
| **TCR** | T cell receptor |
| **TM** | Transmembrane subunit |
| **TME** | Tumor microenvironment |
| **Vif** | Viral infectivity factor |
| **Vpr** | Viral protein r |
| **Vpu** | Viral protein u |
| **WT** | Wild type |

# 1 Introduction

## 1.1 HIV and the AIDS Pandemic

### 1.1.1 Epidemiology

The Acquired Immunodeficiency Syndrome (AIDS) and its etiological agent the human immunodeficiency virus (HIV) remain a major global public health issue. HIV caused one of the most widespread and deadliest pandemics, with an estimated 75 million infections worldwide and 32 million AIDS-related deaths since the start of the pandemic[1] (Figure 1A). Disproportionally affected are middle- and low-income countries (Figure 1B). Sub-Saharan Africa for example makes up about 12% of the world's population, but harbors 2/3 of all people living with HIV (PLWH). In 2019, approximately 38 million people were HIV-infected globally, roughly 1.7 million newly contracted the virus and 770,000 died due to AIDS-related illnesses (Figure 1C). The latter number shrank considerable by more than 55% since it peaked in 2004 with 1.7 million. However, while the number of annual HIV infections declined globally by 23% since 2010, in recent years it remained static and even rose in around 50 countries, specifically in Eastern Europe, Central Asia, Middle East and North Africa (Figure 1D).

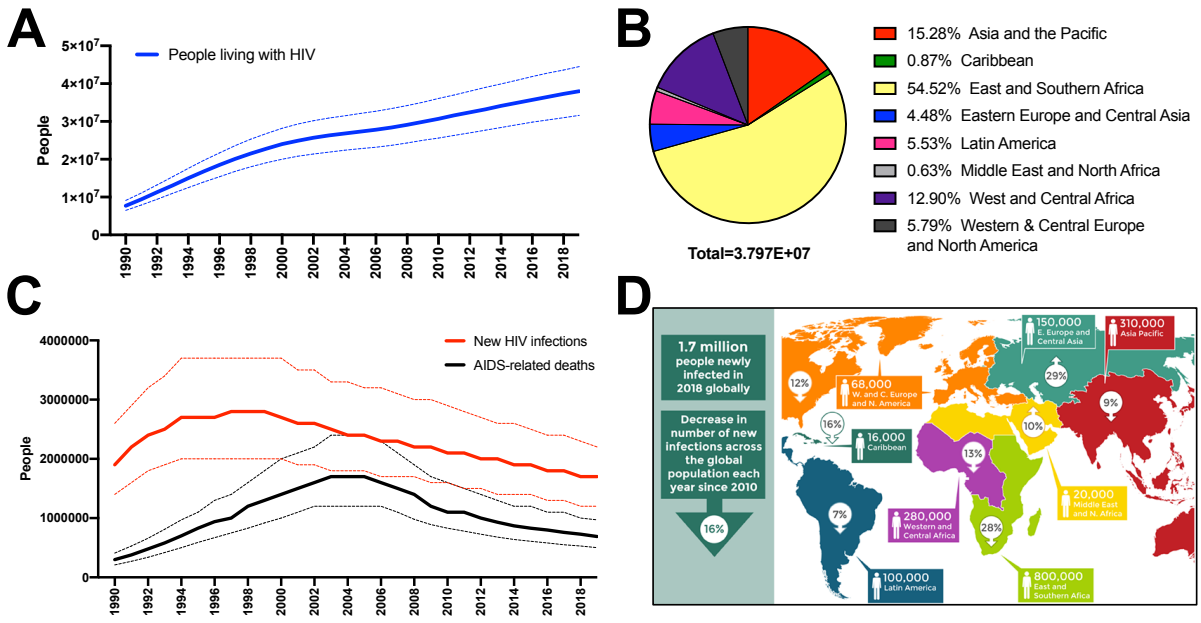


**Figure 1: Global HIV and AIDS statistics.** Data gathered from UNAIDS, 2020[1]. (A) Approximate number of PLWH worldwide. Dashed lines indicate upper and lower estimates. (B) Epidemiological estimates of PLWH classified by region. (C) Estimated global number of annual new HIV infections and AIDS-related deaths. Dashed lines indicate upper and lower estimates. (D) Number of new HIV infections in 2018 and change since 2010. Figure adapted from Avert[2].

### 1.1.2 History

Almost 40 years have passed since the first public announcement by the Center for Disease Control (CDC) on 5 June 1981, marking the official beginning of the history of the epidemic. A rare pattern of lung infections was described in five young, healthy gay men in Los Angeles[3]. Simultaneously, an atypical aggressive cancer was discovered in a small group of men in New York and California[4,5]. By the end of that year, 337 cases of individuals with severe immune deficiency had been reported – almost half had succumbed to the disease[6]. Two years later, the underlying pathogen, HIV was discovered by the group of Luc Montagnier at the Pasteur Institute[7], and received its official name in May 1986[6]. To date, almost 400,000 HIV and AIDS related studies have been published, making HIV one of the most intensively investigated and best characterized human viruses (Figure 2).

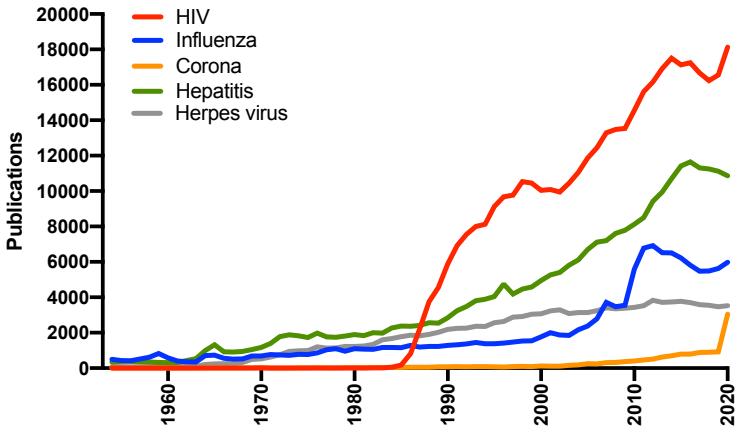


**Figure 2: Time course of papers published annually for indicated human viruses[8].** Graphs show hits on PubMed per year using the search terms as indicated in the figure legend. Data from: 25/01/2021.

### 1.1.3 Transmission

HIV is typically transmitted through certain body fluids such as blood, seminal, vaginal, and rectal fluids, as well as breast milk. The most common path of HIV transmission is through unprotected (condomless) sexual intercourse. For a transmission to happen the infected body fluid needs to contain enough virus and to get in contact with vulnerable or broken skin and mucous membranes. Other non-sexual transmissions comprise sharing unsterilized drug injection equipment, blood transfusions, or exposure from an infected mother to her child during pregnancy, childbirth and breast feeding (mother-to-child transmission).

Importantly, for the virus to be transmitted, the HIV-positive person has to have detectable viral loads defined as > 50 RNA copies/ml. Numerous studies have shown that if a person's viral burden is undetectable, the chance of passing on the virus is effectively zero and proven the consensus U=U (Undetectable=Untransmittable) scientifically sound[9–12].

### 1.1.4 Classification

HIV is an enveloped RNA virus and a member of the lentivirus genus within the family of *Retroviridae*. Two types of HIV have been described, HIV-1 and HIV-2. HIV-1 is the

predominant virus and more virulent type[13], accounting for 95% of global HIV infections. The two types differ in their genomic sequence by more than 50%[14,15]. HIV-1 is further divided into 4 groups: M, O, N and P, where HIV-1 group M is the most prevalent. Group M is subdivided into 9 clades that represent known genetically distinct subtypes. Recombination of different subtypes can result in new hybrid variants which are termed circulating recombinant forms (CRF) (Figure 3). Clade B represents the dominant clade in the Americas, Western Europe and Australia, and, while it constitutes only 12% of HIV infections worldwide, the vast majority of clinical HIV research has been acquired for this clade. In contrast, clade C is common in Southern Africa and India and constitutes almost 50% of PLWH.

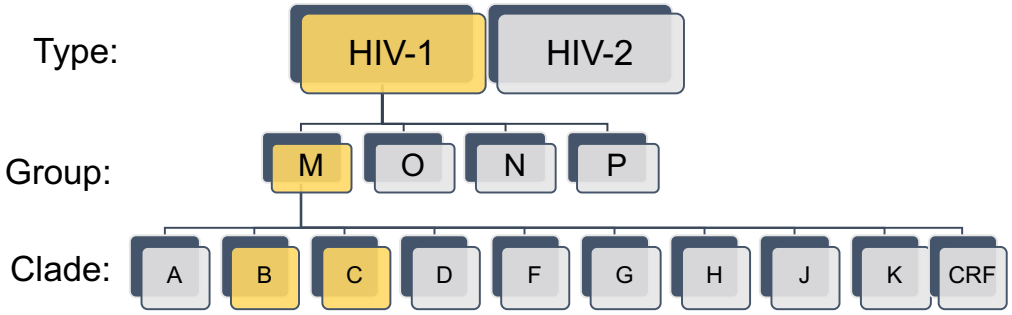


**Figure 3: HIV classification.** HIV-1 and HIV-2 are the two known HIV types. HIV-1 is further classified in groups and clades. The majority of HIV-1 isolates belong to group M which is further subdivided into 9 clades and circulating recombinant forms (CRFs). The most prevalent forms of HIV are highlighted in yellow. Figure is adapted from Avert[2].

### 1.1.5 HIV Structure and Components

HIV particles are spherical and vary in size from 90-260 nm[16,17]. Each particle is composed of two identical single-stranded, positive-sensed RNA molecules that code for 9 genes (Figure 4). Three of the genes encode for the canonical polyproteins Gag, Pol and Env. The Pol polyprotein is cleaved into viral enzymes including the reverse transcriptase (RTr), integrase (IN) and protease (PR). The polyprotein Gag contains major structural components including nucleocapsid (NC), capsid (CA or p24), and matrix proteins (MA or p17). *Env* encodes for the

viral surface polyprotein gp160, which is processed into surface receptors gp120 (SU) and gp41 (TM). The remaining six genes *vif, vpu, nef, vpr, rev,* and *tat* encode for regulatory and accessory proteins. The viral genome is flanked on both ends by long terminal repeats (LTRs). The 5'LTR contains the promoter for viral transcription and the 3'LTR ensures polyadenylation of newly synthesized transcripts.

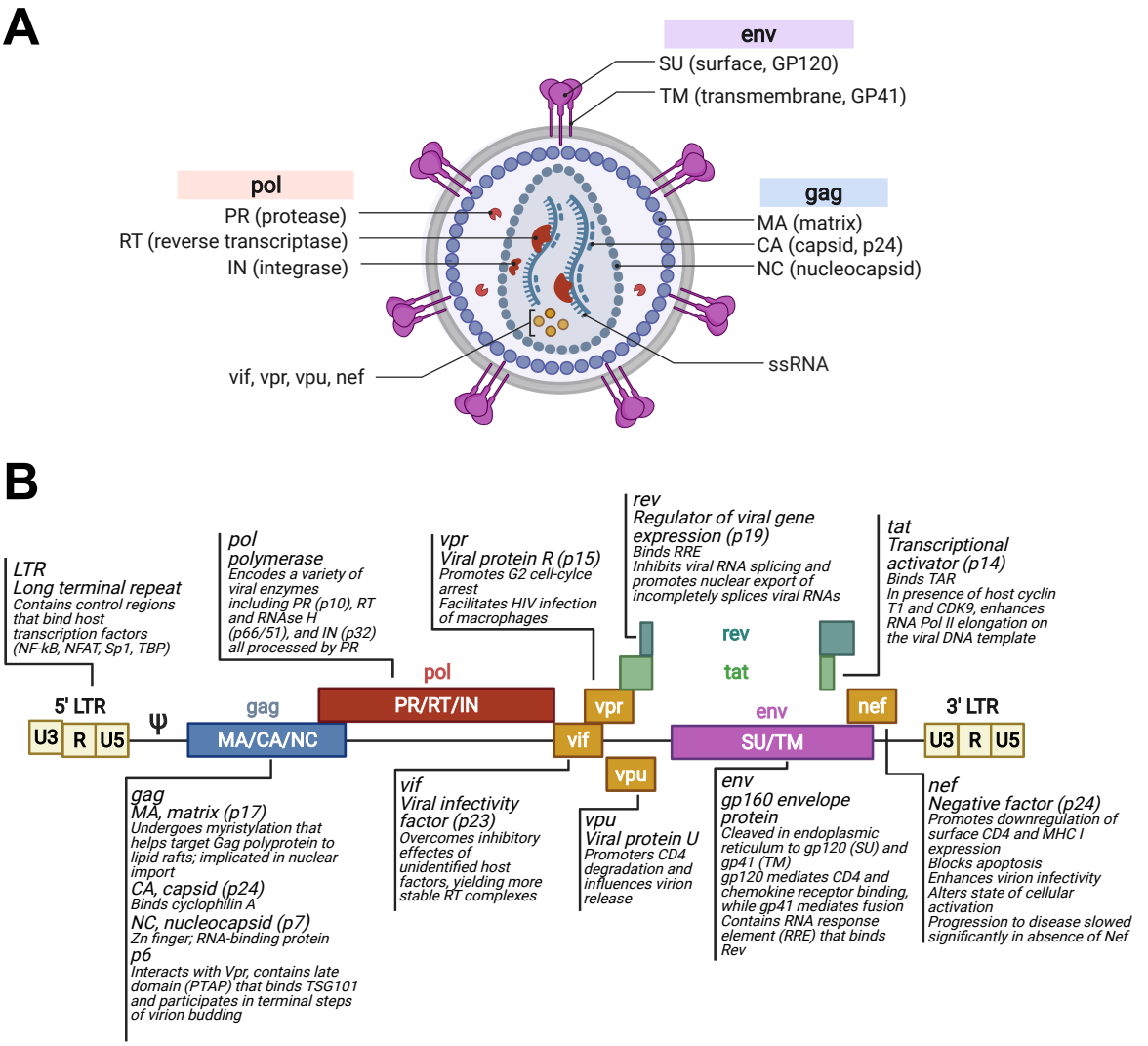


**Figure 4: HIV particle structure and genome.** (A) Simplified schematic of an HIV virion and its major structural components. (B) Genetic organization of the HIV genome adapted from Greene & Peterlin (2002)[18]. The 9 kilobase HIV genome contains nine genes encoding for 15 proteins, which functions are briefly described. Note that some viral proteins are not incorporated into viral particles.

In a mature viral particle, the viral RNA genome is tightly bound by NC proteins and several viral enzymes including RTr and IN. Together, the components assemble to ribonucleoprotein complexes (RNPs) that are encapsidated by CA proteins forming the characteristic cone-shaped core. The capsid is enclosed by viral MA proteins, ensuring the integrity of the viral particle. A lipid bilayer of host cell origin makes up the viral envelope. The trimeric gp120/gp41 heterodimers protrude as viral spikes from the HIV envelope and mediate viral entry and fusion with the plasma membrane of a target cell.

### 1.1.6 HIV Replication Cycle

Intracellular replication of HIV follows a sequence of complex steps that require a highly regulated and coordinated interplay of viral and host proteins. Figure 5 depicts the life cycle schematically, highlighting the main events that lead to reproduction of infectious particles[19]. Infection is initiated by binding of the viral envelope protein gp120 to the surface protein CD4 and, subsequently, co-receptors CCR5 or CXCR4 of the target cell (step 1)[20,21]. This interaction triggers fusion of the viral envelope and cellular plasma membrane which is mediated by the envelope transmembrane subunit gp41[20,21]. The HIV capsid enters the cell and is soon after uncoated by cellular cyclophilin A proteins, releasing viral genome and enzymes into the cytoplasm (step 2)[22]. The viral RTr removes viral proteins that are attached to the single strand RNA and generates a complementary DNA (cDNA) strand. Upon first cDNA strand synthesis, RTr degrades the RNA strand and produces double-stranded viral DNA (step 3). Reverse transcription is extremely error prone and causes mutations that can facilitate viral evolution and thus drug resistance and immune evasion[23]. The viral DNA is transported into the nucleus and inserted into the host's chromosome by the viral IN (step 4)[24,25]. Importantly, at this point,

the viral life cycle bifurcates. The integrated viral DNA, named provirus, can remain dormant for extended periods of time, which represents the latent stage of HIV infection. Alternatively, the productive stage of HIV infection may proceed, which is activated by cellular transcription factors such as NF-κB, supporting synthesis of viral messenger RNA (mRNA) and genomic RNA (step 5). Some transcripts undergo RNA splicing while others remain incompletely spliced or unspliced, full-length RNA. Through these alternative splicing processes, HIV gene expression is strictly balanced and divided into an early and late phase. Fully spliced viral mRNAs encode for Nef, Tat, and Rev and can be exported and translated immediately by the host cell translation machinery. Nef (negative factor) reshapes the infected cell on multiple levels (activation, apoptosis, defense) to optimize viral replication and infectivity[26–31]. Tat (transcriptional transactivator) critically modulates viral transcription[32,33] and Rev is essential for the nuclear export of intron-containing viral RNA species[34–36]. These late transcripts encode for structural and enzymatic proteins Gag, Env, and Pol as well as accessory proteins Vpr, Vpu and Vif. Rev accumulates in the nucleus where it binds to the viral mRNA transcripts that retain intron sequences and directs their nucleus exit, inducing the expression of HIV late genes and translocation of the viral RNA genome to the cytosol. All viral components are ultimately assembled at the host cell plasma membrane where budding of immature HIV particles occurs (step 6). The Env polyprotein gp160 is processed through the endoplasmic reticulum and Golgi apparatus where it is finally cleaved by host cell proteases into gp120 and gp41[37]. Gag and Gag-pol polyproteins associate with the viral RNA genome. During or upon release of newly formed virions, the packaged viral protease cleaves the Gag polyprotein into its functional units MA, CA, and NC proteins, yielding mature, infectious HIV particles (step 7)[38].

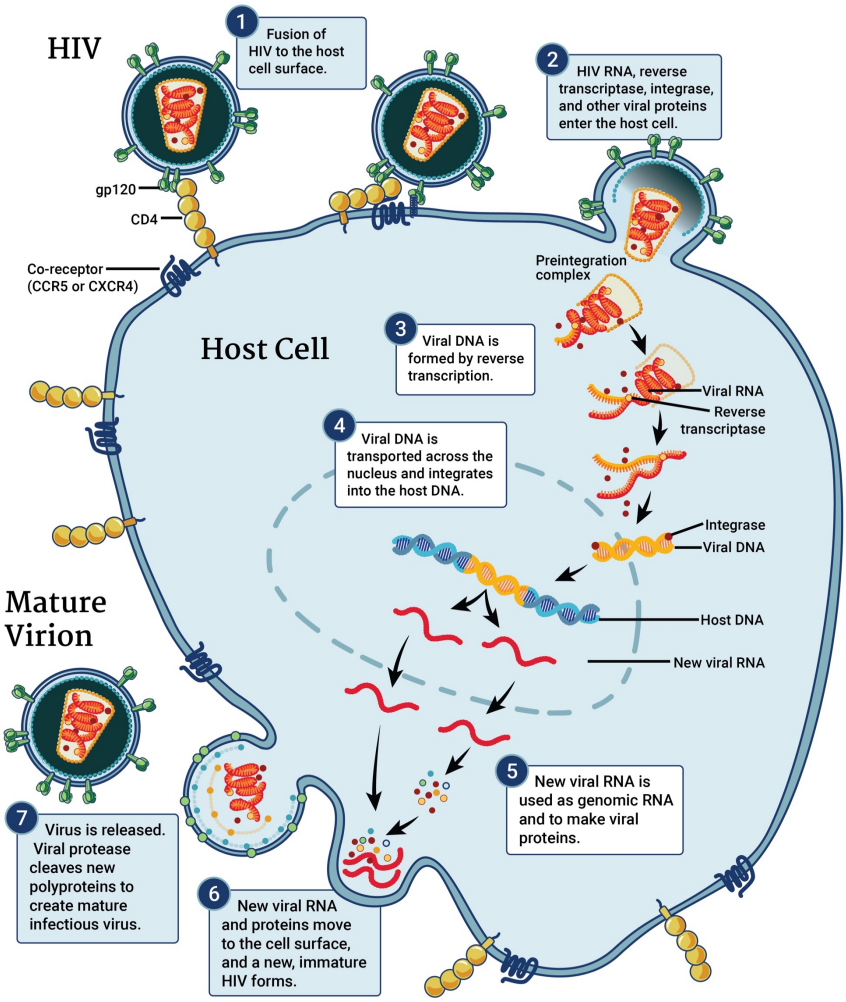


**Figure 5: Illustration of the HIV replication cycle.** (1) HIV binds to host cell surface receptors and fuses with the plasma membrane. (2 and 3) Viral genomic RNA and enzymes are released into the cytoplasm where viral DNA is synthesized by RTr. (4) Viral DNA is transported into the nucleus and integrated into the host's genome. (5) Upon transcriptional activation of the provirus, viral proteins and genomic RNA are synthesized. (6) Viral components form new immature virions that bud at the plasma membrane. (7) Upon virion release, viral protease accomplishes maturation of infectious particles. Figure obtained from NIAID.NIH[19].

### 1.1.7 Disease Progression and Treatment

At the systemic level, an untreated HIV infection is multifaceted and multiphasic with an overall mortality rate of more than 90%[39]. It is typically divided into three phases: 1) acute primary infection, 2) clinical latency, and 3) symptomatic infection with progression to AIDS (Figure 6).

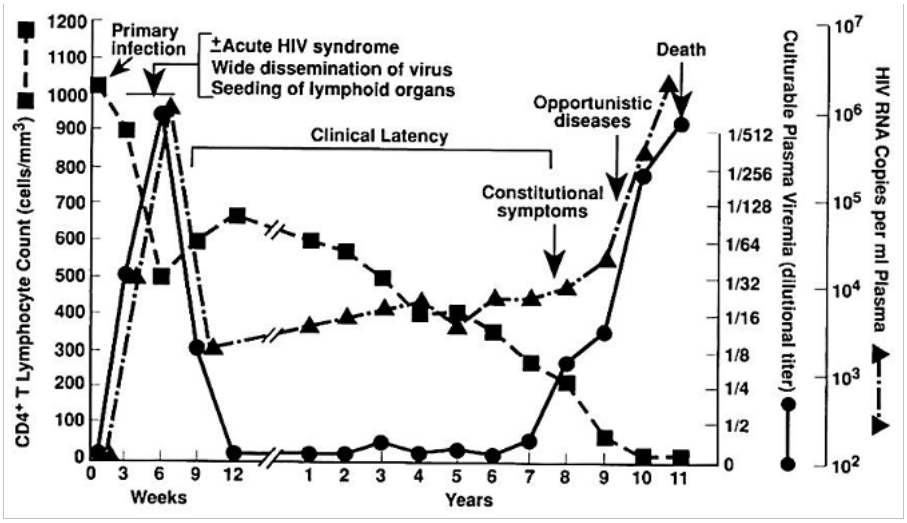


**Figure 6: Typical progression of an untreated HIV infection.** Throughout the course of infection CD4+T cell counts regress and immunodeficiency proceeds while HIV constantly replicates. Figure taken from A. S. Fauci et al. (1996)[40].

Upon primary infection, HIV quickly disseminates throughout the entire host body, preferentially to lymphoid tissues. High plasma viremia and a moderate drop in CD4+ T cells are hallmarks of this initial phase of HIV infection. It can last up to 4 weeks and involves the establishment of an appropriate cellular and humoral immune response to combat the virus[37]. During this phase, up to 70% of infected people experience nonspecific, flu-like symptoms[40].

While the immune response leads to a dramatic downregulation of virus replication, it fails to completely eliminate HIV. The number of peripheral CD4+ T cells continues to decline over the course of infection while HIV transitions from an acute to a chronic infection with persistent viral replication. This mostly asymptomatic phase can last between 10-15 years where the immune system is constantly challenged by slow but continuous viral replication leading to a progressive deterioration and exhaustion of the immune system.

The last phase is characterized by severe damage of the immune system. Viral loads increase to peak levels and opportunistic infections that would normally be controlled cause severe symptoms and illnesses. When CD4+ T cell counts fall below 200 cells/ml, the final stage

of HIV infections, AIDS, has been reached. Importantly, disease progression is highly variable on the individual level and can range from less than one year to long-term nonprogression (<5% of infected people[41–43]).

The unprecedent global effort of scientists to dissect HIV biology, pathogenesis and disease (Figure 2) has enabled the development of various antiviral therapeutics over the last three decades. The first FDA-approved drug for treating HIV infection was zidovudine (AZT) in March 1987. AZT had been previously used as cancer drug but showed promising potency as antiviral regimen[44]. However, high toxicity, uncertainty about long-term effects, and the emergence of drug-resistant HIV variants diminished its applicability as single antiviral agent[45]. A revolutionary breakthrough was achieved in 1995-1996 with the discovery of HIV protease inhibitors as a new class of antiviral drugs[46,47] and the introduction of highly active antiretroviral therapy (HAART) that combines at least three drug types targeting main viral enzymes[48]. Advancements in viral load monitoring and HIV testing further transformed diagnosis and treatment[6].

Today, more than 30 different antiretroviral drugs are available and HIV treatment could be reduced to a single daily pill, turning a once inevitably fatal disease to a chronic manageable condition[49–51].

## 1.2 The Need for an HIV Cure

The advent of HAART was accompanied by the false hope for an ending of the HIV/AIDS crisis. Indeed, deployment of HAART led to an immediate decrease in AIDS-related deaths[6] and dramatically decreased HIV-related morbidity and mortality up until today (Figure 1).

Importantly, HAART was also proven to prevent viral transmission once viral burden falls below the detectable threshold[9–12]. However, a cure for HIV is not achieved.

Despite unquestionable success and immense global investment, access to ART remains challenging especially in resource-limited settings. In 2020, 26 million of 38 million PLWH received HIV treatment[1]. In addition, current ART requires daily, lifelong, expensive medication and strict adherence. Moreover, ART-treated individuals may experience adverse side effects, ongoing morbidity and accelerated aging[52] along with stigma and discrimination[53–56]. An individual's health is never fully restored and the development of HIV-associated disorders an existing risk[57,58]. Given the substantial burden associated with daily treatment, not just at the individual level but also on global and national health resources renders the sustainability of ART and its worldwide distribution uncertain[59].

The main barrier to an HIV cure, lies within the nature of the virus itself. ART regimens target viral proteins and thus inhibit different steps of the viral life cycle potently suppressing viremia to undetectable levels. The efficacy of ART is thereby dependent on the expression of viral proteins and thus can only affect active viral replication. HIV, however, can persist in a latent state, integrated in the host genome with little to no protein expression. Latently-infected cells harboring silent provirus constitute the so-called latent reservoir[60]. These cells are invisible to the immune system and may survive for years even in the presence of ART[61–63]. Although latently-infected cells are assumed to be extremely rare[64–66] they are able to reinvigorate spreading rapidly and almost all HIV-infected persons experience rapid viral rebound, accompanied by pretreatment viral loads in the plasma within weeks upon discontinuation of ART[61,67]. Thus, a true cure for HIV infection can only be accomplished upon neutralization of the latent reservoir.

### 1.2.1 HIV Latency and the Latent Reservoir

The HIV reservoir persists virtually indefinitely within a small pool of latently-infected cells and represents the main obstacle for a full eradication of HIV infection. Viral reservoirs are found in a variety of anatomical sites and cell types (Figure 7).

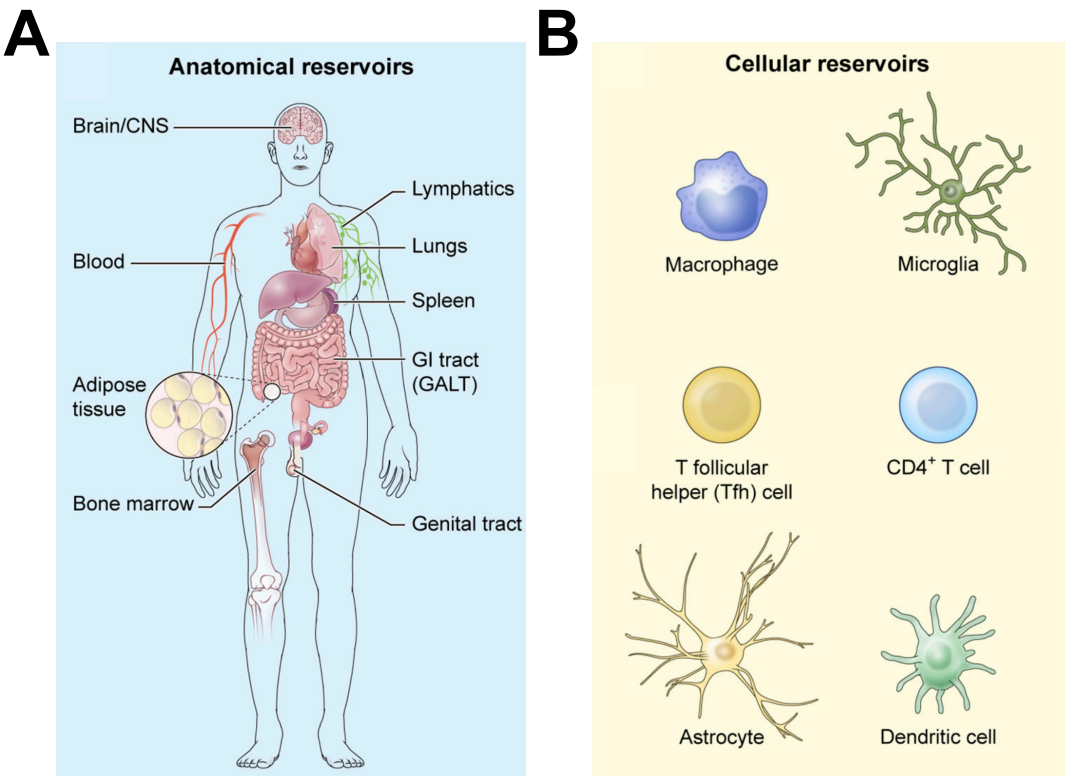


**Figure 7: HIV reservoir sites.** HIV persists in different (A) anatomical compartments and (B) cell types. Figure adapted from Henderson et al. (2019)[68].

CD4+ T cells constitute one of the best characterized HIV reservoirs up to date. The CD4+ T cell compartment is highly diverse and different subsets are distinguished by differentiation state, functional programs and homing capacities. In ART-suppressed individuals, latent provirus is primarily detected in memory CD4+ T cells including central ($T_{CM}$), transitional ($T_{TM}$), and effector ($T_{EM}$) cells, but the field is constantly evolving, and further subsets have been identified as viral reservoirs such as CD4+ T stem cell-like memory cells ($T_{SCM}$)[69], regulatory T cells (Tregs)[70], and T follicular helper (Tfh) cells[71]. The importance and contribution of specific

CD4+ T cell subsets to a long-term functional reservoir have been extensively reviewed by D.A. Kulpa and N. Chomont (2015)[72].

In recent years, the myeloid cell compartment, including macrophages and microglia cells, gained increasing attention as relevant niches for viral persistence and HIV pathogenesis as reviewed by J. H. Campbell et al. (2014)[73]. In that context, the focus has turned towards the central nervous system (CNS) as immune privileged sanctuary site for HIV persistence, especially in the presence of ART[74,75].

While most studies of HIV latency have been conducted by analyzing peripheral blood[76], it is clear that HIV persists to a great extent in tissues such as lymph nodes, spleen, gastrointestinal tract, and CNS[64,72,77–80]. These sites of the viral reservoir have been characterized far less than circulating leucocytes given the complexity to access the respective tissue specimen. Nevertheless, it will be of utmost importance to understand viral persistence in tissues, compare it to the periphery and include new insights in the development of curative approaches.

Viral reservoirs are established within days upon primary infection[81–83] and thus not preventable with available treatment options. A prominent example is the 'Mississippi Child', who received ART two days after birth for 18 months but experienced viral rebound 27 months after treatment interruption[84,85]. This and other studies demonstrated though, that starting treatment at the earliest timepoint possible (early ART) consequently impacts the size of the reservoir leading to clinical benefits for HIV-infected individuals[86,87].

Multiple factors impact the specific fate of a virus-infected cell and viral persistence during therapy. Residual low-level replication[88,89] and clonal expansion of latently-infected cells[90,91] contribute to viral persistence and maintenance of the HIV reservoir. Key molecular

mechanisms that determine latency include proviral integration sites[92–97], transcriptional interference with host genes[98], abundance of required host transcription factors such as NF-κB and NFAT[99–101], epigenetic modifications[102–107], as well as posttranslational mechanisms like impaired RNA processing and nuclear export functions[108–110].

### 1.2.2 The Status Quo of HIV Cure Approaches

A handful of singular events in the history of AIDS mark milestones in HIV cure efforts and reignited enthusiasm in the scientific community that remission is possible. The first person to be cured of HIV was Timothy Ray Brown, also known as the 'Berlin Patient', who received stem cell transplant therapy in 2007 intended to treat his acute myeloid leukemia[111]. Two further individuals, the 'Duesseldorf Patient'[112–114], and 'London Patient', Adam Castillejo[115,116], underwent similar procedures in 2013 and 2019, respectively, and remain in HIV remission since treatment interruption[117]. All three individuals received haemopoietic stem cell transplants from donors with a homozygous deletion in CCR5 (CCR5Δ32), the dominant co-receptor for HIV. While stem cell transplantation as universal HIV cure strategy is unrealistic due to the scarcity of suited donor material, high cost, inherent complexity and the risk for the patient, these successes inspired the field to continue and intensify the search for preventative measures and curative interventions.

Other hopeful but rare individuals are categorized as post-treatment[86,118] and elite controllers[119]. These individuals sustain ART-free virologic suppression for different periods of time based on so far insufficiently characterized mechanisms. A better understanding of the molecular and immunological basis underlying acquired and spontaneous viral suppression will help to conceptualize feasible HIV cure strategies moving forward.

Two main types of an HIV cure are currently investigated: a functional cure, and a sterilizing cure (Figure 8). A functional cure achieves long-term viral suppression below detectable levels in the absence of ART. In contrast, a sterilizing cure eliminates all infected cells and thus completely eradicates the viral reservoir.

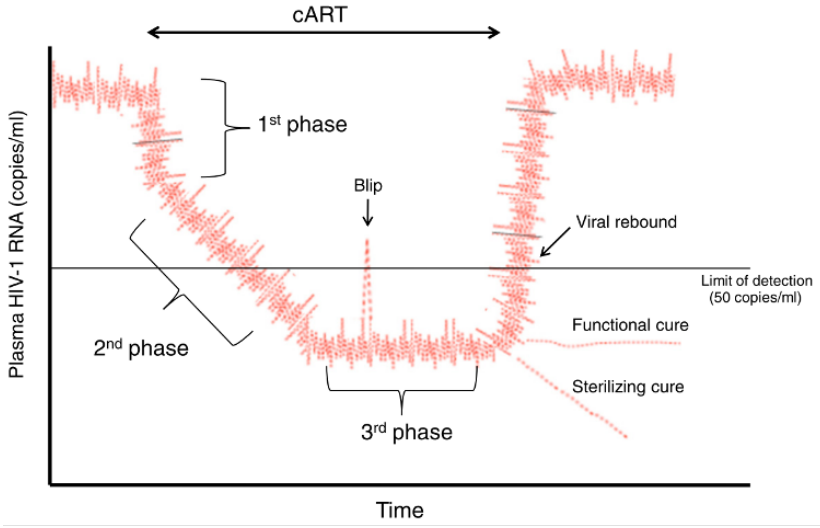


**Figure 8: Existing and hypothetical antiretroviral treatments.** In phase one, initiation of ART leads to a rapid decay of plasma viral levels due to deterioration and immunological clearance of short-lived productively-infected cells. Phase two is characterized by elimination of cells with a half-life of about 14 days. This not fully characterized cellular compartment may comprise partially activated CD4+ T cells, macrophages or dendritic cells. The true latent reservoir is responsible for the low but constant residual viremia in the third phase. Occasional rapid viral rebound can be observed (blips). Upon cessation of ART, plasma HIV RNA quickly reaches pretreatment levels (viral rebound). A functional cure would keep viremia below detection limits while a sterilizing cure would achieve complete elimination of HIV. Figure taken from C. V. Lint et al. (2013)[120]. cART = combination antiretroviral therapy.

Multiple HIV cure strategies are currently pursued as recently summarized by Schwarzer and colleagues[121] (Figure 9). One extensively explored method is 'shock and kill'[122]. Here, potent HIV latency reversing agents (LRAs) are utilized to activate expression of latent proviral genes in order to facilitate clearance of infected cells by either viral cytopathic effects or host immune response mechanisms. However, so far, most LRAs either failed to adequality reverse latency *in vivo*, exhibit toxic side effects, or activate only a small fraction of the reservoir[123]. Some recently discovered new classes of LRAs such as SMAC mimetics[124–126], activating the

noncanonical NF-κB pathway, and GSK-3 inhibitors[127], activating the AKT/mTOR signaling cascade, hold great promise and may help to unleash the full potential of shock and kill approaches[128,129].

A conceptually contrary strategy is referred to as 'block and lock'[130]. This approach strives to drive infected cells into a deep latent state and might offer significant advantages over shock and kill: for example, it circumvents the potentially harmful consequences of viral reactivation in immune-privileged anatomical compartments such as the CNS (a grave hazard that may accompany shock and kill attempts) and avoids the risk of reseeding or broadening viral reservoirs. However, HIV infections would not be cleared, which may lead to i.e. sustained HIV-related stigma and discrimination.

Rapid advances in molecular biology and biotechnology, specifically the revolutionary discovery of CRISPR/Cas9 editing in mammalian cells, have reinvigorated gene editing as antiviral strategies. These techniques exploit a range of DNA-binding proteins such as transcription activator-like effectors (TALEs), Zinc finger proteins (ZFPs), homing endonucleases (HEs), and CRISPR/Cas9[131,132] to target and manipulate proviral DNA. Anti-HIV gene therapies are designed to directly attack the provirus, HIV dependency host factors, or both simultaneously[133–136]. While studies have reported promising results in culture settings[137–141] and could even demonstrate successful *in vivo* editing in humanized mouse models[142–145], delivery and safety measures have to be improved to ensure an effective and scalable deployment of these gene therapy methods[121].

Lastly, immunological approaches instrumentalizing different aspects of the immune system to achieve an HIV cure are on the rise[146]. These immune interventions comprise T cell-based therapies[147–149], engineered killer cells[150], targeting checkpoint inhibitors[151–153],

harnessing effector functions of T cells and natural killer cells (NKs)[146,154], and enhancing broadly neutralizing antibodies (bNAbs) in order to facilitate antibody dependent cellular cytotoxicity (ADCC)[155–158].

Whether a functional or sterilizing cure is aspired, the combination of multiple strategies will most likely give the highest chance for a successful and durable neutralization of the viral reservoir.

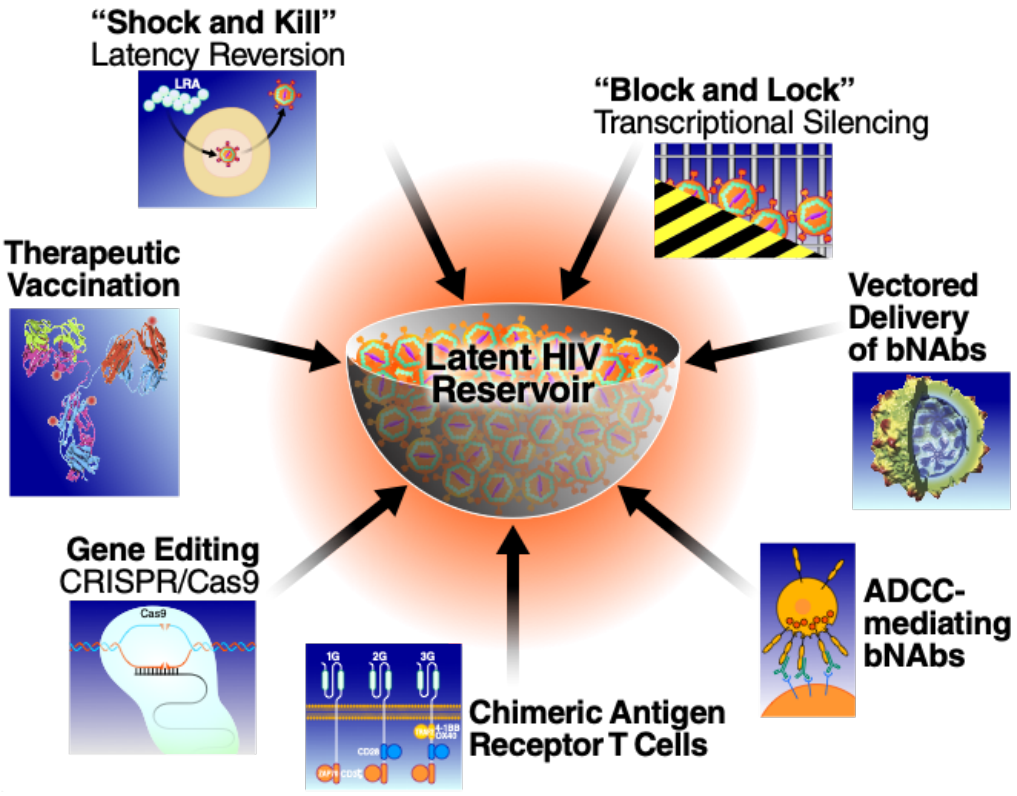


**Figure 9: Overview of major HIV cure strategies.** Figure taken from Schwarzer et al. (2020)[121]. bNAbs = broadly neutralizing antibodies, ADCC = antibody dependent cellular cytotoxicity.

### 1.2.3 The Search for Biomarkers of Persistent HIV

The identification of reliable biomarkers or unique expression patterns in HIV latently-infected cells would significantly facilitate the development of specific and effective HIV cure approaches. Such factors could contribute to HIV cure research in three important ways: 1) refine and broaden our understanding of HIV latency mechanisms and the biology of viral

persistence, 2) enable accurate quantification of viral reservoirs to assess viral burden and efficacy of therapeutic interventions, and 3) provide potential therapeutic targets to specifically affect and eradicate viral sanctuaries. However, the ability of HIV to lay dormant as well as the heterogenous and dynamic nature of the viral reservoir greatly complicate this endeavor.

Several non-viral markers of HIV latently-infected cells have been described and were reviewed in detail by G. Darcis et al. (2019)[159]. Briefly, studies have reported associations between HIV DNA and the expression of immune checkpoint molecules including PD-1, CTLA-4, LAG-3, and TIGIT[160,161]. Further, expression levels of CD2 in CD4+ T cells were reported to identify HIV latently-infected cells[162], while CD20[163] and CD30[164] expressing CD4+ T cells were found to be enriched for HIV RNA. Descours et al. (2017)[165] proposed CD32a as viral reservoir marker and described an unprecedent 1000-fold enrichment in HIV DNA comparing CD32a+ vs CD32a- CD4+ T cells. However, this finding has been thoroughly scrutinized in subsequent studies and incited a controversial discussion. Numerous reports challenged the initial finding and attributed the results to technical inaccuracy[166–169], while others confirmed or extended the association between CD32a expression and the viral reservoir[170,171].

While considerable progress has been made, the incomplete understanding of HIV latency and persistence during suppressive therapy hamper HIV cure attempts. To this day, a clear distinction of HIV latently-infected cells and accurate identification of viral reservoirs remains impossible.

In my thesis project, I addressed this gap and participated in the pursuit of better reservoir markers and determinants of viral persistence. By implementing a systems approach combined with an *in vitro* infection model for HIV latency, I obtained gene expression profiles of HIV-

infected primary cells, specifically focusing on the identification of expression patterns unique to latently-infected cells.

## 1.3 The Toolbox

### 1.3.1 HIV Reporter Viruses

HIV latently-infected cells are extremely rare and phenotypically indistinguishable from healthy cells *in vivo*. Therefore, several *in vitro* model systems have been established, enabling the study of HIV latency in cell culture settings. Often, HIV reporter viruses are used as tool to discriminate infected from uninfected cells (Figure 10).

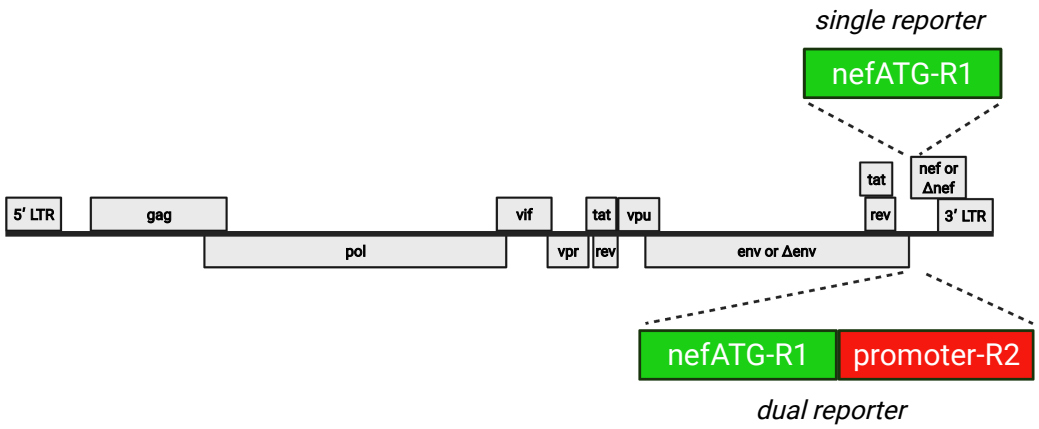


**Figure 10: Genomic organization of HIV reporter viruses.** Single reporter constructs contain a reporter gene under the control of the viral LTR. Reporters are usually integrated right before or in place of the *nef* gene using the start codon of *nef* (nefATG). Dual reporter viruses harbor an independent transcription unit, often placed behind the first reporter, comprising a promoter that drives constitutive expression of the second reporter. Infectious clones carry a full-length HIV genome while single round variants are often *env* and *nef* deficient. R = reporter.

Single reporter viruses contain an LTR-driven marker, usually a fluorescent protein such as GFP, indicating active viral infection. Dual reporter viruses carry an additional marker controlled by an independent promoter that reveals successful viral integration, also in the absence of active viral transcription[172,173]. Molecular clones have been generated as infectious wildtype (WT) or single round variants. The latter harbors a mutated *env* gene thus requiring

a complementing Env expression in trans in order to generate infectious virus particles. Due to their incomplete viral genome, such virions do not cause spreading infections and enable cell culture under lower biological safety conditions. All reporter systems allow for detection and purification of infected and uninfected cells and with dual reporter viruses even a further discrimination of uninfected, productively-infected, and latently-infected cells.

### 1.3.2 NanoString Technology

Nowadays, ample techniques exist to characterize cells and assess their transcriptional and proteomic expression profile. Several methods, including fluorescence *in situ* hybridization and quantitative PCR for RNA detection or western blotting for protein detection, are highly sensitive, but also very narrow in terms of their targeting breadth. These are of great use to investigate a limited number of already identified candidate molecules and confirm or disprove hypotheses. In contrast, RNA-sequencing and mass spectrometry are completely unbiased approaches and enable the detection and semi-quantification of thousands of analyte types in parallel. However, these approaches entail time-consuming and cumbersome downstream bioinformatic analyses.

Here, I employed a relatively new technique, the NanoString nCounter Analysis System, which has been mostly applied in cancer research thus far, for the expression profiling of HIV-infected cells. A great advantage of this method is the possibility to detect DNA, RNA and protein targets simultaneously through molecular barcodes that enable a multiplexed detection of up to 800 analyte types in one single reaction. This gene expression breadth enables an in-depth characterization of cellular HIV infection phenotypes in a highly

quantitative and sensitive format. In addition, streamlined bioinformatic resources allow for rapid data and analysis turnover accelerating the discovery of biological concepts.

The foundation of the NanoString nCounter technology are specific oligonucleotide probe pairs that hybridize to complementary nucleic acid sequences present in a sample (Figure 11A). Each probe is 50 nucleotides long. The capture probe is biotinylated and immobilizes targeted nucleic acids. The reporter probe on the other hand, carries a fluorescent barcode with 4 colors at 6 positions and permits specific identification of the respective target. RNA and DNA molecules are detected directly while protein detection is enabled by oligonucleotide-labeled antibodies.

NanoString assays follow a simple, quick and straightforward procedure (Figure 11B). Nucleic acid targets are bound by the probe pair in solution forming target-probe-complexes. Excess probe is removed in subsequent washing steps and the target-probe-complexes immobilized on a cartridge via the biotin moiety of the capture probe. The NanoString platform, in my case the nCounter SPRINT Profiler, scans and images the sample cartridge using an internal automated fluorescence microscope. A digital analyzer then counts the fluorescent barcodes and provides data as digital counts thus directly quantifying a given analyte type in the respective sample.

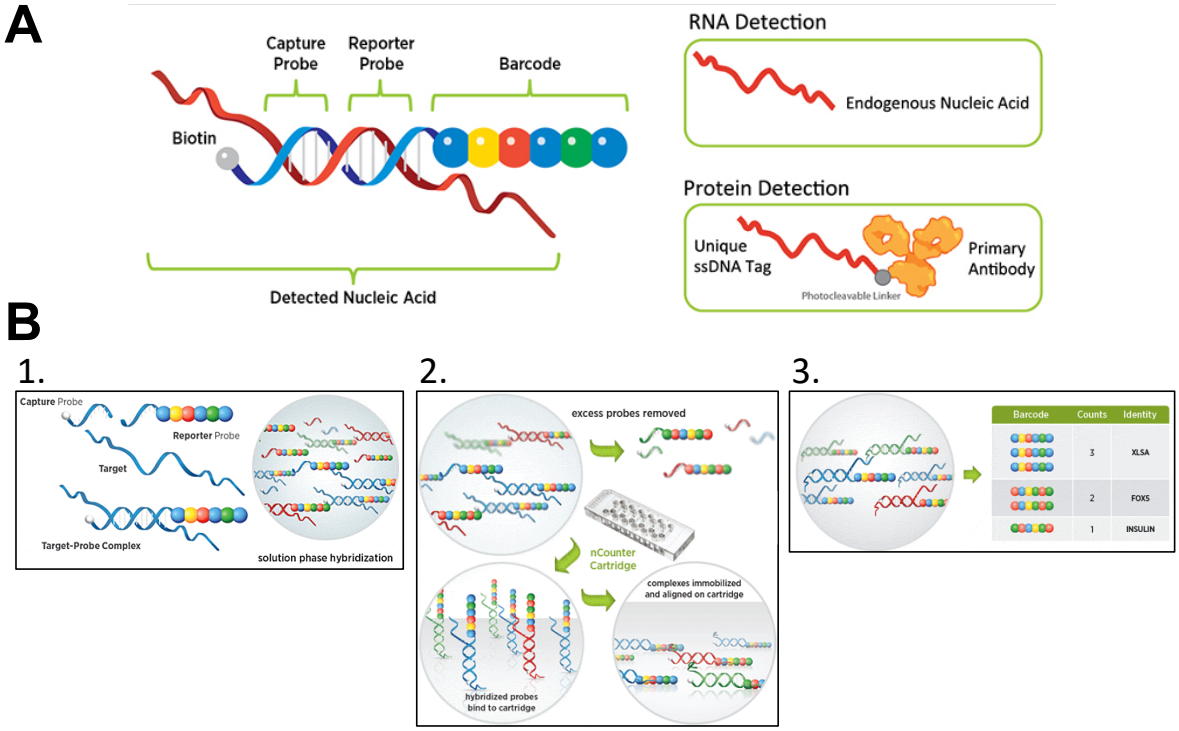


**Figure 11: Illustration of the NanoString nCounter technology.** (A) NanoString digital counting technology is based on molecular probe pairs that allow detection of nucleic acid targets. DNA and RNA molecules are bound directly while proteins are detected using synthetic oligonucleotide-tagged antibodies. (B) Workflow of nCounter assays. 1. The probe pair hybridizes with its target molecule in solution. 2. The nCounter instrument performs several washing steps to remove excess probe. After purification, target-probe-complexes are immobilized and aligned on the nCounter cartridge. 3. A designated region is scanned and imaged by automated fluorescence microscopy. The digital analyzer counts fluorescent barcodes and provides data reflecting total abundance of an analyte type in a given sample.

# 2 Aim of the Study

Highly active antiretroviral therapy (HAART) effectively suppresses human immunodeficiency virus (HIV) replication and dramatically improves health and life expectancy of people living with HIV (PLWH). However, current treatment regimens fail to eradicate HIV infections. The main barrier for an HIV cure are latently-infected cells, forming the so-called latent viral reservoirs in which the virus persists virtually indefinitely. Latently-infected cells are unaffected by ART and invisible to the host's immune system, but capable to rapidly re-initiate viral replication and induce spreading infection once therapy is discontinued. Thus, a true cure for HIV infections has not been achieved.

A key prerequisite for developing an HIV cure is an in-depth understanding of the nature and biology of the latent reservoir. Cellular markers of dormant HIV infections are needed as they could shed light on mechanisms of HIV latency, enable precise measurement of viral reservoirs and, most importantly, allow to target and eliminate HIV-latently infected cells. Hitherto however, no such markers have been convincingly demonstrated. The present study seeks to address some of the aforementioned shortcomings and revolves around two critical questions:

1. **What distinguishes HIV latently-infected cells from other cells?**
2. **How is HIV latency established and/or maintained?**

To address these questions, I utilized primary CD4+ T cells, which constitute the major viral sanctuary, and deployed an *in vitro* HIV infection model that enables identification and isolation of uninfected, latently-, and productively-infected cells. These cells were characterized using NanoString hybridization and fluorescence-based digital counting technology allowing for simultaneous detection of 770 mRNA and 30 protein targets. My goal

was to compare gene expression profiles and analyze cellular pathways in order to identify markers of latency and predict causal relationships that may provide insights into the mechanism of viral persistence.

# 3 Materials & Methods

## 3.1 Materials

### 3.1.1 Chemicals

| Compound | Manufacturer |
|---|---|
| Agarose | Fisher Scientific, Cat. #BP1356-100 |
| CGS-21680 hydrochloride hydrate | Sigma-Aldrich, Cat. #C141-5MG |
| DMOG (Dimethyloxalylglycine) | Sigma-Aldrich, Cat. #D3695 |
| DMSO (Dimethyl sulfoxide) | Sigma-Aldrich, Cat. #D2650-100ML |
| Ethanol, Absolute (200 Proof) | Fisher Scientific, Cat. #BP28184 |
| Ionomycin calcium salt from Streptomyces conglobatus | Sigma-Aldrich, Cat. #10634-1MG |
| PEI (Polyethylenimine) | Polysciences, Inc. Cat. #23966 |
| PMA (Phorbol-Myristate-Acetate) | Sigma-Aldrich, Cat. #10634-1MG |
| Raltegravir potassium | Sigma-Aldrich, Cat. #CDS023737-25MG |
| Saquinavir mesylate | Sigma-Aldrich, Cat. #S8451-50MG |
| SCH-58261 | Sigma-Aldrich, Cat. #S4568-5MG |
| Triton X-100 | Sigma-Aldrich, Cat. #X100 |

### 3.1.2 Equipment and Instruments

| Instrument | Manufacturer |
|---|---|
| Centrifuge 5420 | Eppendorf AG |
| Centrifuge 5804 R | Eppendorf AG |
| LSR II Flow Cytometer System | BD Biosciences |
| MA900 Multi-Application Cell Sorter | Sony Biotechnology Inc. |
| nCounter SPRINT profiler | NanoString Technologies, Inc. |
| S1000 Thermal Cycler | Bio-Rad Laboratories, Inc. |
| TC20 Automated Cell Counter | Bio-Rad Laboratories, Inc., Cat. #1450102 |
| Ultracentrifuge, XL-100K | Beckman-Coulter, Inc. |
| NanoDrop 1000 | ThermoFisher, Scientific |

### 3.1.3 Consumables

| Item | Manufacturer |
|---|---|
| 500 ml Filter System, pore size 0.1 µm, funnel capacity 500ml | Fisher Scientific, Cat. #09-761-181 |
| Cell Counting Slides, Dual-Chamber | Bio-Rad Laboratories, Inc., Cat. #1450011 |
| Corning Cell Culture Treated Flasks, Angled Necks, 175 $cm^2$ | Fisher Scientific, Cat. #10-126-61 |
| Corning Cell Culture Treated Flasks, Angled Necks, 75 $cm^2$ | Fisher Scientific, Cat. #10-126-37 |
| EasyEights EasySep Magnet | StemCell Technologies, Cat. #18103 |
| Falcon 15 ml Conical Centrifuge Tube | Fisher Scientific, Cat. #10263041 |
| Greiner CELLSTAR 96 well V-bottom plate | MilliporeSigma, Cat. #M9686-100EA |
| ImmEdge Hydrophobic Barrier PAP Pen | Vector Laboratories, Cat. #H-4000 |
| Invitrogen Magnetic Stand-96 | Fisher Scientific, Cat. #10579773 |
| nCounter Sprint Cartridge | NanoString Technologies, Inc., Cat. #100078 |
| Steriflip Sterile Disposable Vacuum Filter Units (0.22 µm) | MilliporeSigma, Cat. #SCGP00525 |

### 3.1.4 Cell Culture Media and Reagents

| Reagent | Manufacturer |
|---|---|
| ACK Lysing Buffer | ThermoFisher Scientific, Cat. #A1049201 |
| Alliance HIV-1 p24 Antigen Elisa Kit | PerkinElmer, Cat. #NEK050001KT |
| Bright Glo Luciferase Assay System | Promega, Cat. #E2610 |
| BSA (Bovine Serum Albumin) | Sigma-Aldrich, Cat. # A3059-100G |
| DMEM, high glucose | ThermoFisher, Scientific, Cat. # 11965-118 |
| Dynabeads Human T-Activator CD3/CD28 | ThermoFisher Scientific, Cat. #11132D |
| EasySep Human CD4+ T Cell Isolation Kit | StemCell Technologies, Cat. #17952 |
| FBS (Fetal Bovine Serum), Regular | Corning, Inc., Cat. #35-010-CV |
| Fugene HD transfection reagent | Promega, Cat. #E2311 |
| Lymphocyte Separation Medium | Corning, Inc., Cat. #25-072-CI |
| Opti-MEM (Reduced Serum Medium) | ThermoFisher Scientific, Cat. #31985062 |
| Penicillin/Streptomycin (P/S) | Fisher Scientific, Cat. #11548876 |

| | |
|---|---|
| Recombinant Human IL-2 | PeproTech, Inc., Cat. #200-02 |
| RNA:Protein Immune Profile CS_B2M VRPC B2M-HIPS-12 | NanoString Technologies, Inc., Cat. #121100019 |
| RPMI 1640 Medium | ThermoFisher, Scientific, Cat. #11875-119 |
| Trypan Blue Solution, 0.4% | ThermoFisher, Scientific, Cat. #15250061 |
| Trypsin-EDTA (0.25%) | ThermoFisher, Scientific, Cat. #25200056 |

### 3.1.5 Buffers and Solution

| Reagent | Manufacturer |
|---|---|
| 1X DPBS, no calcium, no magnesium | ThermoFisher, Scientific, Cat. #14190-250 |
| EZ-Link Sulfo-NHS-SS-Biotin | ThermoFisher, Scientific, Cat. # A39258 |
| Target Retrieval Solution | Agilent Dako, Cat. #S1700 |
| TBS, Tris Buffered Saline, 10X Solution, pH 7.4 | Fisher Scientific, Cat. #BP24711 |

### 3.1.6 Molecular Biology Reagents

| Reagent | Manufacturer |
|---|---|
| AscI, Restriction Endonuclease | New England Biolabs, R0558S |
| FseI, Restriction Endonuclease | New England Biolabs, R0588S |
| LB Agar AMP 100 ug/ml (100 mm) | Teknova, Inc., Cat. #50-841-787 |
| LB Agar KAN 50 ug/ml (100 mm) | Teknova, Inc., Cat. #50-190-7951 |
| LB Broth, Miller (Pre-Buffered Capsules) | Fisher BioReagents, Cat. #BP9731-500 |
| Phusion High-Fidelity DNA Polymerase | New England Biolabs, M0530S |
| Plasmid Plus Maxi Kit | QIAGEN, Cat. #12963 |
| Quick Alkaline Phosphatase, Calf Intestinal (Quick CIP) | New England Biolabs, M0525S |
| T4 DNA Ligase | New England Biolabs, M0202S |

### 3.1.7 Antibodies and Other Staining Reagents

| Antibody/Reagent | Provider |
|---|---|
| Alu-repeats DNA probe Cy5-conjugated, GCCTCCCAAAGTGCTGGGATTACAG | PNA Bio, Inc. |
| APC anti-Human CD73 (Ecto-5'-nucleotidase) | BioLegend, Inc., Cat. #344006 |

| | |
|---|---|
| APC-Cy™7 Mouse Anti-Human CD25 Clone M-A251 | BD Pharmingen Cat. #557753 |
| Donkey anti-Goat IgG (H+L) Cross-Adsorbed Secondary Antibody, Alexa Fluor 594 | ThermoFisher Scientific, Cat. #A-11058 |
| Goat anti-Mouse IgG (H+L) Cross-Adsorbed Secondary Antibody, Alexa Fluor 647 | ThermoFisher Scientific, Cat. # A-21235 |
| HIV-1 Gag-pol mRNA probe | Advanced Cell Diagnostics, Inc., Cat. #317691 |
| Anti-HIV-1 gp120 Antibody | NIH HIV Reagent Program, Cat. #1476, Lot: 160183 |
| Anti-HIV-1 Integrase Antibody | NIH HIV Reagent Program, Cat. #7374, Lot: 110157 |
| Anti-HIV-1 Nef Antibody | NIH HIV Reagent Program, Cat. #2949, Lot: 140216 |
| Anti-HIV-1 Tat Antibody | NIH HIV Reagent Program, Cat. #705, Lot: 180001 |
| Anti-HIV-1 Vpr Antibody | NIH HIV Reagent Program, Cat. #11836, Lot: 150149 |
| HIV-Nef DNA probe Alexa Fluor 488-conjugated, GCAGCTTCCTCATTGATGG | PNA Bio, Inc. |
| Anti-HIV-1-p24 Antibody | GeneGex, Cat. #GTX40774 |
| Human TruSTain FcX | BioLegend, Inc., Cat. #422301 |
| PNA ISH detection kit | Agilent Dako, Cat. #K5201 |
| ProLong Gold Antifade Mountant with DAPI | ThermoFisher Scientific, Cat. #P36931 |
| RNAscope 2.5 HD Assay - RED | Advanced Cell Diagnostics, Inc., Cat. #322360 |
| Streptavidin, Alexa Fluor 647 Conjugate | ThermoFisher Scientific, Cat. # S21374 |
| Streptavidin, Alexa Fluor 680 Conjugate | ThermoFisher Scientific, Cat. # S32358 |
| V450 Mouse Anti-Human CD69 Clone FN50 | BD Horizon Cat. #560740 |
| Zombie Violet Fixable Viability Kit | BioLegend, Inc., Cat. #423113 |

### 3.1.8 Plasmids

| Plasmid | Provider |
|---|---|
| $HIV_{DFI}$ | Verdin lab, Buck Institute |
| $HIV_{DFII}$ | Generated in this work |
| $HIV_{Luc}$ (NL4.3-Luciferase) | Greene lab, Gladstone Institutes |
| mKO2-N1 | Addgene, Cat. #4625 |
| pENV (pSVIII 92HT593.1) | NIH HIV Reagent Program, Cat. #3077 |

### 3.1.9 Primers

| Primer | Sequence |
|---|---|
| $mKO2_{HIVdfii}$ FW | AGAAGGCGCGCCATGGTGAGTGTGATTAAACC |
| $mKO2_{HIVdfii}$ RV | TTCTGGCCGGCCTTAGCTATGAGCTACTGCAT |

### 3.1.10 Biological Material

| Material | Provider |
|---|---|
| **Primary human samples** | |
| TRIMA Leukoreduction Chamber | Vitalant |
| **Eukaryotic cell lines** | |
| HEK293T | ATCC, Cat. #CRL-3216 |
| J-Lat 11.1 | Verdin lab, Buck Institute |
| J-Lat 5A8 | Greene lab, Gladstone Institutes |
| J-Lat 6.3 | Verdin lab, Buck Institute |
| Jurkat, clone E6-1 | ATCC, Cat. #TIB-152™ |
| **Prokaryotic Cell lines** | |
| E. coli DH5 $\alpha$ | ThermoFisher Scientific, Cat. #18258012 |
| E. coli Stbl3 | ThermoFisher Scientific, Cat. #C737303 |

### 3.1.11 Software

| Software | Provider |
|---|---|
| A plasmid editor (ApE) | M. Wayne Davis, Utah, USA |
| Advanced Analysis 2.0 | NanoString Technologies, Inc. |
| Cytoscape 3.8.2 | Institute for Systems Biology |

| | |
|---|---|
| FlowJo 10.7.1 | Becton Dickinson & Company (BD) |
| GraphPad Prism 9.0.1 | GraphPad Software, Inc. |
| NIS-Elements-AR | Nikon Instruments Europe B.V. |
| nSolver 4.0 | NanoString Technologies, Inc. |
| SnapGene Viewer | GSL Biotech LLC |
| Venn diagram Generator | Bioinformatics&Evolutionary Genomics |

## 3.2 Methods

### 3.2.1 Molecular Biology

**Molecular Cloning.** The 1st generation dual reporter virus construct R7GEmC[172] (kindly provided by Dr. Eric Verdin) was adapted by ligation-based molecular cloning. Briefly, R7GEmC was linearized by enzymatic digest using FseI and AscI (both ThermoFisher) in order to excise the mCherry open reading frame. Then, mKO2 was PCR amplified from the template mKO2-N1 (Addgene) using primers containing matching restriction sites. Subsequently, the lentiviral vector was dephosphorylated using Quick CIP (NEB), purified and subjected to ligation with the digested and gel-purified PCR product utilizing T4 DNA ligase (ThermoFisher). Finally, circularized plasmid DNA was transformed by heat-shock in chemically competent Stbl-3 E. coli (Life Technologies) for subsequent antibiotics selection and Sanger sequencing (Elim Biopharm) of positive clones.

**Plasmid amplification and preparation.** Transformed Stbl-3 cells were grown in 2-5 ml of lysogeny broth with 0.1 mg/ml Ampicillin (LB Amp) for 4-8 hours prior to inoculation of large-volume flask with 100-300 ml LB Amp for overnight growth. 16 hours later, cells were pelleted by centrifugation for 15 min at >3000 g and subjected to plasmid preparation using Plasmid Plus Maxi Kits (QIAGEN) following the manufacturer's protocol. The DNA

concentration of isolated plasmid DNA was spectrophotometrically determined using a NanoDrop 1000 (ThermoFisher) and DNA aliquots were stored at 4°C.

### 3.2.2 Cell Culture and Treatment

**Cell lines and cell culture.** HEK293T were obtained from ATCC and were cultured in DMEM supplemented with 10% FBS and 10% Penicillin/1% Streptomycin (DMEM+/+) at 37°C, 5% $CO_2$ unless stated otherwise. J-Lat 5A8 cells were kindly provided by Warner C. Greene (Gladstone Institutes). All other J-Lat clones were a gift from Eric Verdin (Buck Institute). Jurkat E6-1 cells were obtained from ATCC. All suspension cells were cultured in RPMI 1640 supplemented with 10% FBS and 10% Penicillin/1% Streptomycin (RPMI+/+) at 37°C, 5% $CO_2$ unless stated otherwise.

**Virus production.** HIV-1 viruses were generated by transfection of proviral DNA into HEK293T cells via polyethylenimine (PEI, Polysciences) transfection protocol. Env-pseudotyped $HIV_{DFII}$ stocks were produced by co-transfecting plasmids encoding $HIV_{DFII}$ and a plasmid encoding HIV-1 dual-tropic envelope (pSVIII-92HT593.1) at a ratio of 3:1 into HEK293T cells at 50-60% confluency grown in 175 $cm^2$ culture flasks. Each flask was transfected with a total amount of 30 µg DNA. The transfection mix was prepared in 2 ml Opti-MEM (ThermoFisher) as follows: DNA plasmids were diluted in Opti-MEM first, then PEI was added at a ratio of 3:1 PEI:DNA (90 µg PEI). The transfection mix was vortexed for 15 sec and incubated for 15 min at RT. Culture medium was replaced with 20 ml fresh DMEM + 10% FBS without P/S, and 2 ml transfection mix was added to each flask. 16h post transfection, P/S-free medium was replaced with standard culture medium (DMEM+/+), and cells were incubated for another 24h at 37°C, 5% $CO_2$. For replication competent HIV NL4-3 Luciferase (a kind gift from Dr. Warner Greene),

lentiviral vectors were introduced by Fugene HD transfection according to the manufacturer protocols. Cell supernatants were collected 48h post transfection, centrifuged at 4°C for 10 min at 4000 rpm (~ 3390 x g) and subsequently filtered using 0.22 µm membrane vacuum filter units (MilliporeSigma) to remove cell debris. Virus preparations were concentrated by ultracentrifugation at 20,000 rpm (~ 50,000 x g) for 2h at 4°C and resuspended in complete media for subsequent storage at -80°C. Virus concentration was estimated by p24 titration (HIV-1 alliance p24 ELISA kit, PerkinElmer).

**J-Lat cell latency reversal.** J-Lat 5A8 cells (seeded at $1x10^6$ cells/ml) were incubated with CGS21680 (Sigma-Aldrich) or SCH-58261 (Sigma-Aldrich) at 37°C for 1h at increasing doses in RPMI+/+, followed by stimulation with 20 nM PMA / 1 µM Ionomycin (PMA/I). Untreated cells or cells treated with 0.5% DMSO served as negative controls. 7h after PMA/I reactivation, cells were washed 2x with PBS and viral transcriptional activity, reflected by GFP expression was measured using LSR II flow cytometer (BD Biosciences).

**Leucocyte isolation and primary cell culture.** Peripheral blood mononuclear cells (PBMCs) from HIV-seronegative donors (Vitalant) were isolated by Ficoll-Hypaque density gradient centrifugation at 2000 rpm (~ 850 x g) at RT for 30 min, without brake. PBMCs were immediately processed to isolate CD4+ T cells by negative selection using the EasySep Human CD4+ T Cell Isolation Cocktail (StemCell Technologies) according to manufacturer's protocol. Purified CD4+ T cells were cultured in RPMI+/+.

**CD4+ T cell *in vitro* activation and infection.** CD4+ T cells from peripheral blood were stimulated with αCD3/αCD28 activating beads (ThermoFisher) at a concentration of 1 bead/cell in the presence of 100 U/ml IL-2 (PeproTech) in RPMI +/+ for 3 days (initial seeding

concentration 1x$10^6$ cells/ml). At the day of infection, cells were spinoculated in 96-well V-bottom plates in 50 µl RPMI+/+ with 100 ng ($HIV_{DFII}$) of p24 per 1×$10^6$ cells with 5×$10^6$ cells total per well for 2 h at 2350 rpm (1173 × g) at 37°C. After spinoculation, all cells were returned to culture in the presence of 30 U/ml IL-2. Pre-stimulated CD4+ T cells stayed in αCD3/αCD28 activating beads during spininfection and subsequent cell culture. For hypoxia experiments, cells were treated with 500 µM DMOG (or mock-treated with 0.5% DMSO) two days after αCD3/αCD28 bead stimulation and 24h before $HIV_{DFII}$ spininfection. Cells were kept in DMOG containing RPMI+/+, in presence of activation beads and IL-2 until sample collection 4 days post infection.

**CD4+ T cell *in vitro* infection and latency reversal.** Initially, CD4+ T cells were isolated from peripheral blood as described above and subjected to fluorescence-activated cell sorting (FACS) of CD73+ and CD73- cells. To that aim, cells were stained with APC anti-human CD73 (Biolegend) diluted in PBS (1:20) in 100 µl final volume for 20 min at RT. Cells were then washed twice with PBS and resuspended in 500 µl – 1000 µl PBS to achieve high cell concentrations (20 - 40x$10^6$ cells/ml) for FACS. Cells were sorted into 15 ml conical tubes containing 1.5 ml RPMI+/+. Cells were cultured for 24h, then infected and rested in the presence of ART to establish *in vitro* latency[174]. Briefly, 100 ng of purified NL4-3-Luciferase was added per 1x$10^5$ sorted cells, which were then infected by spinoculation as described above. 24h post virus exposure, 5 µM saquinavir (protease inhibitor) was added to the cell cultures to suppress spreading infection. 5 days later, cells were stimulated with αCD3/αCD28 beads (or left untreated) in the presence of 30 µM raltegravir (integrase inhibitor) to prevent new infections. 24h after stimulation, luciferase activity was quantified using the bright glo luciferase assay system (Promega).

### 3.2.3 Flow Cytometry and Cell Sorting

**Cell staining and processing.** Freshly isolated CD4+ T cells were stained for viability, using the fixable Zombie viability dye (1:100; BioLegend) according to the manufacturer's protocol. Subsequently, antibodies for cell surface staining diluted in PBS (1:50 or 1:100) were added and incubated for 20 min at RT. For flow cytometry, cells were washed and fixed in 1% paraformaldehyde (PFA) in PBS after the staining. FACS experiments were performed with live, unfixed cell samples. Flow cytometry analyses were performed on the LSR II flow cytometer (BD Biosciences) or MA900 Multi-Application Cell Sorter (Sony Biotechnologies). All fluorescent-based sorts were conducted on the latter instrument.

**Flow cytometry data analysis and gating.** Data were analyzed and visualized using the FlowJo software (v.10.4.2). Crosstalk compensations was performed using single-stained samples for each of the fluorochromes and isotype controls were employed to assess antigen positivity and enable specific gating. FACS and flow cytometry gating was performed as follows: first, single live cells were selected from FSC/SSC scatter plots, sub-gated on Zombie low/negative cells. Then, antibody gates (CD73, CD69 or CD25) were defined based on suited isotype controls. Gating of $HIV_{DFII}$ reporter expression was based on non-infected, mock-treated (*in vitro* activated) negative control samples to account for activation-dependent increase of cellular background fluorescence.

### 3.2.4 Expression Profiling via NanoString

Quantitative RNA and protein expression data were generated using the nCounter Vantage 3D RNA:Protein Immune Cell Profiling Assay and the nCounter SPRINT profiler (NanoString Technologies), comprising 770 RNA and 30 protein targets as well as positive and negative

controls. 100,000 viable, sorted cells were used per sample, which were processed according to the manufacturer's instructions. RNA and protein expression values were normalized and analyzed using the nSolver Analysis Software 4.0 and the add-on Advanced Analysis Software 2.0.115 (NanoString Technologies). Normalization genes for each sample were automatically selected by the software based on the geNorm algorithm. Biological replicates were grouped according to sample type and the differential expression of each analyte-type (RNA or protein target) was determined in cross-comparisons among all sample types by considering inter-donor differences as confounding variable unless otherwise stated. Intersections of significant targets of individual differential expression analyses were visualized in a Venn diagram using an open source platform from Bioinformatics & Evolutionary Genomics[175].

Based on the differential expression of each gene, gene sets pre-defined by nanoString, representing different pathways included in this assay, were analyzed by calculating global significance scores for each gene set within each sample as follows: undirected global significance statistic = $\left(\frac{1}{p}\sum_{i=1}^{p} t_i^2\right)^{\frac{1}{2}}$, where ti is the t-statistic from the ith pathway gene. The directed global significance statistic is similar to the undirected global significance statistic, but rather than measuring the tendency of a pathway to have differentially expressed genes, it measures the tendency to have over- or under-expressed genes. It is calculated similarly to the undirected global significance score, but it takes the sign of the t-statistics into account: Directed global significance statistic = $sign(U)|U|^{1/2}$ where U = $\left(\frac{1}{p}\sum_{i=1}^{p} sign(t_i) * t_i^2\right)$ and where sign(U) equals -1 if U is negative and 1 if U is positive (MAN-10030-02[176]).

### 3.2.5 RNA Sequencing

Freshly isolated CD4+ T cells from healthy blood donors were sorted based on their CD73 expression as described above. $3x10^6$ cells were collected per sample and stored as dry cell pellets at -80 °C. RNA preparation, library preparation and mRNA sequencing were conducted at Genewiz (USA). Paired-end sequencing was performed using the Illumina NovaSeq 6000 instrument to obtain a minimum of 20 million read pairs per sample with a read length of 2x150 bp. Sequence reads were trimmed to remove possible adapter sequences and nucleotides with poor quality using Trimmomatic v.0.36. The trimmed reads were mapped to the Homo sapiens GRCh38 reference genome available on ENSEMBL using the STAR aligner v.2.5.2b. Unique gene hit counts were calculated by using featureCounts from the Subread package v.1.5.2. The hit counts were summarized and reported using the gene_id feature in the annotation file. Only unique reads that fell within exon regions were counted. After extraction of gene hit counts, the gene hit counts table was used for downstream differential expression analysis. Using DESeq2, a comparison of gene expression between samples was performed adjusting for the donor effect as confounding variable. The Wald test was used to generate p-values and $\log_2$ fold changes. Genes with an adjusted p-value < 0.05 (Benjamini-Hochberg method) and absolute $\log_2$ fold change > 1 were called as differentially expressed genes for each comparison. A gene ontology analysis was performed on the statistically significant set of genes by implementing the software GeneSCF v.1.1-p2. The goa_human GO list was used to cluster the set of genes based on their biological processes and determine their statistical significance. A list of genes clustered based on their gene ontologies was generated.

### 3.2.6 *In Situ* Detection of HIV and Cellular Markers

The experimental procedure for the immunofluorescence staining and parallel detection of viral nucleic acids has been described and gradually optimized in a series of previous publications[177–179]. In its ultimate version, the protocol enables the detection of HIV-integrated DNA, viral mRNA, viral proteins, and several cellular markers in the same assay. Sample preparation, data acquisition and subsequent analyses were conducted in the laboratory of Dr. Eliseo Eugenin.

**Tissue samples.** Tissues from ART-suppressed individuals who have been on treatment for at least 6 months and had viral loads below clinical detection limits (<50 RNA copies/ml), as well as tissues from HIV-negative and ART-naïve viremic individuals with high plasma loads (>50 RNA copies/ml) were part of an ongoing research protocol approved by Rutgers University. Further clinical data and additional information are available and will be provided upon request by the lead contact Eliseo Eugenin (eleugeni@utmb.edu). All tissues were obtained with full, written consent from the study participants and freshly collected specimens were immediately fixed with 4% PFA, then mounted into paraffin blocks and subjected to tissue sectioning and ultimately to analysis by immunostaining.

**Staining procedures.** Paraffin-embedded slides containing the tissue samples were consecutively immersed in the following solutions: xylene for 5 min (2 times), 100% EtOH for 3 min, 100% EtOH for 3 min, 95% EtOH for 3 min, 90% EtOH for 3 min, 70% EtOH for 3 min, 60% EtOH for 3 min, 50% EtOH for 3 min, miliQ $H_2O$ for 3 min. Then, tissue was encircled with ImmEdge Pen to reduce the reagent volume needed to cover the specimens. Finally, slides were immersed in miliQ $H_2O$ for 3 min. For Protein K treatment, tissues were incubated with

proteinase K diluted 1:10 in 1X TBS (PNA ISH kit) for 10 min at RT in a humidity chamber. Next, slides were immersed in miliQ H2O for 3 min, then immersed in 95% EtOH for 20 sec and finally, the slides were let air-dry for 5 min. For HIV DNA probe hybridization tissues were incubated with 10 µM PNA DNA probe for Nef-PNA Alexa Fluor 488 and Alu-PNA Cy5. Next, slides were placed in a pre-warmed humidity chamber and incubated at 42°C for 30 min, then the temperature was raised to 55°C for an additional 1 h incubation. Subsequently, tissues were incubated using Preheat Stringent Wash working solution (PNA ISH kit) diluted 1:60 in 1X TBS for 25 min in an orbital shaker at 55°C. Slides were equilibrated to RT by brief immersion in TBS for 20 sec. HIV mRNA detection followed the manufacturer's protocol for RNAscope 2.5 HD Detection Reagent-RED. Probe for HIV Gag-pol was added to the tissue samples and incubated for 30 min at 42°C and then 50 min at 55°C. Next, samples were incubated in Preheat Stringent Wash working solution diluted 1:60 in 1X TBS (PNA ISH kit) for 15 min in an orbital shaker at 55°C. Finally, slides were immersed in 1X TBS for 20 sec. For HIV or cellular protein detection antigen retrieval was performed by incubating slide sections in commercial antigen retrieval solution (Dako) for 30 min in a water-bath at 80°C. Next, slides were removed from the bath and allowed to cool down in 1X TBS. Samples were permeabilized with 0.1% Triton X-100 for 2 min and then washed in 1X TBS for 5 min three times. Unspecific antibody binding sites were blocked by incubating samples with freshly prepared blocking solution. Afterwards, sections were incubated overnight at 4°C using a humidity chamber (10 ml of Blocking solution: 1 mL 0.5 M EDTA, 100 ul Fish Gelatin from cold water 45%, 0.1 g Albumin from Bovine serum Fraction V, 100 ul horse serum, 5% human serum, 9 mL miliQ $H_2O$). A primary antibody was added to the samples diluted in blocking solution and incubated at 4°C overnight. Then, slides were washed in 1X TBS 5 min for three times to eliminate unbound antibodies.

Secondary antibodies were added at the appropriate dilutions and incubated for 2h at RT. Slides were washed three times in 1X TBS for 5 min to eliminate unbound antibodies. Next, slides were mounted using Prolong Diamond Antifade Mount medium containing DAPI. Slides were kept in the dark at 4°C.

**Image acquisition and analysis.** Cells were examined by confocal microscopy using an A1 Nikon confocal microscope with spectral detection and unmixing. Image analysis was performed using the Nikon NIS Elements Advanced Research imaging software. The automated image segmentation and analysis is based on the following premises: For detection of HIV-integrated DNA, first, automatic or manual detection of cells that are positive for HIV-DNA and second, the HIV-DNA probe has to colocalize with DAPI and Alu repeats staining with a Pearson's correlation coefficient of at least 0.8 as described previously[180]. For HIV-integrated DNA, these two conditions are essential, or the signal is considered negative or unspecific. For detection of HIV-mRNA, first, low colocalization with DAPI or Alu-repeats (0.2 Pearson's correlation coefficient or below) and second, presence in cells with HIV-DNA signal. The sensitivity, accuracy and specificity of the system was previously validated in the laboratory of our collaborator in two well characterized T cell lines A3.01 (uninfected) and ACH-2 (HIV-infected) and two monocytic cell lines, HL-60 (uninfected) and OM-10 (HIV-infected).

### 3.2.7 Quantification and Statistical Analysis

Statistical details are given in the figure legends. All statistical analyses were performed using GraphPad Prism software versions 9. P-values $\leq 0.05$ were considered statistically significant. A Student's two-tailed t-test was used for two-way column analyses. ANOVA tests

were used for multiple comparisons. P-values are denoted in figure panels. Data are presented as means with error bars indicating standard error of the mean (SEM) unless otherwise stated.

# 4 Results

## 4.1 Development of an Experimental Workflow for Expression Profiling of HIV-infected Cells

The overall objective of this work was to identify expression signatures and biomarkers of latent HIV infections. In general, a thorough characterization of the latent HIV reservoir is hampered by two crucial, biological obstacles. Firstly, latently-infected cells are extremely infrequent - it was estimated that approximately only one in a million CD4+ T cells harbors latent provirus in the blood of ART-treated individuals[64] - making their isolation and investigation extremely challenging. Secondly, HIV latently-infected cells, by definition, do not express viral genes and are virtually indistinguishable from their healthy counterparts. This fact often renders an unequivocal identification of latently-infected cells difficult or even impossible[181].

In order to circumvent these limitations, I sought to employ an HIV infection model that allows for identification and isolation of latently- and productively-infected cells, as well as uninfected bystander cells[172]. The model involved infection of blood-derived primary CD4+T cells from healthy donors with a single round, recombinant HIV dual-reporter virus called HIV Duo-Fluo II ($HIV_{DFII}$).

**Generation of an improved dual reporter virus.** The deployed dual-color reporter virus $HIV_{DFII}$ encodes for two separate fluorescent markers (Figure 12). In this construct, the LTR-driven enhanced green fluorescent protein (eGFP) in place of the *nef* gene reports transcriptional activity of the integrated provirus and thus represents productive infection. The second, spectrally distinct reporter mKusabira-Orange2 (mKO2) is under the control of an EF1α

promoter. The EF1α promoter and mKO2 were inserted as an independent transcriptional cassette between eGFP and the 3'LTR. Thus, mKO2 is constitutively expressed once the virus is integrated and allows for the detection of infected cells independent of viral LTR activity, including latent infection.

Here, $HIV_{DFII}$ was adapted from the previous dual-color HIV reporter version HIV Duo-Fluo I ($HIV_{DFI}$)[83,172]. By molecular cloning, I exchanged the latent reporter mCherry in $HIV_{DFI}$ with the brighter fluorescent protein mKO2 to improve detection of latently-infected cells (Table 1).

**Table 1: Attribute comparison of fluorescent proteins mCherry and mKO2[182].** $\lambda_{ex}$ = Excitation maximum, $\lambda_{em}$ = Emission maximum, EC = Extinction coefficient, QY = Quantum Yield.

| Name | $\lambda_{ex}$ | $\lambda_{em}$ | Stokes | EC | QY | Brightness | pKa | Aggregation | Maturation | Lifetime | kDa |
|---|---|---|---|---|---|---|---|---|---|---|---|
| mCherry | 587 | 610 | 23 | 72,000 | 0.22 | 15.84 | 4.5 | monomeric | 15.0 | 1.4 | 26.72 |
| mKO2 | 551 | 565 | 14 | 63,800 | 0.62 | 39.56 | 5.5 | monomeric | 108.0 | N/A | 24.46 |

Of note, $HIV_{DFII}$ is replication-deficient due to a mutated *env* gene, limiting the viral replication cycle to a single round infection. This prevents not just spreading viral infection, but also envelope-associated cell toxicity[183] and eliminates the necessity of antiretroviral drugs in cell culture systems. Replication-competent viruses would otherwise, in absence of ART, quickly overwhelm cultures with continuous productive infections, leading to strong cytopathic effects and a rapid decline of CD4+ T cell numbers.

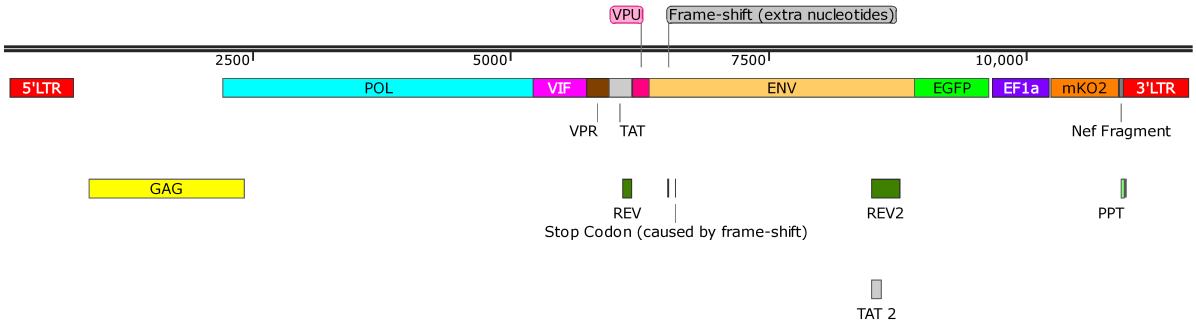


**Figure 12: Genomic organization of the dual-color reporter virus $HIV_{DFII}$.** The virus harbors a non-sense mutation in the ORF of *env*, limiting infections to a single round. eGFP replaced the *nef* gene and is under the

control of the viral LTR. An independent transcription unit was inserted downstream, comprising an EF1α promoter that drives the expression of mKO2 and that is constitutively active upon viral integration into the host's genome. Cells expressing eGFP alone or eGFP and mKO2 are considered productively-infected; cells expressing mKO2 alone are considered latently-infected; cells lacking the expression of either reporter are considered uninfected.

A critical aspect to consider in HIV persistence studies is the activation state of infected cells. Activated CD4+ T cells are highly susceptible for HIV infection while resting or naïve CD4+ T cells are not, or only marginally permissive to HIV as they impede viral infection and replication at several steps of the viral life cycle[184]. However, HIV replication is tightly linked with the cellular activation state and infections in activated cells are heavily skewed towards active viral replication. The latent reservoir in contrast is generally believed to predominantly reside in resting CD4+ T cells[185]. Nevertheless, it has been recently demonstrated that latency can still be established early after initial infection, even in fully stimulated CD4+ T cells[83,173]. Noteworthily, whether HIV reservoirs *in vivo* are established in activated cells prior to their transition to quiescence or forthright in resting CD4+ T cells is still under debate[186].

**Activation of CD4+T cells *in vitro* dramatically increases the frequency of $HIV_{DFII}$ infection.** I performed a pilot experiment to identify experimental conditions that permit maximal frequencies of latently-infected cells. To this aim, blood derived CD4+ T cells were either activated *in vitro* through T cell receptor (TCR) stimulation using αCD3/αCD28 beads or left unstimulated prior to $HIV_{DFII}$ infection. Then, cells were analyzed by flow cytometry to assess T cell activation and infection levels. Expectedly, αCD3/αCD28 stimulation led to a dramatic increase in cells expressing activation markers CD69 and/or CD25 (Figure 13A and B), and an almost 4-fold increase of $HIV_{DFII}$ infected CD4+ T cells compared to unstimulated CD4+ T cells (Figure 13C). Unfortunately, infection levels in resting CD4+T cells were so low that an analysis, let alone isolation of reasonable numbers of latently-infected cells, seemed

infeasible. Therefore, I performed *in vitro* stimulation prior to infection for the majority of my subsequent experiments.

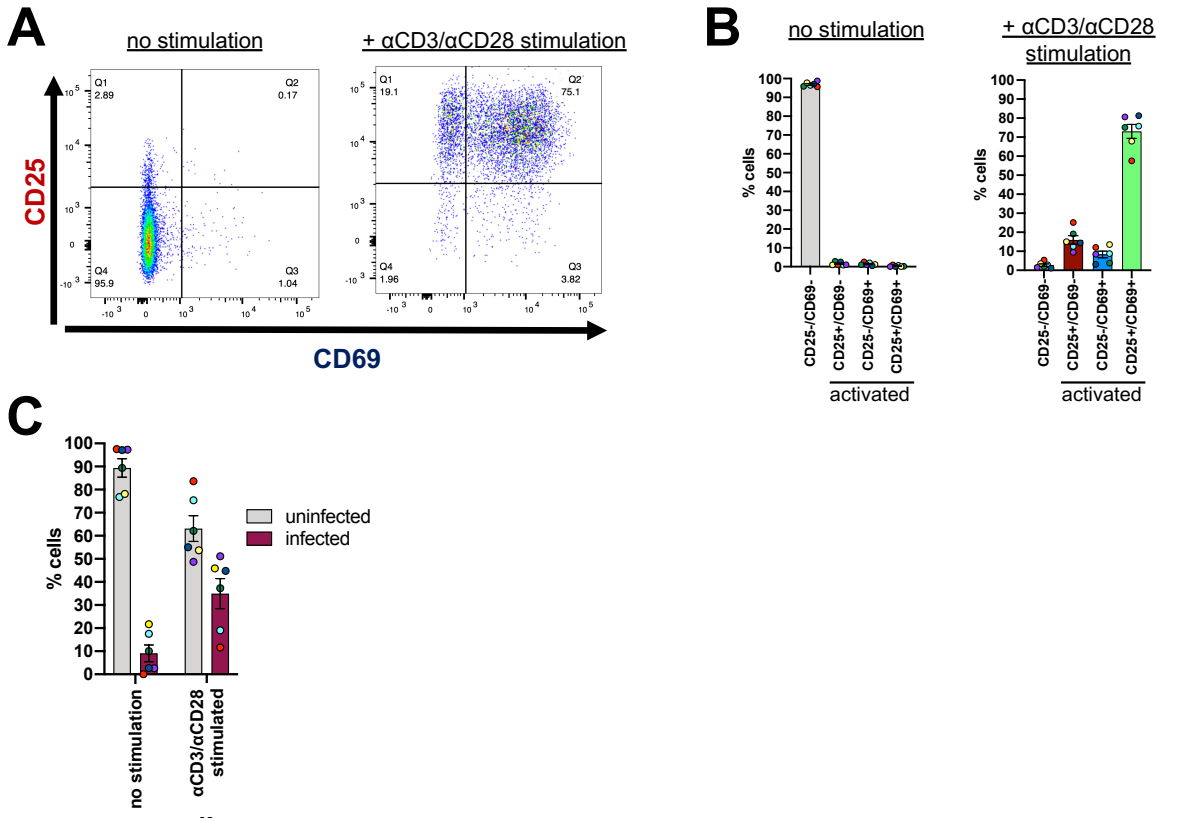


**Figure 13: Activation of primary CD4+ T cells *in vitro* profoundly affects $HIV_{DFII}$ infection.** The frequency of live, single, activated CD4+ T cells was determined based on activation markers CD69 (early activation) and CD25 (late activation). Cells were either left untreated or stimulated with αCD3/αCD28 beads for three days and subsequently infected with $HIV_{DFII}$. $1x10^6$ cells were then stained with anti-CD25 and anti-CD69 fluorescent antibodies to measure surface expression using flow cytometry. (A) Shown are representative flow plots from one donor for CD25/CD69 surface expression in unstimulated and αCD3/αCD28 stimulated cells before $HIV_{DFII}$ infection. (B) The frequency of CD25/CD69 expressing cells was quantified three days post stimulation for 6 donors. (C) Data represent the frequency of $HIV_{DFII}$-infected cells left untreated or stimulated with αCD3/αCD28 beads measured for 6 donors four days after $HIV_{DFII}$ infection. Colors indicate each donor. Error bars show standard error of the mean (SEM).

## 4.2 Expression Profiling of $HIV_{DFII}$-infected Cells Using NanoString

In the course of this work, I established and optimized a workflow for cell processing, infection and isolation, as well as downstream gene expression profiling as depicted in Figure 14. The ultimate goal of this experiment was to thoroughly characterize HIV latently-infected,

primary CD4+ T cells and to identify cellular factors that distinguish them from uninfected and productively-infected cells. To this aim, blood-derived primary CD4+ T cells were purified from six healthy donors, stimulated with αCD3/αCD28 beads, and infected with $HIV_{DFII}$. Cultures were maintained for 4 days to allow for completion of viral integration and replication, and then subjected to FACS in order to separate latently- and productively-infected, as well as uninfected cells. Finally, sorted samples were characterized using the NanoString nCounter platform enabling multiplexed detection of predefined 770 mRNA and 30 protein targets. For each donor control samples were collected, which comprised untreated cells (no exposure to αCD3/αCD28 stimulations beads and $HIV_{DFII}$ infection), cells infected with $HIV_{DFII}$ only (no αCD3/αCD28 stimulation), and cells stimulated with αCD3/αCD28 beads only (no $HIV_{DFII}$ infection).

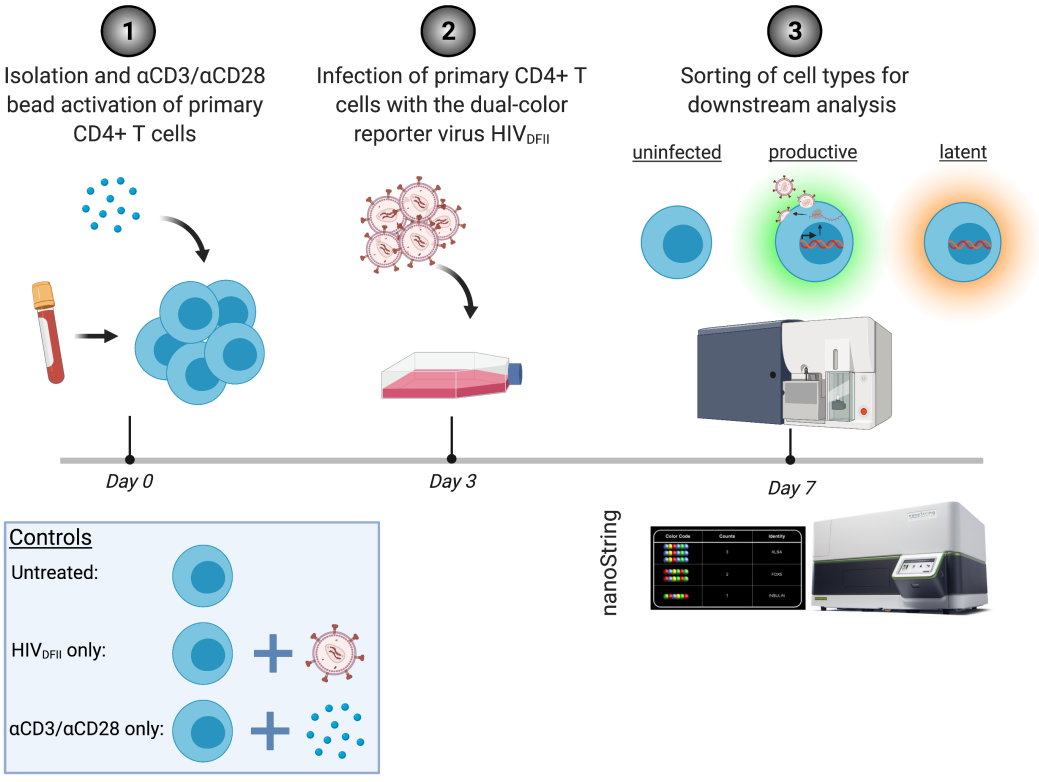


**Figure 14: Experimental workflow of cell processing, infection and, purification for downstream characterization using nanoString.** (1) Isolation of blood-derived primary CD4+ T cells from healthy donors and

subsequent stimulation with αCD3/αCD28 beads were performed on the same day. (2) Cells were spinoculated with $HIV_{DFII}$ for 2h at 37°C three days post bead stimulation. (3) Cells were cultured for 4 days in the presence of beads and $HIV_{DFII}$ and then sorted based on their fluorescence signal using FACS. Untreated cells (no exposure to αCD3/αCD28 stimulation beads and $HIV_{DFII}$), cells infected with $HIV_{DFII}$ only (no αCD3/αCD28 bead stimulation), and cells stimulated with αCD3/αCD28 beads only (no $HIV_{DFII}$ infection) were collected for each donor and served as control samples.

### 4.2.1 Sorting of $HIV_{DFII}$-infected Cells

**Latently infected cells can be sorted despite low frequency in primary cell samples.** FACS allows for simultaneous sample acquisition and single cell sorting. Here, I assessed the frequency of uninfected, productively- and latently-infected cells, while collecting different cell samples for subsequent NanoString analysis. As expected, a low frequency of latently-infected cells (mKO2+ events) was found for all 6 donors with an average of less than 0.5% (Figure 15A and B). In contrast, uninfected (GFP-/mKO2- events) and productively-infected cells (GFP+ and GFP+/mKO2+ events) could be rapidly collected in large numbers, with frequencies of up to 60% and 40%, respectively.

**Productively-infected cells do not show double positivity.** Of note, the majority of GFP+ cells did not show additional mKO2 signal (Figure 15A). Taking into account that the latter fluorophore is controlled by a constitutive promoter it stands to reason that productively-infected cells would exhibit positivity for both fluorophores. However, this phenomenon has been reported before[187] and it is assumed that transcription from the viral LTR during productive infection interferes with the activity of the EF1a promoter and thus diminishes expression of the latent reporter mKO2. Whether this transcriptional interference is due to steric hindrance or competition for transcription factors between promoters remains to be resolved.

**All sorted samples show significant enrichment of the respective cell populations.** In order to assess the purity of all sorted samples, small aliquots were subjected to another round of flow cytometry analysis post processing (Figure 15C). Sorted uninfected samples showed the highest purity across all donors and comprised close to 100% double negative cells, while sorted productively-infected samples reached a purity of more than 90% in 4 out of 6 donors. Sorted latently-infected samples consisted of about 60% mKO2 positive cells, which showed a clear enrichment of latently-infected cells in these samples, albeit with a notably lower purity than other sorted specimens.

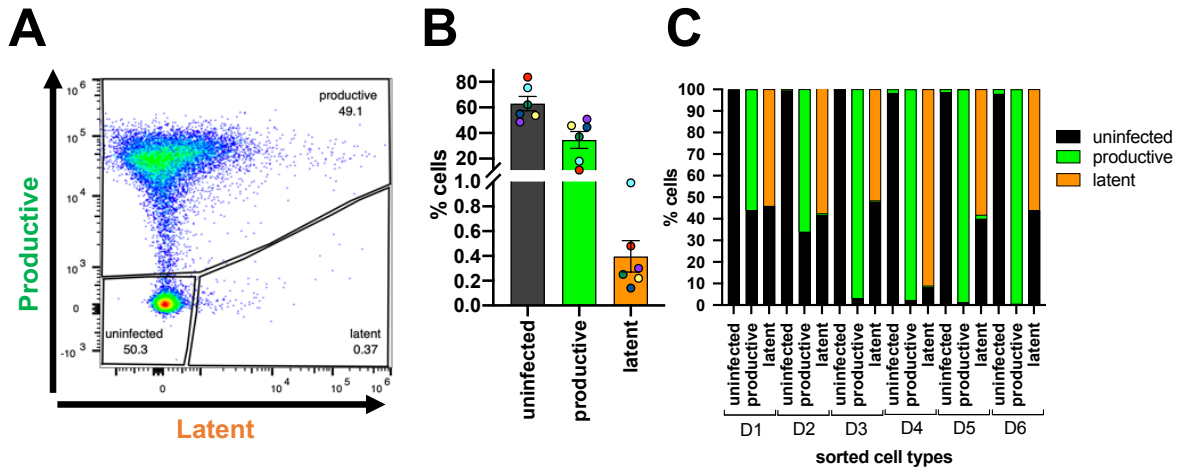


**Figure 15: $HIV_{DFII}$ infection and sorting of primary CD4+T cells enables enrichment of latently-infected cells.** (A) Live, single cells were sorted based on their reporter expression using FACS 4 days post $HIV_{DFII}$ infection. Gating of sample types is demonstrated in the representative flow cytometry plot for one donor. Events lacking the expression of both reporters were considered uninfected; eGFP+ and eGFP+/mKO2+ events were considered productively-infected; mKO2+ events were considered latently-infected. (B) Bar graph represents the distribution of infected cells of all six donors. (C) Data show the percentage of cells composing the sorted samples for each donor normalized to the total gated events. Colors indicate the same donor. Error bars show SEM.

### 4.2.2 NanoString Analysis

All previously collected samples (6 donors with 6 sample types each) were subjected to NanoString analysis, followed by data processing and statistical evaluation. Two samples,

$HIV_{DFII}$ only of donor 2 and 5 (D2 and D5), failed the proprietary quality controls and were removed from following analyses.

**Response to TCR stimulation dominates expression patterns across samples and donors.** First, a principal component analysis (PCA) and heatmap of the normalized data were generated to provide a general overview of the results (Figure 16). PCA is an unsupervised method to reveal and display the similarity between samples based on a distance matrix. PCA plots thereby visualize the overall effect of experimental covariates and batch effects (Figure 16A). Here, each sample was labeled according to its 'sample type' and 'donor ID'. Considering principal component 1 (PC1), which captures the highest level of variance in the data, samples clearly clustered based on *in vitro* activation. Precisely, all untreated and $HIV_{DFII}$ only samples formed one cluster and were distant to the other samples, which had been exposed to αCD3/αCD28 beads. Thus, the response of CD4+ T cells to TCR stimulation determined the greatest variance in expression signatures between samples. This observation was reflected as well in the hierarchical clustering of normalized data (Figure 16B), revealing a strong association between expression signatures and T cell responses to *in vitro* stimulation.

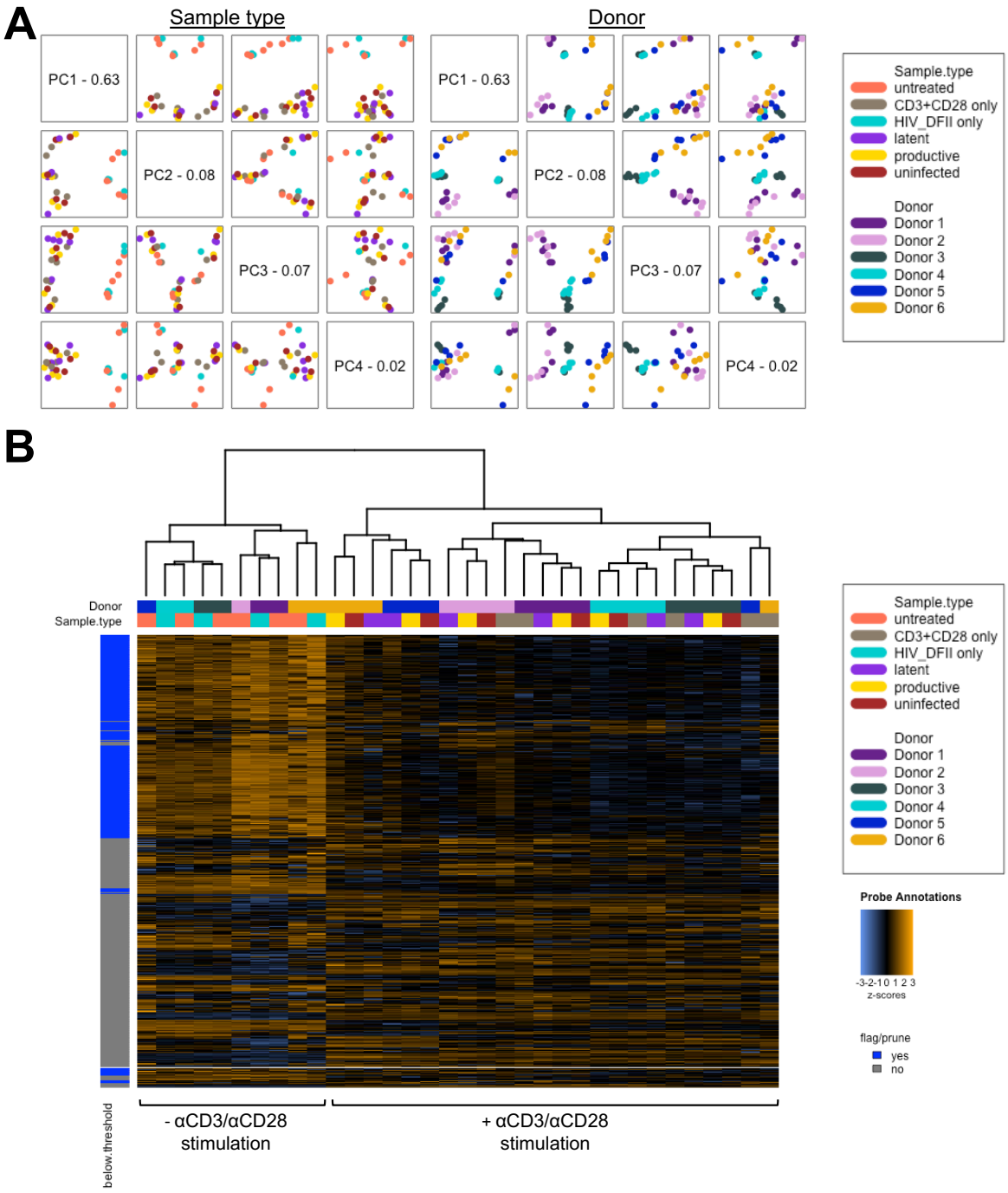


**Figure 16: General overview of NanoString data reveals sample clusters connected to *in vitro* activation.** (A) Displayed are principal component analyses, which transform and display high-dimensional gene expression data on a 2D plane based on a distance matrix. Each dot represents one sample and is colored by the attributes 'sample type' or 'donor' (color legend on the right). Principal component 1 (PC1) captures the highest level of variance, followed by PC2, PC3 and PC4. Each PC is plotted twice vs the other (image is diagonally mirrored). The diagonal boxes denote the PC name and its contribution to the total variance in percent. Plots in the same row show this specific PC on their y-axis and plots in the same column display this PC on their x-axis. Samples with similar features are clustered together while differing samples are further apart. (B) Heatmap visualizing normalized gene expression data. Each row shows counts of a single probe (target) and each column represents an individual sample. Colored horizontal bars along the top of the heatmap identify assigned sample attributes (see color legend). The

vertical blue bar on the left indicates probes whose counts have fallen below threshold in all samples in blue. These will be trimmed out of further analyses. The data are plotted by z-score and scaled with relation to the average probe performance across all samples, giving all genes equal mean and variance. Hierarchical clustering was used to generate dendrograms. Distance between samples reflects their similarity to each other.

**Canonical markers do not correlate with $HIV_{DFII}$ infection state.** Since the response to TCR stimulation was discovered to dominate cellular expression patterns, I further investigated if there was a correlation between the response to TCR stimulation and $HIV_{DFII}$ infection – in other words, if the fate of a cell to be latently-infected was mainly determined by its activation state.

Initially, the normalized expression levels of generic T cell surfaces markers CD45, CD45RO, and CD4 were compared between samples, with the main focus on latent infection (Figure 17A). CD45, a protein tyrosine phosphatase, receptor type C, exists in various isoforms, which are expressed in specific cell types at specific differentiation stages[188]. Naïve T cells typically express CD45RA, while activated and memory T cells are marked by CD45RO surface expression. Comparing the expression of CD45 in latent to other samples did not reveal significant differences. In contrast, CD45RO was significantly upregulated in latently-infected cells compared to non-activated, but not compared to other stimulated samples, reflecting the expected cellular response to *in vitro* stimulation. CD4 expression was similar between all samples except for productively-infected cells (Figure 17A), which exhibited considerably lower CD4 surface expression compared to almost all other samples (p-values not shown). Since HIV is known to downregulate CD4 expression through regulatory activity of multiple viral proteins[28,189–193], this result was predicted and confirmed ongoing viral gene expression in productively-infected samples.

**Definition of a panel-specific set of activation markers.** To exploit the high dimensional nature of the NanoString analysis and to further explore T cell activation as a causative factor for HIV infection fate, I defined an expression signature for TCR stimulation based on the predefined NanoString panel targets. To this aim, I performed a differential gene expression analysis that compared normalized target expression in αCD3/αCD28 only samples vs untreated samples (Figure 17B) and selected the 6 protein hits exhibiting the most extreme $\log_2$ fold changes and highest statistically significances: CD25, OX40, PD1, GITR, ICOS, and CD127. All of these surface proteins were significantly upregulated upon αCD3/αCD28 stimulation, except for CD127, which was significantly downregulated.

**Panel-specific activation markers do not correlate with HIV latency.** The 6 hits were defined as activation markers and examined in context of $HIV_{DFII}$ infection, specifically latent infection, by comparing their normalized linear count between all samples (Figure 17C). Expectedly, expression of the 6 activation markers differed significantly between latently-infected and both non-activated sample types. In contrast, comparing expression levels of the activation markers between latently-infected and other *in vitro* activated sample types did not reveal significant differences, with one exception: ICOS.

No additional correlation was discovered between the expression of activation markers and latently-infected cells suggesting that other factors than T cell activation are involved in the establishment and maintenance of latent infection.

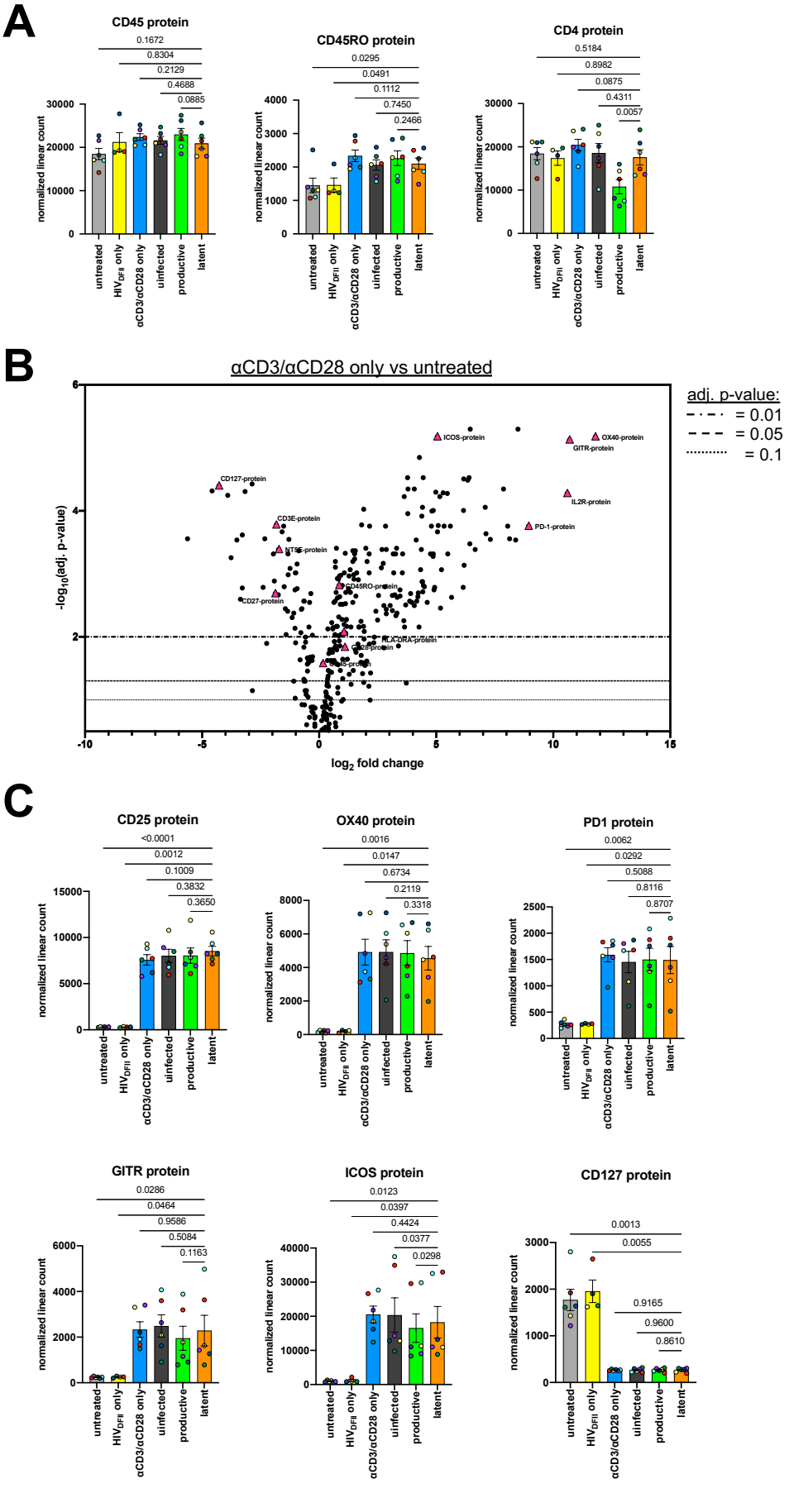
A
CD45 protein
0.1672
0.8304
0.2129
0.4688
0.0885
CD45RO protein
0.0295
0.0491
0.1112
0.7450
0.2466
CD4 protein
0.5184
0.8982
0.0875
0.4311
0.0057
normalized linear count
untreated
HIVDFII only
αCD3/αCD28 only
uinfected
productive
latent
B
αCD3/αCD28 only vs untreated
adj. p-value:
= 0.01
= 0.05
= 0.1
ICOS-protein
OX40-protein
GITR-protein
CD127-protein
IL2R-protein
CD3E-protein
PD-1-protein
CD45RO-protein
CD27-protein
-log10(adj. p-value)
log2 fold change
C
CD25 protein
<0.0001
0.0012
0.1009
0.3832
0.3650
OX40 protein
0.0016
0.0147
0.6734
0.2119
0.3318
PD1 protein
0.0062
0.0292
0.5088
0.8116
0.8707
GITR protein
0.0286
0.0464
0.9586
0.5084
0.1163
ICOS protein
0.0123
0.0397
0.4424
0.0377
0.0298
CD127 protein
0.0013
0.0055
0.9165
0.9600
0.8610

**Figure 17: Latently-infected cells are not characterized by a different T cell activation state.** (A) Bar graphs represent the average normalized linear expression levels of generic T cell markers CD45, CD45RO and CD4 in all samples for all 6 donors. (B) The volcano plot visualizes the differential expression analysis, comparing normalized target expression in αCD3/αCD28 only samples vs untreated samples of all six donors. Each data point in the scatter plot represents one target species. Protein targets are highlighted as pink triangles. The $\log_2$ fold change of each target is displayed on the x-axis and the $-\log_{10}$ of its adjusted (adj.) p-value (using the Benjamini-Hochberg method) on the y-axis. Horizontal lines indicate adj. p-value thresholds. (C) Bar graphs show the average normalized linear expression levels of defined T cell activation markers for all 6 donors. Colors dots indicate individual donors. Error bars show SEM.

### 4.2.3 Focused NanoString Analysis of Sorted Samples

Next, I explored what cellular factors determined the fate of cells exposed to $HIV_{DFII}$. In particular, I asked the question whether I can identify gene expression patterns that correlate with the respective infection state of the three sorted cell populations. Do latently-infected cells show transcriptional features that clearly distinguish them from productively-infected or uninfected cells? Importantly, all sorted samples had been stimulated with αCD3/αCD28 beads and exposed to virus, so that gene expression differences should directly reflect HIV-related cellular properties.

**The donor effect dominates expression signatures within virus-exposed, sorted samples.** This analysis followed the same steps as describe above. First, all considered samples were subjected to PCA, which revealed a distinct clustering of samples based on their donor origin rather than a correlation with $HIV_{DFII}$ infection (Figure 18A). This phenomenon was further highlighted in a histogram that bins p-values according to their relative abundance with respect to a specific confounding variable. A striking association was found between the frequency of significant p-values and the attribute 'donor', meaning that almost all genes were differentially expressed between samples from different donors, whereas only a small fraction of genes was found to be distinctly different between samples of the same donor (Figure 18B).

This observation was also reflected in heatmaps and the associated dendrograms, which were based on normalized data rather than raw counts and therefore accounted for generic batch effects and other experimental confounders (Figure 18C). In summary, global gene expression differences were greater between samples obtained from different donors than differences between the $HIV_{DFII}$ infection state. Since the purpose of this work was to decipher expression signatures of $HIV_{DFII}$ infection rather than differences between donors, the attribute 'donor' was henceforward defined as an additional batch effect ('donor effect'). Accordingly, target expression levels were adjusted by defining the 'donor' attribute as confounding variable allowing for data interpretation of biological covariates.

**Latently-infected cells exhibit unique features.** Importantly, I observed that within each donor expression patterns between uninfected and productively-infected cells clustered more closely while latently-infected cells remained distinct (Figure 18C, red arrows). This finding highlighted that overall gene expression patterns significantly differed between samples. In fact, NanoString analysis revealed specific transcripts and proteins for latently-infected cells, suggesting that latently-infected cells were characterized by factors besides the absence of viral protein production, which is also a feature of uninfected cells.

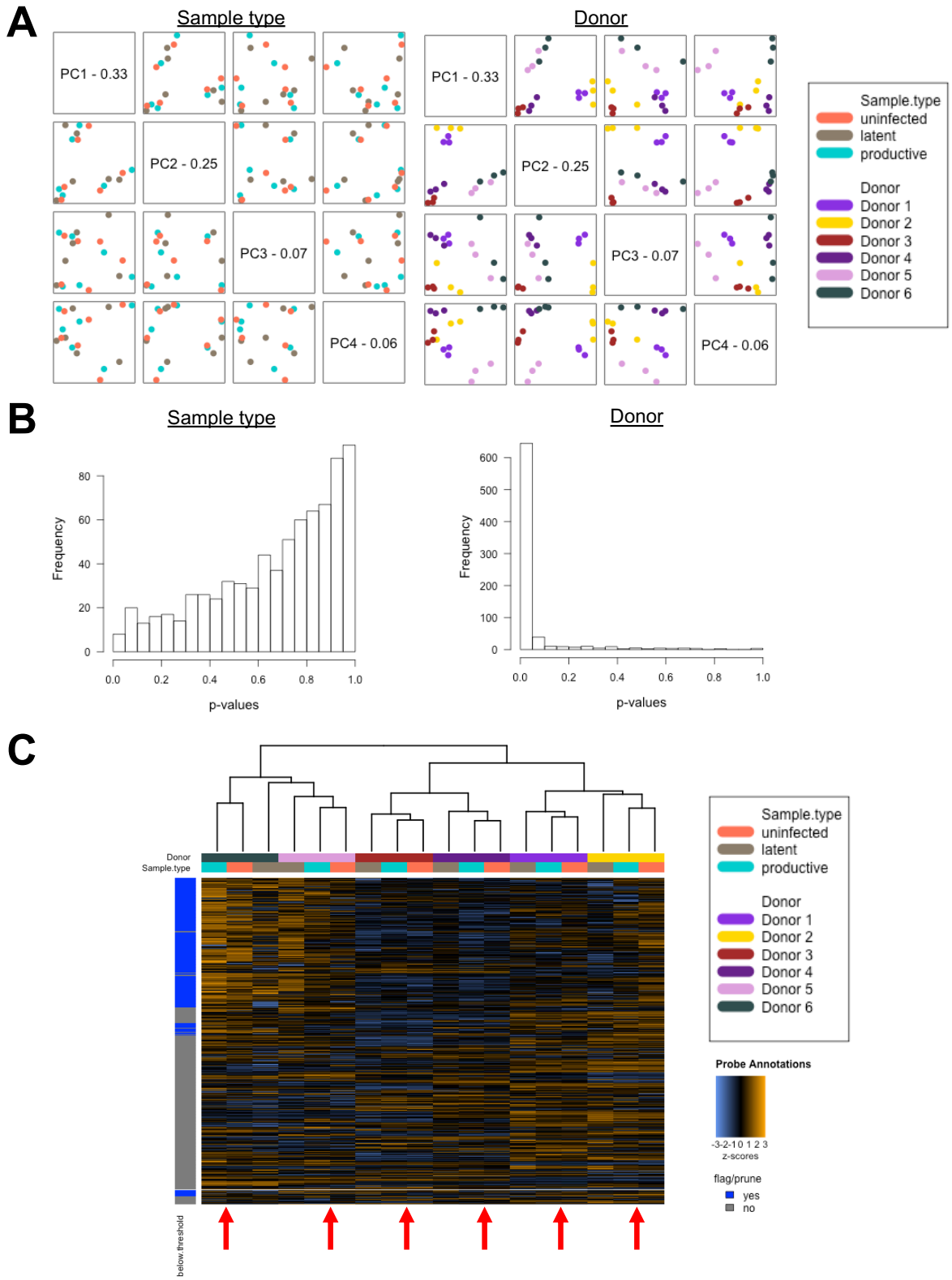


**Figure 18: Sorted samples reveal a donor-dependent clustering of gene expression profiles and unique latency signatures.** (A) PCA plots, as described in Figure 16, show the first 4 PCs of virus-exposed, sorted samples from six donors. (B) Histograms displaying the frequency of p-values associated with assigned sample attributes 'sample type' or 'donor'. (C) Heatmap, as described in Figure 16, visualizes normalized data of virus-exposed, sorted samples. Red arrows highlight clustering of uninfected and productively-infected samples within each donor.

**Latently-infected cells show deregulation in multiple signaling pathways**. To uncover discrete features of latently-infected cells, I performed comprehensive analyses comparing target expression and signaling pathways between latently-, productively- and uninfected cells (Figure 19). Comparing uninfected vs latently-infected cells with an adj. p-value cutoff < 0.1 revealed 16 targets that were differentially expressed (Figure 19A). Among these were two protein targets: HLA-DRA and NT5E protein. HLA-DRA protein was downregulated and NT5E protein upregulated in latent cells. Differential expression analysis between productively- and latently-infected cells with an adj. p-value cutoff < 0.1 resulted in 36 significant hits (Figure 19B). These included CD4 protein and also NT5E protein. CD4 protein was significantly downregulated in productively-infected cells as observed before (Figure 17A) and NT5E protein was upregulated in latently-infected cells. Based on the differential expression analyses, changes in signaling pathways were analyzed by grouping targets into specific gene sets. To this aim, undirected and directed global significance scores were measured for defined pathways (Figure 19C and D). The undirected global significant score represents the significance of differential expression (Figure 19C) while the directed global significance score demonstrates the extent to which the regulation of given pathway has changed (Figure 19D). 'Antigen Processing', 'Adhesion', 'Pathogen Defense', and 'Interleukins' pathways were among the most significantly changed pathways in latently-infected cells compared to both other samples. 'Interleukins' and 'Pathogen Defense' pathways were significantly upregulated while 'Antigen Processing' was reduced in latently-infected cells. 'Adhesion' was decreased in latent samples compared to productively-infected cells but increased in latently-infected cells compared to uninfected cells.

**27 cellular targets distinguish latently-infected cells from uninfected and productively-infected cells.** In the next step, I examined which specific genes showed differential expression between latently-infected cells and both, productively- and uninfected cells. To identify such factors, individual, differential expression analyses were overlaid using a p-value cutoff at $p < 0.05$, revealing 27 targets that were uniquely changed in latent infection (Figure 19E). Among the hits was one protein target, NT5E (CD73) protein, while all others were mRNA targets (Table 2). The list further included three mRNAs encoding for transcription factors, 6 that encoded for cytokines and 11 encoding for surface proteins. The latter were especially interesting in context of latent infection, since surface proteins expressed on latently-infected cells could be exploited easily as biomarker and therapeutic target.

The relationship between targets specific for latent infection was then investigated by utilizing the open-source software Cytoscape. The target list was uploaded onto the platform and interfaced with the STRING database to generate a detailed protein-protein interaction network (Figure 19F). The chemotactic factor IL8 (or CXCL8) was found to have the most immediate connections (17 first neighbors), followed by the transcription factor STAT1 (15 first neighbors) and the cytokine CSF2 (15 first neighbors) suggesting that these proteins may be key elements of the observed gene expression phenotypes.

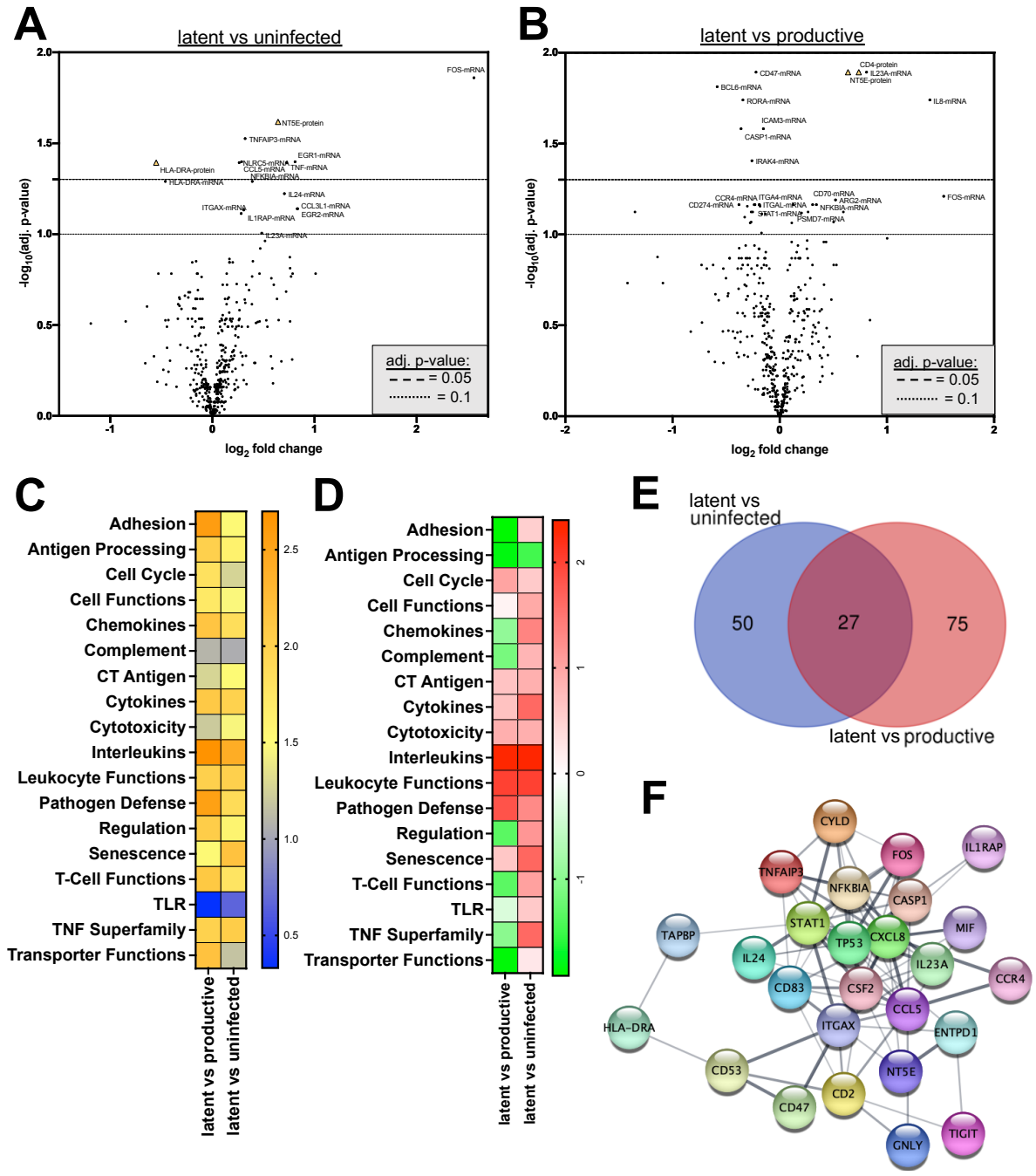


**Figure 19: Latently-infected cells possess unique expression signatures.** Volcano plots, as described in Figure 17, depict differential mRNA and protein target expression between latent and (A) uninfected or (B) productively-infected cells. The top 20 hits in each comparison are labeled. Heatmaps showing (C) undirected and (D) directed global significance scores for signaling pathways based on differential gene expression analysis. (E) Venn diagram illustrating overlapping hits from the differential expression analyses 'latent vs uninfected' and 'latent vs productive' using a p-value cutoff $p < 0.05$. (F) A protein-protein interaction network of targets uniquely changed in latently-infected cells was generated in Cytoscape 3.8.2. Applied was the STRING database for Homo sapiens with a default confidence score of 0.4. Thickness of lines between nodes depicts confidence score with a thicker line representing a higher score. HLA-DRB3 was not recognized by the software and thus excluded from the interaction network.

**Table 2: Targets identified in the differential expression analyses comparing latently-infected cells to both other sorted samples with a p-value cutoff at p < 0.05.** Targets are sorted by p-value of latent vs productive comparison.

| | latent vs uninfected | | latent vs productive | |
|---|---|---|---|---|
| Target | log2 fold change | p-value | log2 fold change | p-value |
| IL23A-mRNA | 0.483 | 0.00365 | 0.81 | 0.0000954 |
| CD47-mRNA | -0.106 | 0.0151 | -0.221 | 0.000114 |
| NT5E-protein | 0.644 | 0.000111 | 0.638 | 0.000119 |
| IL8-mRNA | 0.785 | 0.0114 | 1.4 | 0.000295 |
| CASP1-mRNA | -0.166 | 0.0434 | -0.361 | 0.000519 |
| FOS-mRNA | 2.56 | 3.18E-05 | 1.53 | 1.57E-03 |
| CCR4-mRNA | -0.15 | 0.032 | -0.237 | 0.0028 |
| NFKBIA-mRNA | 0.39 | 0.00118 | 0.342 | 0.00281 |
| STAT1-mRNA | -0.12 | 0.0326 | -0.19 | 0.00286 |
| CD53-mRNA | -0.145 | 0.0132 | -0.184 | 0.00345 |
| ITGAX-mRNA | 0.282 | 0.00267 | 0.263 | 0.00408 |
| IL24-mRNA | 0.705 | 0.00152 | 0.592 | 0.00466 |
| TNFAIP3-mRNA | 0.321 | 0.000206 | 0.203 | 0.00492 |
| TAPBP-mRNA | -0.16 | 0.00714 | -0.168 | 0.00534 |
| GNLY-mRNA | -0.303 | 0.0441 | 0.431 | 0.0104 |
| HLA-DRA-mRNA | -0.46 | 0.00119 | -0.318 | 0.0114 |
| CCL5-mRNA | 0.286 | 0.000383 | 0.169 | 0.0114 |
| CD2-mRNA | 0.238 | 0.0174 | 0.252 | 0.0133 |
| TP53-mRNA | -0.151 | 0.0134 | -0.143 | 0.0174 |
| HLA-DRB3-mRNA | -0.325 | 0.0273 | -0.356 | 0.018 |
| ENTPD1-mRNA | -0.529 | 0.0109 | -0.467 | 0.0209 |
| CSF2-mRNA | 0.577 | 0.0157 | 0.528 | 0.0241 |
| MIF-mRNA | 0.101 | 0.0189 | 0.0942 | 0.0258 |
| CD83-mRNA | 0.33 | 0.0188 | 0.284 | 0.0361 |
| CYLD-mRNA | -0.165 | 0.032 | -0.156 | 0.0404 |
| TIGIT-mRNA | -0.335 | 0.0387 | -0.328 | 0.0424 |
| IL1RAP-mRNA | 0.308 | 0.00238 | 0.175 | 0.0451 |

### 4.2.4 Identification of Markers Specific for Latent Infection

My previous analyses specifically focused on populations of cells that were recently stimulated and exposed to virus. In ART-suppressed, otherwise healthy individuals however, the majority of CD4+ T cells is likely in a resting state and has not encountered HIV. Therefore, to emulate this *in vivo* situation, I now considered all acquired samples, including non-activated and non-virus exposed, in the downstream analysis.

**CD39 mRNA, IL8 mRNA, and CD73 protein expression levels correlate with latent infection.** Target expression in latently-infected cells was compared to all other sample types

using a p-value cutoff at $p < 0.05$. Of note, the number of targets meeting the p-value threshold was relatively low in differential expression analyses between latent infection and sorted, $HIV_{DFII}$-exposed samples (Table 3). In contrast, comparing latent infection to samples that were not exposed to $HIV_{DFII}$ yielded > 100 significantly changed targets (Table 3). This illustrated two things: first, already the exposure to $HIV_{DFII}$ alone heavily influenced expression signatures of cells; and second, while latently-infected cells exhibited distinct expression patterns, these signatures were very subtle.

**Table 3: Number of differentially expressed genes from pairwise-comparisons of latent cells to all other samples.** Differential target expression between samples was compared with a p-value cutoff at < 0.05.

| Sample type | Number of DE targets |
|---|---|
| **Uninfected** | 18 |
| **Productive** | 15 |
| **CD3/CD28 only** | 108 |
| **$HIV_{DFII}$ only** | 308 |
| **untreated** | 316 |

The individual differential expression analyses were graphically overlaid, and the overlap of specific hits was visualized with a Venn diagram (Figure 20A). Three hits were identified that were significantly changed in latent cells with respect to all other comparators: IL8 mRNA, CD39 mRNA and NT5E (CD73) protein. Strikingly, this result did not only include a key protein hit from my previous analyses (CD73), but also three genes, which were already known to interact with each other according to the STRING database (Figure 20B). The data showed that IL8 mRNA was significantly upregulated in latently-infected cells compared to all other samples (Figure 20C). CD39 mRNA was upregulated in latently-infected cells compared to non-activated samples and downregulated in latent cells compared to activated samples, while

CD73 protein results trended reversely. Expression levels of CD73 protein were lower in latent cells compared to non-activated samples but higher in latent cells compared to activated samples (Figure 20C).

Taken together, this comprehensive analysis revealed clear evidence for unique gene expression patterns in latently-infected cells. Importantly, the observed differential expression levels of IL8 mRNA, CD39 mRNA and CD73 protein could not only be leveraged as biomarkers for latent infection, but it may also suggest a common cellular pathway as underlying cause of their deregulation.

As CD73 occupied a central position in all previous analyses and was the only significant hit already detected at the protein level, subsequent experiments were focused specifically on this surface protein.

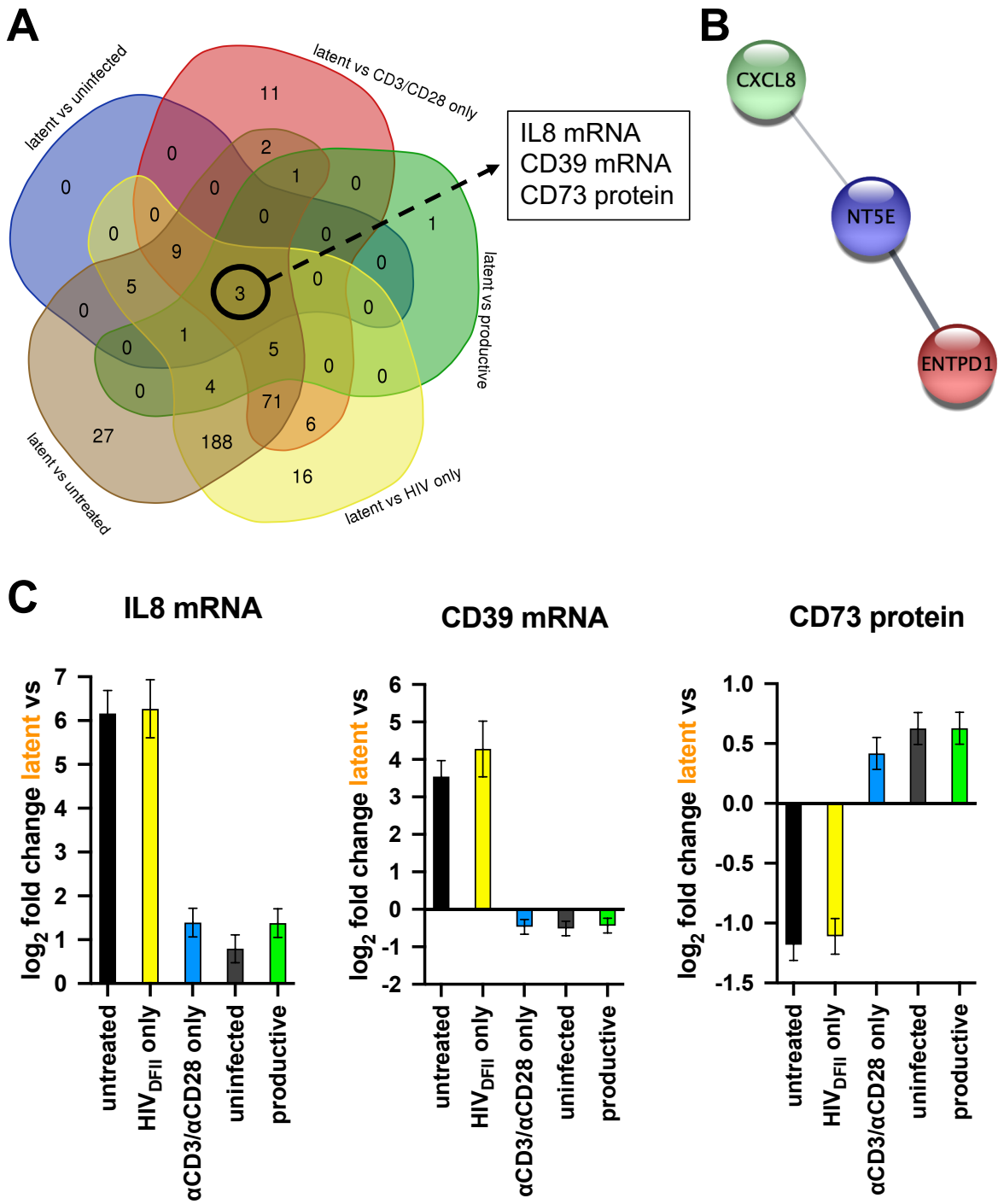


**Figure 20: IL8 mRNA, CD39 mRNA and CD73 protein are uniquely expressed by latently-infected cells.** (A) Venn diagram displaying differential expression hits from comparisons of latently-infected cells with all other samples using a p-value cutoff at $p < 0.05$. (B) The protein interaction network of the three hits IL8 (CXCL8), CD39 (ENTPD1), and CD73 (NT5E) was generated as described in Figure 19. (C) Bar graphs depict the $\log_2$ fold change of the three targets IL8 mRNA, CD39 mRNA, and CD73 protein between latent cells and all other samples. Error bars show standard deviation (SD).

## 4.3 Investigating the Relationship Between CD73 and HIV Latency

A large body of work has established that the ectonucleotidase CD73 contributes to adenosine production and signaling by converting AMP to adenosine. However, to better understand the relevance of CD73 in the context of HIV infections and particularly HIV persistence, I first investigated how the expression of CD73 itself is regulated. The CD73 promoter contains a multitude of binding motifs for different transcription factors including SP1, AP-2 and SMAD family proteins[194,195]. Interestingly, cAMP responsive elements were described as well[194] indicating a direct regulation of CD73 expression based on metabolite abundance. Furthermore, at least one hypoxia-response element (HRE) was identified in the promoter region[196] allowing for direct binding of hypoxia-inducible factors (HIFs). In this context, HIF-1α was demonstrated to control CD73 expression, with CD73 typically being increasingly expressed under hypoxic conditions[197]. Given my previous finding of a CD73-upregulation in latently-infected cells, I raised the hypothesis that hypoxia may be the underlying cause of both, increased CD73 expression and HIV latency.

***In vitro* induction of hypoxic responses.** In order to test my hypothesis, I applied the same HIV latency model as before, comprising *in vitro* activation and $HIV_{DFII}$ infection of primary, blood-derived CD4+T cells from healthy donors. In addition, however, I treated cells with dimethyloxalylglycine (DMOG) to mimic hypoxic conditions (Figure 21). In most mammalian cells, HIF-1α is constitutively expressed, but under normoxic conditions targeted for proteasomal degradation by prolyl hydroxylases (PHDs). The activity of PHDs is reduced upon oxygen deprivation, which in turn stabilizes and activates HIF-1α. Using a PHD inhibitor such as DMOG chemically inhibits PHD activity and thus leads to induction of hypoxic

responses even under normal oxygen levels in cell culture. Therefore, cells were treated with DMOG 24h before $HIV_{DFII}$ infection and were cultured under hypoxic conditions until sample collection. 0.5% DMSO treatment served as mock control. Expression levels of CD73 and $HIV_{DFII}$ infection state of mock- and DMOG-treated cells were measured using flow cytometry 4 days post virus exposure. Samples not exposed to $HIV_{DFII}$ served as control for infection.

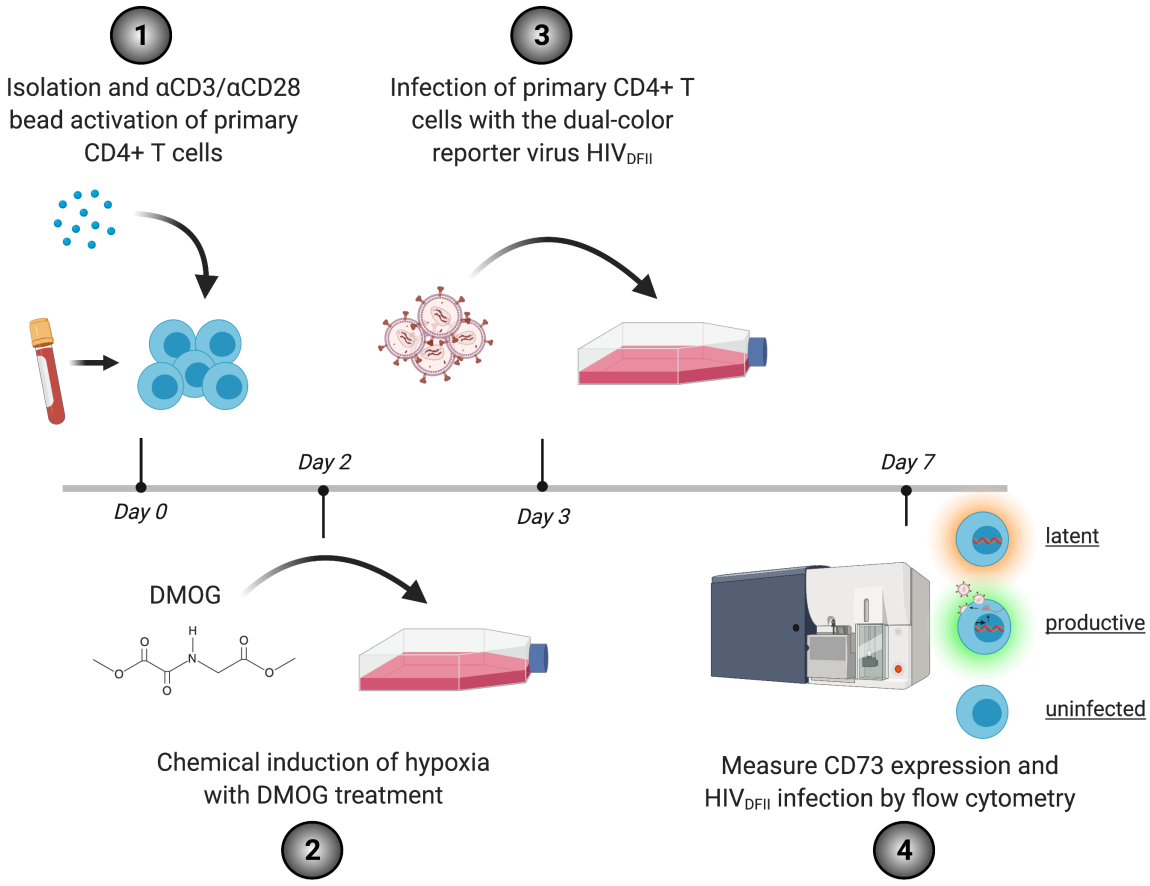


**Figure 21: Experimental workflow for $HIV_{DFII}$ infection under hypoxic conditions.** (1) Blood-derived primary CD4+ T cells were isolated from seven healthy donors and activated with αCD3/αCD28 beads on the same day. (2) 48h post activation, cells were treated with 500 µM DMOG to mimic hypoxic conditions or mock-treated with 0.5% DMSO. (3) Three days post activation and 24h post hypoxia induction, cells were spinoculated with $HIV_{DFII}$ for 2h at 37°C or left unexposed as control. (4) Cells were cultured for another 4 days under hypoxic conditions (or mock treatment) in the presence of beads and $HIV_{DFII}$. Expression of CD73 and the distribution of $HIV_{DFII}$-infected cells was measured using flow cytometry.

**Hypoxia enhanced CD73 expression and HIV latency.** DMOG treatment drastically affected CD73 expression in CD4+ T cells and led to a 2.5-fold increase of CD73+ cells compared to

mock-treated cells, independent of $HIV_{DFII}$ exposure (Figure 22A and B). More importantly, latent infection became significantly more abundant under hypoxic conditions with a 33.6% increase upon DMOG treatment (Figure 22C and D). In contrast, the distribution of uninfected or productively-infected cells did not alter significantly between culture conditions.

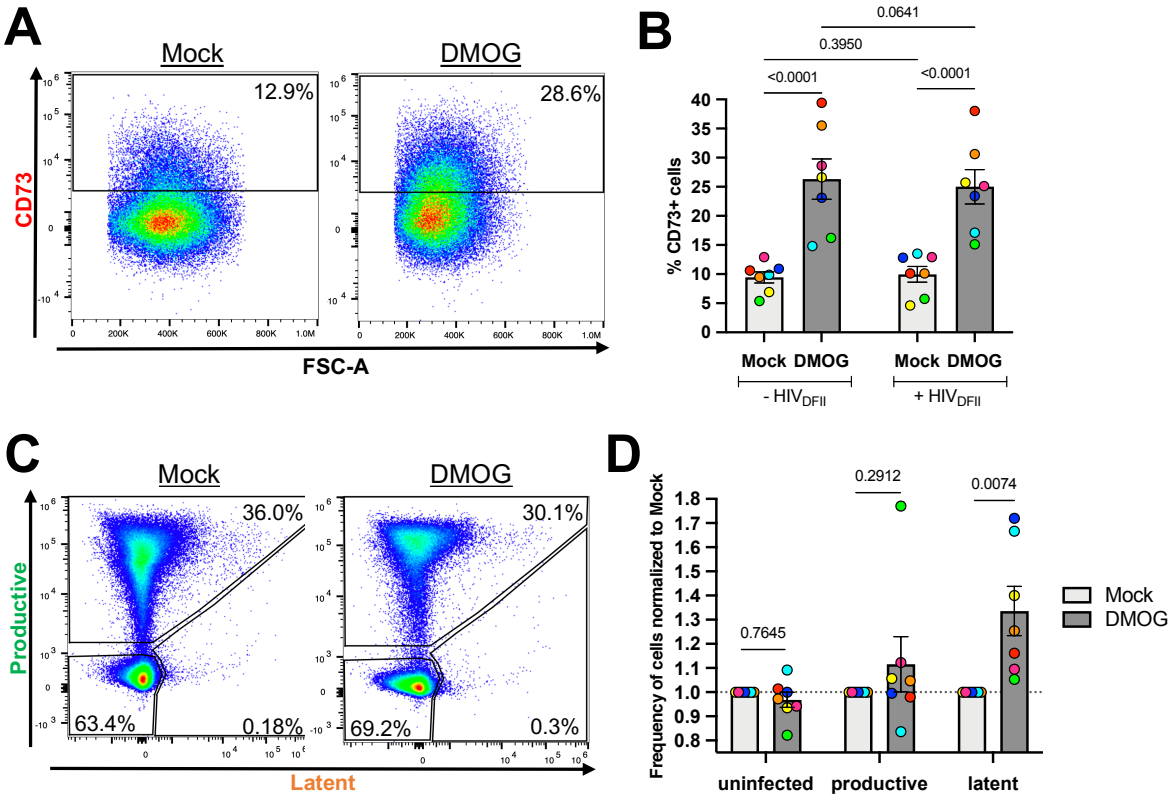


**Figure 22: Hypoxic conditions increase the frequency of CD4+ CD73+ T cells and facilitate latent infection.** CD73 expression levels in mock- or DMOG-treated and $HIV_{DFII}$-exposed or non-exposed primary CD4+ T cells were measured using flow cytometry 4 days post $HIV_{DFII}$ spinoculation. (A) Representative flow plots from one donor illustrate CD73 surface expression of live, single cells that were not exposed to $HIV_{DFII}$ upon mock or DMOG treatment. (B) The average frequency of CD73+ cells in respective culture conditions was determined in 7 donors in presence and absence of $HIV_{DFII}$ infection. (C) Representative flow plots from one donor showing $HIV_{DFII}$ infection profiles 4 days post $HIV_{DFII}$ exposure upon mock or DMOG treatment. (D) The frequency of DMOG-treated, $HIV_{DFII}$-infected cells was normalized to mock-treated $HIV_{DFII}$-infected cells within each donor to account for donor variability. Colored dots indicate results from individual donors. P-values were obtained by two-way ANOVA with Fisher's Least Significant Difference (LSD) test and are displayed within the diagram. A p-value of $p<0.05$ was considered significant. Error bars show SEM.

**Latent infections enrich for CD73+ cells.** I next examined CD73 expression within uninfected, productively- and latently-infected cells (Figure 23A) in the context of mock and DMOG

treatment (Figure 23B and C). In analogy to my previous NanoString analysis (Figure 20C), CD73+ cells were significantly more abundant among latently-infected cells compared to uninfected and productively-infected cells (see mock sample in Figure 23A). This was also reflected in CD73 MFIs, which indicated an overall increase of CD73 expression in latently-infected cells. The flow cytometry results thus confirmed my previous findings from bulk NanoString experiments at the single cell level.

**Enrichment of CD73+ cells in latent infection is reinforced upon hypoxia.** The flow cytometry data also showed that induction of hypoxic responses led to a general increase of CD73+ cells in uninfected, productively- and latently-infected cells. However, latent infection was further enriched for CD73+ cells with up to 60% (average ~40%) of latently-infected cells being CD73+ upon DMOG treatment (Figure 23B). This was again accompanied by a significantly higher mean CD73 surface expression in latently-infected cells (Figure 23C).

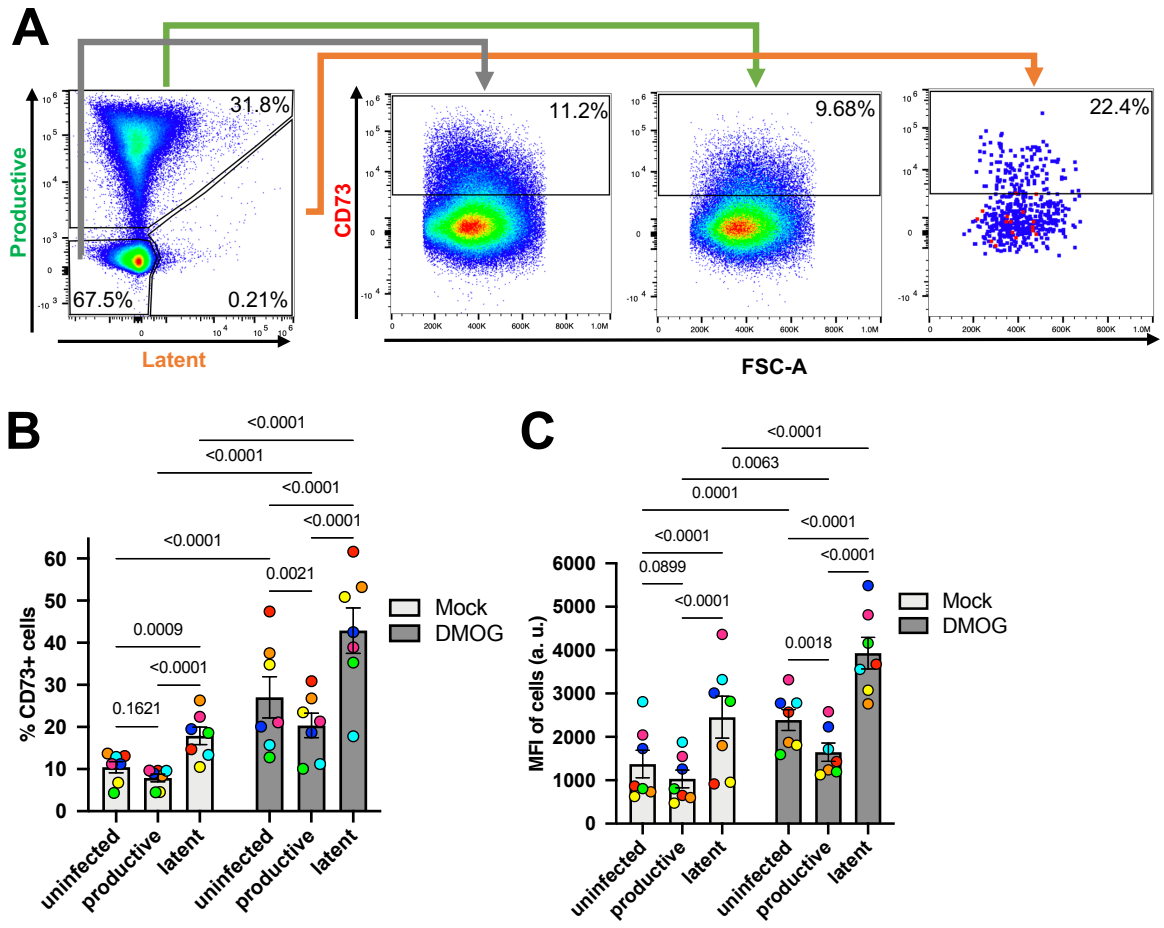


**Figure 23: The enrichment of CD73 positivity in latently-infected cells and CD73 surface expression of latent cells is reinforced under hypoxic conditions.** (A) Flow plots displaying the applied gating strategy to analyze CD73 expression in $HIV_{DFII}$-infected cells. Data shown are from a single donor upon mock treatment and are representative for all seven donors. (B) The Frequency of CD73+ cells and (C) CD73 surface expression per cell reflected by the mean fluorescence intensity (MFI) is displayed for 7 donors. Colored dots indicate individual donors. P-values displayed within the diagrams were generated by performing a two-way ANOVA with Fisher's LSD. P-value threshold for significance was at $p < 0.05$. Error bars show SEM.

**Latently-infected cells are enriched in the CD4+ CD73+ T cell compartment**. Last, I approached the analysis from a different angle and determined $HIV_{DFII}$ infection profiles in the CD73+ and CD73- CD4+ T cell compartments (Figure 24A). Before, I asked the question, whether latency is associated with increased CD73 positivity. Now, I examined whether CD73+ cells enrich for the latent reservoir. Importantly, also from this perspective, a clear correlation was discovered between CD73 expression and latency. The data showed a significant increase of latently-infected cells in CD73+ compared to CD73- cells with a 3-fold enrichment of latent

infection within the CD73+ T cell compartment (Figure 24B). Taking into account the average frequency of CD73+ cells among CD4+ T cells (~10%), this data implied that approximately 25% of the overall CD4+ T cell reservoir resides in CD73+ cells. Interestingly, the enrichment of latent cells in the CD4+ CD73+ T cell compartment did not significantly differ between mock- and DMOG-treated samples (Figure 24B), indicating that CD73+ cells might possess specific features that favor the establishment and/or maintenance of latent infection and that are not further modulated by the induction of hypoxic responses.

Overall, flow cytometry data showed a coherent relationship between CD73 expression, hypoxic conditions and the establishment and/or maintenance of HIV latency.

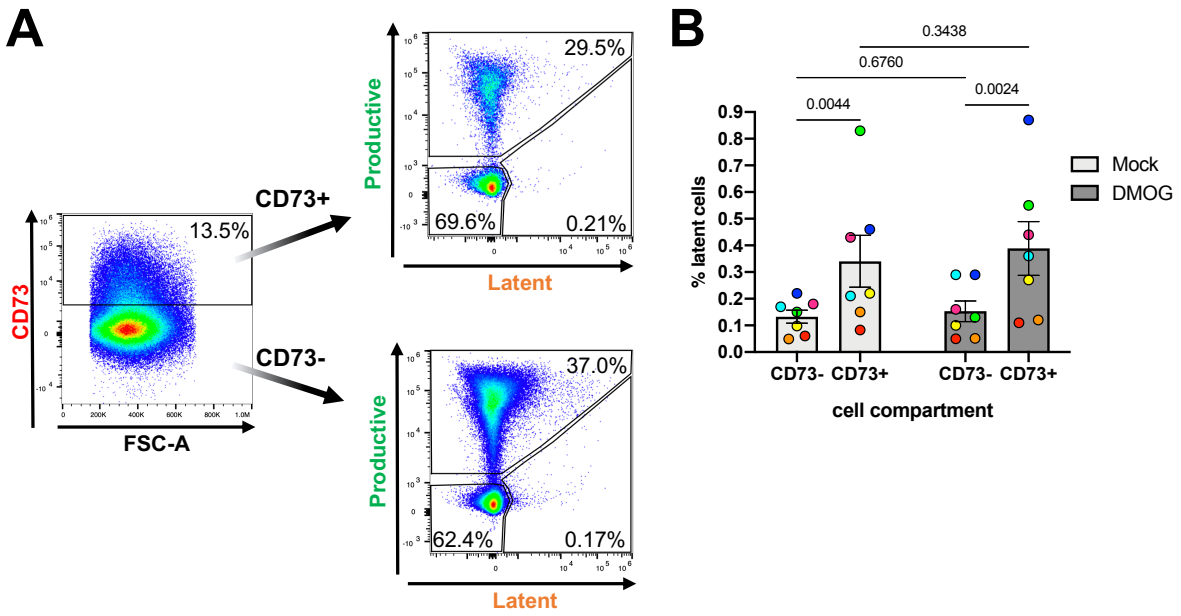


**Figure 24: Latently-infected cells are enriched in the CD4+ CD73+ T cell compartment.** (A) Flow plots display the applied gating strategy to analyze $HIV_{DFII}$ infection profiles in the CD4+ CD73+/- T cell compartments. Data shown are from a single, mock-treated donor and are representative for all seven donors. (B) The average frequency of latently-infected cells was assessed in CD4+ CD73+/- T cells for seven donors. Colored dots indicate individual donors. P-values displayed above bars were generated by performing a two-way ANOVA with Fisher's LSD. P-value threshold for significance was at $p < 0.05$. Error bars show SEM.

## 4.4 Characterization of CD4+ CD73+ T cells

A myriad of information has been collected about the role of CD73 in context of oncogenesis, tumor progression and survival[198]. Hitherto however, little is known about the relevance and function of CD73 in human CD4+ T cells. Here, I aimed to further characterize this specific phenotype by sorting blood-derived, primary CD73+ and CD73- CD4+ T cells and compared their transcriptome by RNA sequencing.

**A small fraction of blood-derived CD4+ T cells express CD73 on the cell surface.** Primary CD4+ T cells were isolated from blood samples of three healthy donors, subsequently stained for CD73 surface expression and sorted into CD73- and CD73+ cells via FACS (Figure 25A). Analysis of the flow cytometric data revealed that CD73 surface expression on CD4+ T cells was generally infrequent and ranged notably between donors from only about 3% to about 23% CD73+ CD4+ T cells (Figure 25B), indicating a broad intrinsic variability of CD73 expression.

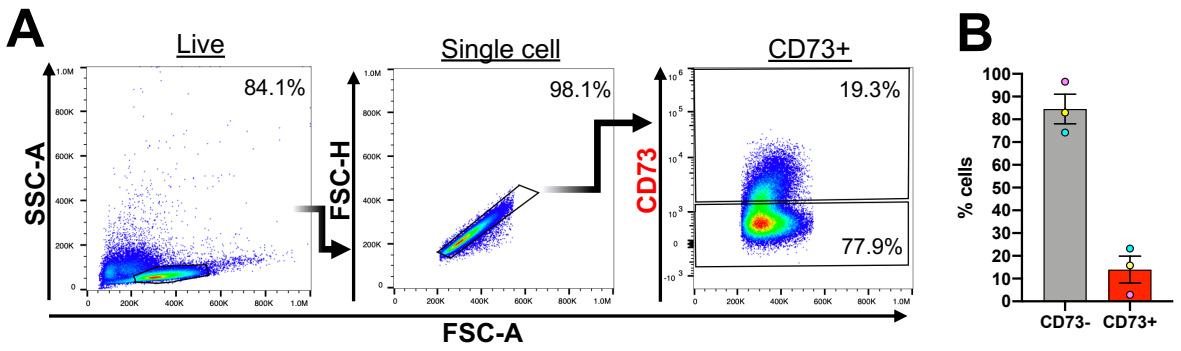


**Figure 25: CD73+ CD4+ T cells constitute less than 1/5 of the blood-derived CD4+ T cell compartment.** (A) Representative flow plots demonstrate the gating strategy for FACS of CD73- and CD73+ CD4+ T cells directly following blood processing, CD4+ T cell isolation and CD73 staining. (B) The frequency of CD4+ CD73+/- T cells was measured for three donors (colored dots). Error bars show SEM.

**CD73+ cells exhibit specific immunoregulation and signaling cascade patterns.** As observed in my previous NanoString experiments, RNA sequencing showed again that

transcriptional phenotypes are dominated by the donor effect. Both, heatmap and associated dendrogram, as well as PCA plots indicated that differences between donors were far greater than differences between the sorted cell populations (Figure 26A and B). Upon adjustment for the donor effect, I found 145 genes that were significantly, differentially expressed between CD73+ and CD73- cells, with 111 upregulated and 34 downregulated genes in CD73+ cells (Figure 26C). Expectedly, *CD73* was most significantly upregulated in CD73+ cells, followed by *CR1, ADAM23, ABCB1 and AUTS2* (Figure 26C, yellow dots). *CLEC17A* exhibited the highest foldchange in CD73+ cells compared to CD73- cells (> 5-fold), followed by *CD73, LINC02397* and *MACROD2* (> 4-fold) (Figure 26C, red dots). Importantly, four of these hits encoded for cell surface proteins, which may serve as additional surface markers for latent infection. Multiple genes were markedly downregulated in CD73+ cells. However, only two of them reached the highest level of statistical significance: *FCER1A* and *NPR3*. A gene set enrichment analysis of all hits yielded a multitude of significantly changed pathways between CD73+ and CD73- cells (Figure 26D). The top five included immune response and endocytic pathways. Interestingly, among the 40 most significantly changed pathways were positive regulation of angiogenesis, regulation of apoptotic processes and furthermore tyrosine kinase signaling cascades.

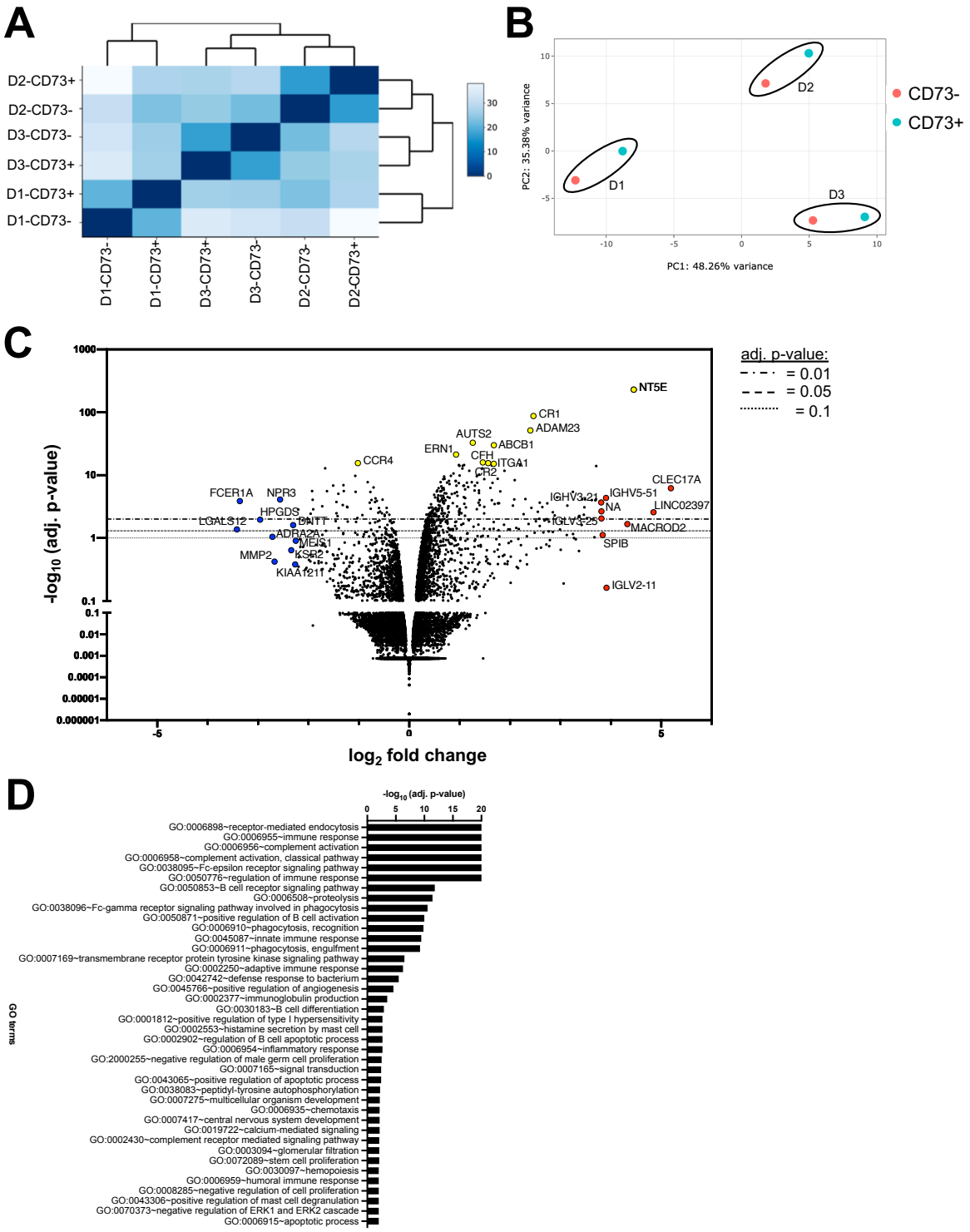


**Figure 26: CD73+ cells feature specific immunoregulation and signaling cascade patterns.** (A) Heatmap depicts overall similarity among sorted samples assessed by their Euclidean distance. Clustering and dendrogram organization reflect relatedness between samples. (B) PCA plot displaying PC1 and PC2. The percentage of the total variance per direction is shown on the respective axes. D = Donor. (C) Global transcriptional changes between CD73- and CD73+ cells are visualized in the volcano plot. Each data point represents a single gene and data were normalized as described in Materials & Methods 3.2.5. The $\log_2$ fold change of the normalized mean hit counts of each gene is on the x-axis and the $-\log_{10}$ of its adj. p-value (using the Benjamini-Hochberg method) on the y-axis.

Horizontal lines indicate adj. p-value thresholds. The top 10 most significantly changed, most upregulated and most downregulated genes are labeled and indicated by yellow, red and blue dots, respectively. (D) Significantly differentially expressed genes were grouped by their gene ontology and the enrichment of gene ontology terms was tested using Fisher exact test. The top 40 gene ontology terms that were significantly enriched with an adj. p-value < 0.05 in the differentially expressed gene sets are displayed in the bar graph.

**The majority of differentially expressed genes in CD73+ cells are part of the same protein-protein interaction network.** To better understand the specific transcriptional profile of CD73+ cells, all significantly differentially expressed hits were uploaded onto Cytoscape and cross-referenced with the STRING database. The resulting protein-protein interaction network was then overlaid with $\log_2$ fold changes and adj. p-values of each gene visualizing directionality and significance of interacting proteins (Figure 27). Out of the 145 hits, 33 were not identified in the database and thus not included in the analysis. Among the remaining 112 genes, 43 genes did not have an interaction partner and were excluded from the network plot. The analysis revealed 5 distinct interaction networks, whereas one network contained the majority of all hits. Within this network (I), a tight clustering of cell surface receptors was apparent (*CD22, CD79A, CR1, CR2, KIT, FCER1A, CD34*) accompanied by several signaling factors (*LYN, BLNK, BLK, BTK, PIK3AP1, TCL1A)* and transcription factors (*IRF8, EBF1, PAX5*). Another cluster (II) comprised downregulation of cell surface proteins *CXCR3*, *CCR4* and *PTGDR2*. The three other networks were not interconnected and based on only 2 to 4 significant hits, which may render the interpretation of their relevance and biological function difficult.

Nonetheless, the majority of identified, differentially expressed genes were part of an intrinsically cross-connected network, pointing towards overlapping signaling cascades and biological processes shared by the entire CD73+ CD4+ T cell compartment.

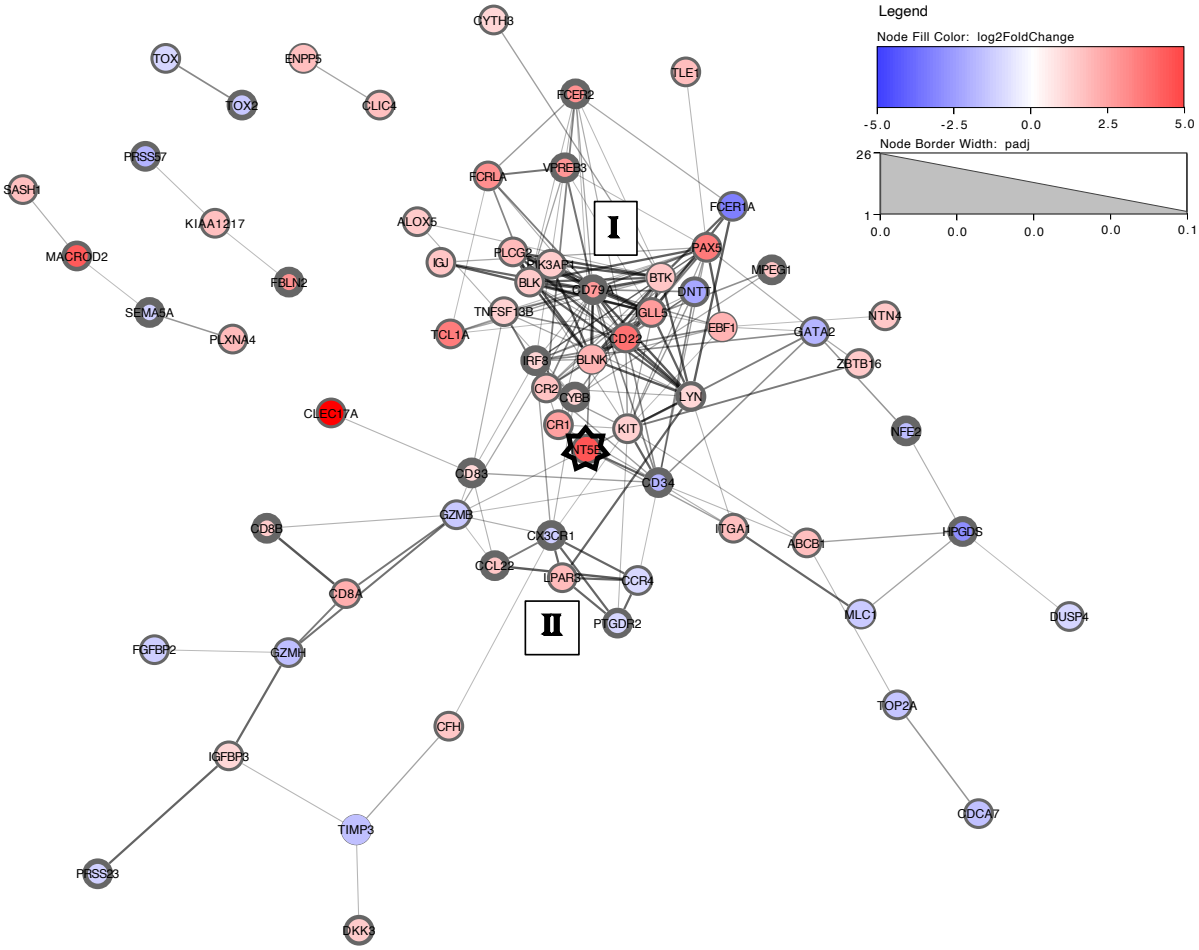


**Figure 27: Differentially expressed genes in CD73+ cells form a large protein-protein interaction network.** The protein-protein interaction network of genes significantly, differentially expressed between CD73- and CD73+ CD4+ T cells was generated in Cytoscape 3.8.2 using the STRING database for Homo sapiens with a default confidence score of 0.4. Thickness of lines between nodes depict score value, with thicker lines indicating greater scores. 33/145 significant hits were not recognized by the STRING database and thus excluded from the interaction network. Genes that were found to interact with at least one other gene are displayed in the network analysis. $Log_2$ fold changes of genes is indicated by node pseudo color and the adj. p-value by node border width. *CD73* (*NT5E*) is highlighted by a star shape. Protein clusters of interest are labeled.

## 4.5 Relevance of the Latent Reservoir in CD73+ CD4+ T cells

An important question regarding cells that harbor proviral sequences is if and to what extent they contribute to the functional HIV reservoir. The intactness of the integrated provirus and inducibility of viral transcription predominantly determine viral spread upon antiretroviral treatment interruption (ATI). My previous data showed that latently-infected cells reside within the CD73+ CD4+ T cell compartment. However, the biological and clinical relevance of this

specific viral reservoir remained elusive. To close this gap, I adapted a primary *in vitro* HIV infection model that was specifically developed and optimized for latency reversal studies[174].

**CD73+ CD4+ T cells comprise an inducible HIV reservoir.** Firstly, I purified primary blood-derived CD4+ T cells and subjected them to FACS for sorting of CD73- and CD73+ CD4+ T cells. Subsequently cells were infected with a recombinant, replication-competent reporter virus that contains a luciferase gene under the control of the viral LTR ($HIV_{LUC}$). After successful infection, cells were maintained in ART-containing media for 5 days to allow for establishment of a latent reservoir. Then, cells were stimulated with αCD3/αCD28 beads for 24h in order to reverse latency. Transcriptional activity of integrated provirus was measured based on luciferase activity in the sorted T cell compartments (Figure 28A). Reactivation of viral transcription was assessed by comparing sample aliquots with or without αCD3/αCD28 stimulation. Viral transcription was clearly induced upon αCD3/αCD28 stimulation in both, CD73- and CD73+ CD4+ T cells compared to unstimulated cells as reflected by a 10-fold and 14-fold increase in LTR-driven luciferase activity, respectively (Figure 28B).

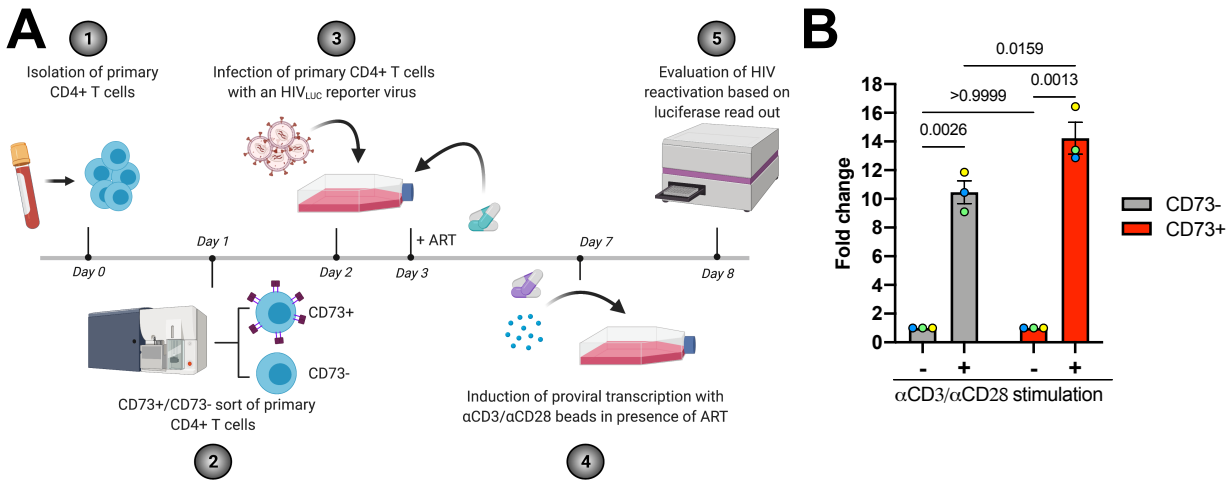


**Figure 28: $HIV_{LUC}$ infected CD73+ CD4+ T cells constitute an inducible HIV reservoir.** (A) The schematic represents the experimental workflow to test reactivation of integrated provirus in sorted CD73- and CD73+ CD4+ T cells. Proviral activity in the sorted CD4+ T cell compartments was measured by quantitating luciferase signals. (B) Data display the average fold change of stimulated over unstimulated cells from the same sample of three

donors. Colors indicate individual donors. P-values above bars were generated by performing a two-way ANOVA with Fisher's LSD. A p-value at $p < 0.05$ was considered significant. Error bars show SEM.

Interestingly, induction of viral transcriptional activity was significantly higher in stimulated CD73+ T cells compared to CD73- T cells. These results unequivocally demonstrated that the CD73+ CD4+ T cell compartment can harbor an inducible latent reservoir *in vitro*, indicating the potential of this compartment to contribute to a spreading infection in PLWH upon ATI.

## 4.6 CD73 as Marker of HIV Latency *in vivo*

The hitherto presented *in vitro* data have consistently demonstrated a direct association between CD73 expression and HIV latency. However, it remained an open question if and how these findings reflect physiological phenomena *in vivo*. To tackle this question, a collaboration was established with Dr. Eugenin and his team at the University of Texas Medical Branch. The Eugenin laboratory has previously developed a sophisticated microscopy imaging pipeline that enables simultaneous detection of integrated HIV-DNA, viral mRNA and HIV protein as well as lineage markers in tissues, followed by automated quantitative image analyses[178].

**Simultaneous *in situ* staining of HIV DNA, RNA and proteins.** Here, our collaborator utilized this approach to concomitantly measure CD73 expression and HIV molecules in lymph node tissues obtained from either: HIV-infected individuals on suppressive ART, viremic individuals, and uninfected controls (Figure 29). Specimens comprised peripheral and inguinal lymph nodes and were stained for CD3, CD73 and HIV markers. CD3 staining was used as lineage marker for T cells and DAPI was included as a counter staining of nuclear DNA. CD73 signals were found across all samples, while HIV detection greatly differed between ART-suppressed and viremic individuals and was absent in uninfected control samples (Figure 29A-C). In lymph nodes of viremic individuals, more than 50% of cells showed positive signal for all

three HIV markers, indicating severe infections and ongoing viral replication (Figure 29D). In contrast, signals for HIV molecules in lymph nodes from ART-suppressed individuals were low and exhibited a gradual reduction in frequency, with HIV DNA positive cells being detected the most and p24 positive cells the least (Figure 29D). This incremental abundance of the different HIV markers illustrated the complex nature of viral replication *in vivo,* where different obstacles have to be overcome at every level of the gene expression cascade. As a result, only a fraction of infected cells expresses viral transcript and only a subfraction of these cells translate mRNAs into functional proteins.

**CD73 expression correlates with HIV persistence in lymph nodes from ART-suppressed individuals.** CD73 expression was then assessed for CD3+ and CD3- cells and (except for uninfected specimen) compared between HIV-DNA+ and HIV-DNA- subsets (Figure 29E). In general, CD73 expression levels of CD3+ cells were significantly higher in ART-suppressed samples compared to uninfected samples. In addition, HIV-DNA+ CD3+ cells in ART-suppressed individuals possessed a significant, 1.6-fold higher CD73 expression compared to the overall CD3+ population. This difference in CD73 expression levels was not observed in untreated, viremic individuals and suggested a specific persistence of HIV infections under ART in the CD73+ CD3+ compartment.

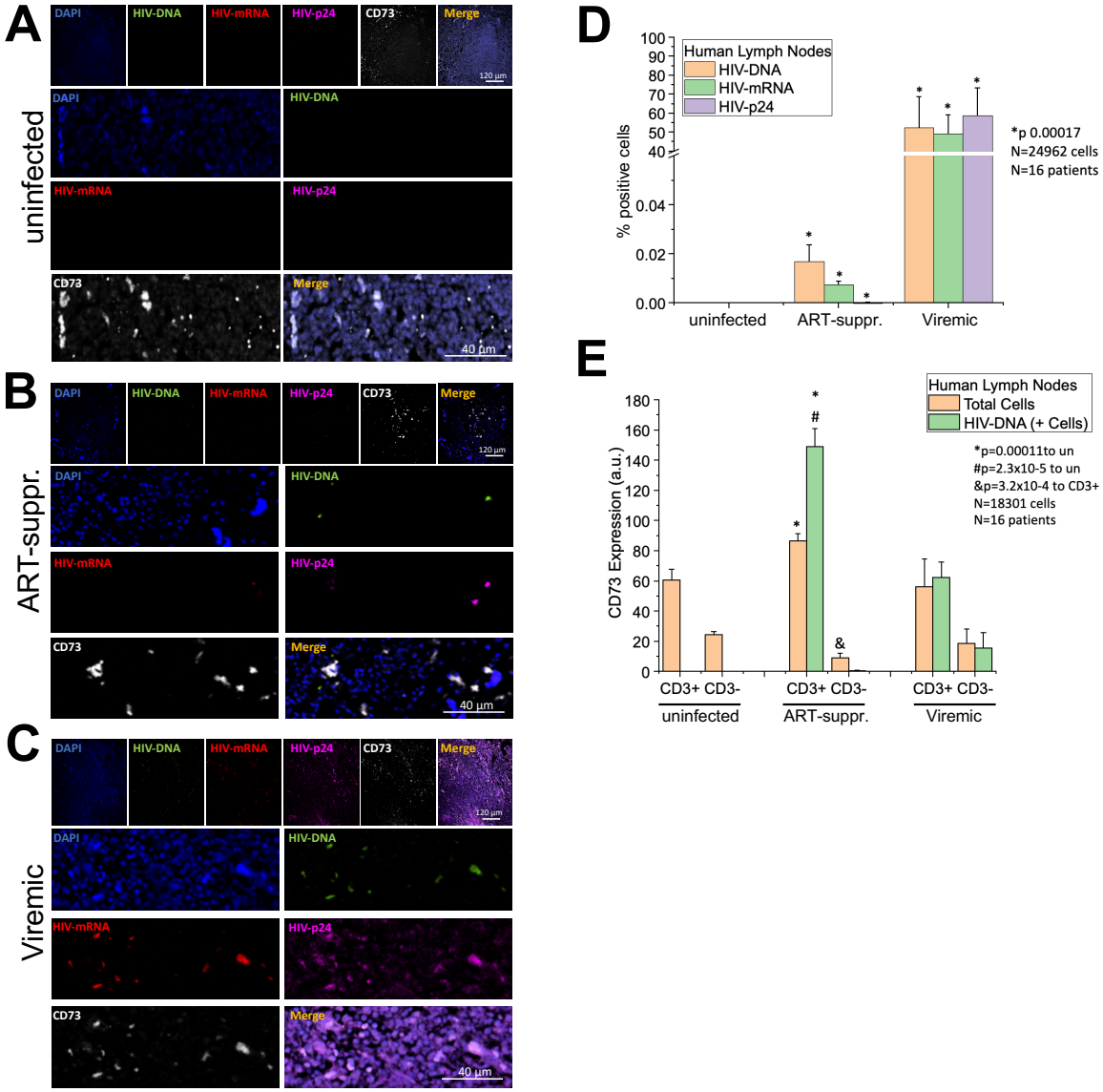


**Figure 29: *In situ* imaging of lymph nodes reveals association between CD73 expression and HIV DNA specifically in ART-suppressed individuals.** Cellular and viral targets were detected by immunofluorescence *and in situ* hybridization assays. Staining, imaging and analyses were conducted in collaboration by members of the Eugenin Laboratory. (A-C) Panels show representative confocal microscopy images for CD73 and HIV molecule staining of lymph node tissue obtained from (A) uninfected, (B) ART-suppressed (suppr.), and (C) viremic individuals. (D) Automated image analysis of tissue sections stained for HIV DNA, mRNA and p24 protein in uninfected (n = 5), ART-suppressed (n = 6), and viremic individuals (n = 5). Bar graphs show the average percentage of cells that exhibit a positive signal for the respective target. Images were analyzed as described in Materials & Methods 3.2.6. Briefly, cells were identified based on DAPI staining and were scored positive for HIV-DNA if a high Pearson correlation between nuclear stain and HIV-DNA signal was found. Conversely, cells were scored positive for HIV mRNA or protein, only if a low correlation was found between DAPI and HIV transcript/protein signal. Detection thresholds were defined based on uninfected samples and suited positive controls. (E) Quantitative CD73 expression analysis in tissue samples from uninfected (n = 5), ART-suppressed (n = 6) and viremic individuals (n = 5). Identification of the T cell compartment (CD3+ cells) and detection of HIV reservoir cells (HIV-DNA+) was followed by quantification

of CD73 signals in the indicated 4 cellular subsets (CD3+ HIV-DNA-, CD3+ HIV-DNA+, CD3- HIV-DNA-, CD3 HIV-DNA+). ANOVA was used to compare the different groups. Relevant statistics are shown in the bar graphs.

## 4.7 The CD73/adenosine Axis as Drug Target in HIV Infection

So far, my data clearly demonstrated a correlation between HIV latency and CD73 surface expression *in vitro* and *in vivo*. Importantly, I found that this correlation was reinforced by the induction of hypoxic responses which led to an overall increase of CD73 positivity among CD4+ T cells, facilitating the preferential enrichment of the latent reservoir in the CD73+ compartment. I therefore hypothesized that a regulation of CD73 expression under hypoxic conditions, and the resulting increase in adenosine signaling could be mechanistically involved in the establishment and/or maintenance of HIV latency. In the final set of experiments, I thus focused on the signaling cascades downstream of CD73. To that purpose, I employed a well-established cell line model of HIV latency that has been extensively used in the past to either test latency reversing agents or investigate the molecular mechanisms of HIV persistence[199,200]. The model system is based on Jurkat cells, an immortalized human T lymphocyte cell line, that have been infected with a fluorescent reporter virus and subsequently subjected to a series of single cell, fluorescence sorts. Individual clones were selected featuring low or no viral transcription at baseline, but significant gene expression from the viral LTR upon reactivation (Figure 30A)[199,200]. Here, I exploited this model to examine how modulation of adenosine receptors by selective agonists and antagonists affects HIV transcriptional activity.

**Blocking the adenosine receptor A2AR promotes HIV latency reversal**. I first measured CD73 surface expression in three J-Lat clones 5A8, 6.3 and 11.1 as well as the parental JurkatE6 cell line (Figure 30B). Between 10-20% of JurkatE6, J-Lat 6.3 and 11.1 cells expressed CD73 on the surface. In strong contrast, about 80% of J-Lat 5A8 cells were CD73 positive. Due to this

remarkably high frequency of CD73 expressing cells, subsequent experiments were focused on this clone. J-Lat 5A8 cells were pretreated with the A2AR agonist CGS21680 (CGS), mimicking adenosine signaling, and antagonist SCH-58261 (SCH), blocking adenosine signaling, for 1h at increasing doses, followed by stimulation with PMA/I, a strong mitogen and latency reversing agent. GFP expression, reflecting HIV transcriptional activity, was assessed 7h later, including from PMA/I only and mock-treated samples (0.5% DMSO). CGS and SCH pretreatment did not compromise cell viability at any dose compared to cells treated with PMA/I only (Figure 30C). Notably, while pretreatment with A2AR agonist CGS did not markedly alter latency reversal, pretreatment with A2AR antagonist SCH significantly promoted latency reversal by PMA/I stimulation and resulted in an evident dose response with a 2-fold increase in the frequency of GFP+ cells at the highest dose of 10 µM SCH (Figure 30D). Thus, selective blocking of A2AR promoted latency reversal without inducing cell toxicity. This finding underlined the potential to pharmacologically manipulate the CD73/adenosine axis in HIV cure approaches. However, it also represented a first piece of evidence supporting the hypothesis that CD73 through its enzymatic functions actively promotes and maintains latency.

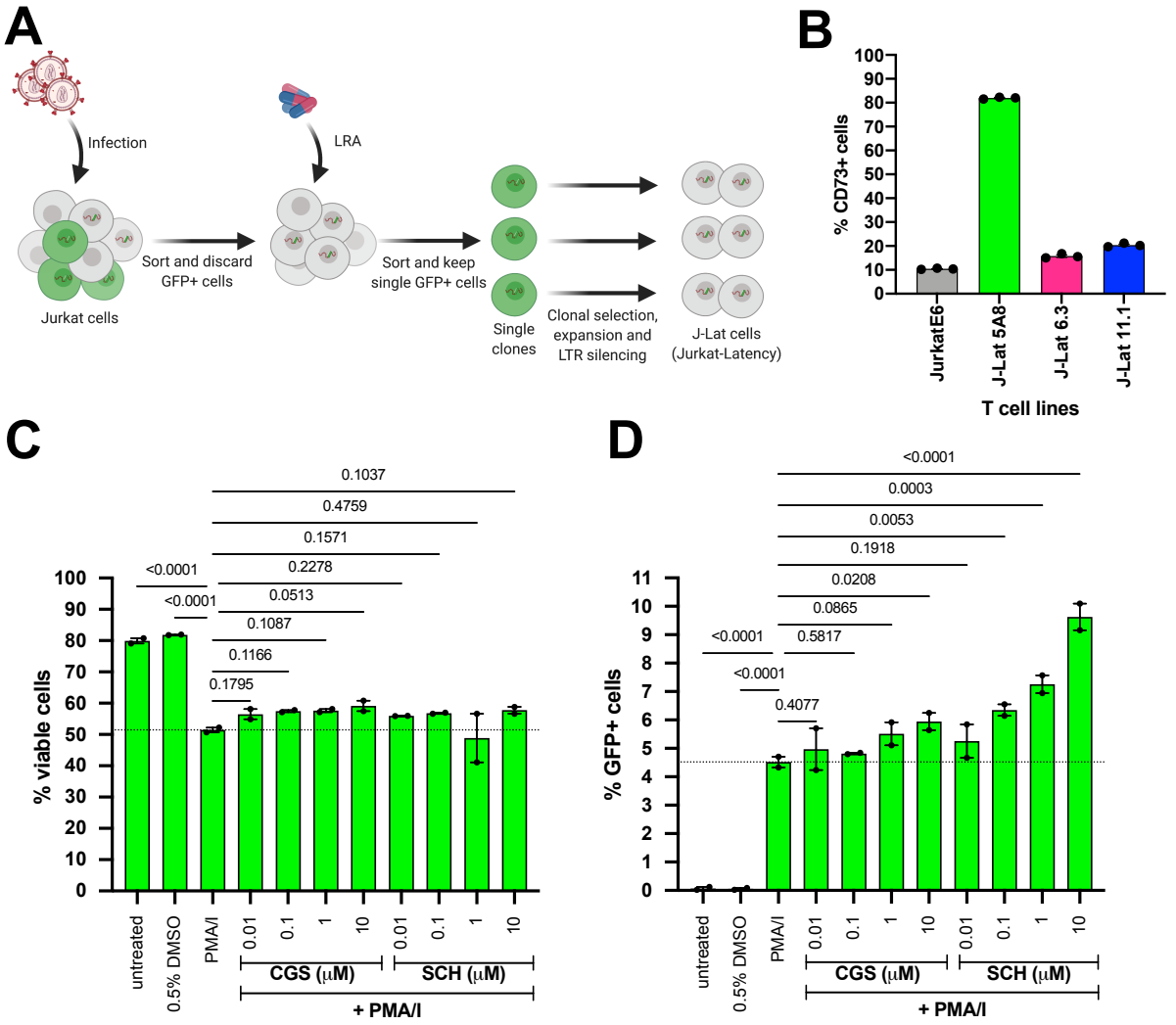


**Figure 30: Blockade of adenosine receptor A2AR facilitates HIV latency reversal.** (A) J-Lat cell clones were generated previously[200,201] and were kindly provided by Warner C. Greene and Eric Verdin. Figure was adapted from Chan JK et al. (2013)[200] and shows how different sub-clones were isolated and propagated. (B) Average frequency of live, single CD73+ cells in the different T cell lines measured via flow cytometry. (C and D) J-Lat 5A8 cells were treated with A2AR agonist CGS21680 (CGS) antagonist SCH-58261 (SCH) at indicated, increasing doses for 1h, followed by treatment with LRA PMA/I. PMA/I treatment alone served as positive control, 0.5% DMSO treatment as mock control. (C) Cell viability based on FSC-A and SSC-A and (D) GFP expression as a reporter of HIV transcriptional activity were assessed 7h post treatment using flow cytometry. Samples were measured in duplicates. P-values above bars were generated by performing a one-way ANOVA with Fisher's LSD. A p-value at $p < 0.05$ was considered significant. Data represent the mean and error bars the SEM.

# 5 Discussion

In recent decades remarkable scientific and biomedical advances have turned the tides in the long-lasting fight against the HIV pandemic. To date, the number of new infections is declining, and HIV-related deaths are steadily shrinking. Further research is necessary, however, into the mechanism of HIV persistence and the biology of chronic HIV infections since a true cure and therefore complete remission from HIV infections remain intangible. The goal of this study was to thoroughly characterize primary HIV latently-infected cells in order 1) to contribute to a deeper understanding of the latent reservoir and 2) to pinpoint potential targets for therapeutic interventions. My work was focused on CD4+ T cells, the major target of HIV infection and an important source of viral rebound upon ART interruption.

Using a dual reporter virus that enables differentiation between uninfected, productively-infected, and latently-infected cells, each population was isolated and, for the first time, characterized by a systems biology approach. Extensive statistical and bioinformatic analyses were applied to elucidate expression signatures, regulatory programs and signaling cascades of HIV-infected cells with special attention to latently-infected cells.

The core finding of this work was an association between surface protein CD73 and HIV latency. To the best of my knowledge, the enrichment of latently-infected cells in the CD73+ CD4+ T cell compartment, that I am reporting here, has not been described previously. I also found indications that CD73 is not just a passive marker of reservoir cells, but moreover that the regulation of CD73 expression as well as its enzymatic function may be linked to HIV persistence. These results provide further insight into the establishment and maintenance of a

significant portion of viral reservoirs and may unveil new therapeutic targets for HIV cure approaches.

## 5.1 Characteristics of HIV Latently-infected Cells

In the following chapter, I will discuss some of the unique features of HIV latently-infected cells that were discovered in the course of this work. Of note, CD73, the inarguably most important hit of this study, will be covered separately.

### 5.1.1 No Causality Between T Cell Activation and Viral Gene Expression

Multiple previous reports have described correlations between T cell activation or exhaustion markers and viral reservoirs[160,202,203]. When scrutinizing the expression of defined activation makers across all stimulated samples, my own data show that the only differentially expressed surface protein was the inducible T cell costimulator ICOS (Figure 17C). ICOS levels were significantly lower in latently-infected cells compared to uninfected, and significantly higher compared to productively-infected cells. ICOS is an immune check point protein and part of the CD28 and CTLA-4 cell surface receptor family. Interestingly, it prevents the apoptosis of pre-activated T cells[204]. Thus, higher expression levels of ICOS on latently-infected cells compared to productively-infected cells could indicate a survival advantage. Importantly, ICOS was also shown to play a crucial role in regulating Tfh cell functions[205] and Tfh cells in turn were identified as major compartment for HIV infection[71,206,207].

In recent years, multiple studies have described an association between the T cell exhaustion marker PD1 (programmed cell death 1) and viral persistence[208]. In contrast, my data showed no correlation between HIV infection or latency and PD1 expression. This discrepancy may be explained by the fact that previous studies were often based on clinical samples from

ART-suppressed individuals rather than *in vitro* HIV infections. The PD1 phenotype is therefore likely established over years of chronic infection and cannot be captured in short-term cell culture experiments. As the HIV reservoir is highly dynamic and divers, it is likely that multiple latency markers exist, reflecting different time points of infection. For instance, my data may suggest that ICOS is involved in the establishment and early maintenance of latency, while PD1 cells may represent T cell reservoirs that persist or emerge during years of chronic infection and ART. As a side note, ICOS and PD1 are both markers for Tfh cells and are directly involved in Tfh cell development and function[209]. One could therefore speculate that both proteins are actually indicative of the same subset of CD4+ T cells albeit at different differentiation states. In that case, my ICOS data may in fact support previous PD1-focused publications.

### 5.1.2 Signaling Pathways Associated with Latent Infection

My initial analysis focused on the pairwise comparison of all sorted cell populations. It should be emphasized that these samples (uninfected, productively-infected and latently-infected) underwent the exact same treatment (T cell stimulation and exposure to virus), which nonetheless led to diverging infection outcomes. This raises the important question which host factors determine the cellular fate upon HIV infection. Are there proteins that are associated with latent, productive or non-successful infection? However, in such consideration one also has to take into account viral remodeling since differential gene expression, in particular in productively-infected samples, will be heavily impacted by the regulatory activity of viral accessory proteins. A prime example of this phenomenon is the downregulation of CD4 I observed in cells with active viral replication. The loss of CD4 expression is mediated through

multiple viral proteins, including Env, Vpu and Nef[28,189–193]. To date viral remodeling is well-understood and has been extensively described in the HIV literature[210]. My study therefore focused on the gene expression profiles of latently-infected cells in which this remodeling should be minimal or absent due to the lack of viral proteins.

My analysis of $HIV_{DFII}$-exposed, sorted samples revealed several pathways, uniquely altered in latently-infected cells (Figure 19C and D). The upregulation of 'Interleukins' and 'Pathogen Defense' in latently-infected cells points towards intracellular signaling cascades that antagonize productive infection. In contrast, the suppression of 'Antigen Processing' in latently-infected cells may indicate the ability of these cells to evade host immunity, a pro-survival effect that could enforce viral persistence. Antigen processing and presentation involve multiple steps and are important for an effective immune response: viral proteins are degraded, and peptide fragments are presented on the cell surface by class I major histocompatibility complex (MHC I) proteins, thus subjecting the infected cells to the lytic activity of cytotoxic T lymphocytes (CTLs) or NK cells. It has long been known that HIV actively modulates antigen presentation pathways[211,212] and has evolved very elaborate fine tuning mechanisms to selectively balance MHC I protein expression, thus preventing recognition and clearance by host immune responses[212]. It stands to reason that such a phenotype could promote immune evasion and long-term survival of latently-infected cells, thus contributing to reservoir maintenance.

### 5.1.3 Specific Genes Associated with Latent Infection

27 targets were uniquely changed in latently-infected cells compared to productive and uninfected samples (Figure 19E and F). All these genes (26/27 hits were identified by the

STRING database) were found to be part of one protein-protein interaction network (Figure 19F) arguing for unique cellular programs, either promoting latency, or modulated by HIV to induce a latent state.

Interestingly, two factors known to be involved in HIV infection were within this network. NF-κBIA mRNA was significantly upregulated and CASP1 mRNA significantly downregulated in latently-infected cells (Table 2). NF-κBIA (NF-κB Inhibitor Alpha) is a master regulator of the transcription factor NF-κB and blocks its activity by sequestering NF-κB proteins in the cytoplasm[213]. NF-κB in turn is a crucial transcription factor of HIV[18,101]. Thus, the detected upregulation of NF-κBIA in latent cells provides a reasonable explanation for the transcriptional quiescence of the provirus. The other aforementioned factor, CASP1 (Caspase-1) is a key regulator of pyroptotic cell death, a highly inflammatory process that has been reported to be a major determinant of HIV pathogenesis and a potent driver of virus-dependent CD4+ T cell depletion[214]. Low expression of CASP1 in latently-infected cells may suggest an increased chance for latently-infected cells to survive HIV infection, thus again contributing to reservoir maintenance and persistence.

My top three interconnected hits were IL8 mRNA (CXCL8), STAT1 (signal transducer and activator of transcription 1) mRNA, and CSF2 (colony-stimulating factor 2) mRNA. The Chemokines *IL8* and *CSF2* were both upregulated in latent cells while *STAT1* was suppressed. IL8 and CSF2 are both involved in inflammatory responses. CSF2 is mainly known to be involved in granulocyte and macrophage development and activity. However, increasing evidence suggests CSF2 as pro-inflammatory factor with varying functions and an important role in autoimmunity when produced from CD4+ T cells[215–217]. Some preclinical and clinical studies reported promising results using CSF2 as adjuvant in ART, but further studies are

necessary to explore its mechanism and therapeutic potential[218]. IL8 is a major mediator of inflammatory responses and has been reported to stimulate HIV replication[219]. Increased IL8 levels have further been shown to be associated with chronic inflammation in HIV-infected individuals[220]. Additional studies are necessary to unravel the contribution and relevance of both, IL8 and CSF2, in HIV latency. STAT1 is an interferon-responsive transcription factor that globally modifies the transcriptional landscape and establishes an antiviral cellular state. HIV directly blocks interferon (IFN)-stimulated genes and activation of STAT1 to evade IFN-induced antiviral responses[221,222]. The subtle but significant downregulation of STAT1 detected here in latent infection may suggest an immediate remodeling of cellular regulatory programs upon infection prior to viral quiescence. Alternatively, latent infections may have selected for cells with inherently lower STAT1 levels. In that case, the question whether there is a causative relationship or otherwise a mere correlation between latency and STAT1 expression merits further attention. Lastly, I found a slight but significant upregulation of CD2 mRNA in latent cells. CD2, an adhesion and co-stimulatory molecule, was previously described to accompany latent infection in memory cells[162]. However, the biology and molecular mechanisms of this reservoir enrichment in CD2+ cells are hitherto only insufficiently understood.

## 5.2 CD73 as Key Player in HIV Persistence

My pairwise comparison of all collected samples identified three targets: IL8 mRNA, CD39 mRNA and CD73 protein, which shared already known interconnections on the protein level and are linked via the adenosine signaling pathway[223] (Figure 20B). A plethora of literature exists about CD39 and CD73 and their orchestrated functionality in purinergic signaling[198,224,225]. CD39, encoded by the *ENTPD1* (ectonucleoside triphosphate

diphosphohydrolase 1) gene, and CD73, encoded by the *NT5E* (5'-nucleotidase) gene, are both ectonucleotides. They are expressed on the cellular surface and successively catalyze processing of extracellular ATP to adenosine, with CD39 hydrolyzing ATP to ADP/AMP and CD73 converting AMP to adenosine[226]. Extracellular adenosine acts as important messenger and triggers divers signaling cascades mediated by different adenosine receptors. Importantly, IL8 expression has been shown to be stimulated by adenosine signaling, and is thus directly connected to the enzymatic function of CD73[227]. The unique differential expression of these three genes in latently-infected cells provides intriguing evidence, that CD73 and the adenosinergic pathway play a pivotal role in HIV latency and the maintenance of viral reservoirs. In the following chapter I will focus specifically on CD73 as central element of the adenosine signaling cascade and investigate its role in context of HIV latent infection.

**HIV latency correlates with CD73 positivity *in vitro* and *in vivo*.** A major discovery of my work was the identification of elevated cell-surface expression of CD73 as signature characteristic of HIV latently-infected CD4+ T cells – an observation that, to the best of my knowledge, has never been described in context of latent HIV infection. This finding was first uncovered by comprehensive NanoString profiling (Figure 20) and validated at the single cell level by flow cytometry (Figure 23 and Figure 24). My data further showed that latent reservoirs established in the CD73+ CD4+ T cell compartment could be reactivated, implying a relevant contribution to a functional reservoir in HIV-infected individuals (Figure 28). Importantly, *in situ* staining and imaging of lymph nodes demonstrated an association between CD73 and HIV persistence during ART, which indicates that CD73 can serve as biomarker of latent infections *in vivo* (Figure 29). Interestingly, the association between CD73 expression levels and HIV was not observed in viremic individuals, suggesting that CD73 expression might offer

a survival advantage for HIV-infected cells to persevere specifically under ART. I surmise that in the absence of treatment, when HIV is not subject to an external, pharmacologic selection pressure, active viral replication dominates and potentially overwrites CD73 effects. It is likely the long-term persistence of HIV under ART that carves out the clear correlation between CD73 and viral latency.

**Previous knowledge about CD73+ CD4+ T cells in HIV infections.** CD73 is not completely unheard-of in the HIV field. Here, I provide a brief overview of the existing literature, covering also CD39+ T cells to take into account the tight mechanistic and functional connection between both ectoenzymes.

Previous studies have investigated the relationship between CD39+ or CD73+ T cell subsets and HIV infection. To data however, none has examined the contribution of these subsets to HIV reservoirs. Notably, while murine Tregs co-express CD39 and CD73[228] and double positivity is fairly abundant in mice, my data and the work of others have demonstrated that only a small fraction of human peripheral CD4+ T cells expresses both ectoenzymes[229–231]. In humans comparably little is known about CD73+ T cells, whereas CD39+ T cell subsets are well understood[229,230]. For CD39 it has been shown that increased activity of CD39-expressing Tregs and altered Treg cell phenotypes in HIV-infected individuals are associated with a more severe HIV disease progression[232–235]. Interestingly, one study reported that HIV replication in activated T cells is repressed by Tregs through a contact- and cAMP-dependent mechanism, involving CD39 and protein kinase A (PKA) activity[236]. Regarding CD73, it was reported that the frequencies of different circulating CD73 expressing T cell subsets decline in HIV-infected individuals[231,237]. However, in ART-suppressed individuals, a significant enrichment of CD73+ CD8+ and CD73+ CD4+ T cells was detected in lymph nodes compared to the periphery with

a significant increase of CD39+ and CD73+ double-positive T regs[237]. This finding suggests a redistribution of T cell subsets upon HIV infection. Lastly, a study from 2015 used simian immunodeficiency virus (SIV)-infected nonhumane primate (NHP) models to elucidate the relevance of the adenosinergic pathway in progressive SIV/HIV infections[238]. The authors discovered a positive correlation between elevated CD39 and CD73 expression, adenosine levels and slow disease progression again indicating that CD73 anti-correlates with active viral replication, thus possibly favoring viral latency. In summary over the last years, increasing circumstantial evidence has demonstrated a critical role for CD73 expression, adenosine production and signaling in HIV infection. My data now show for the first time a direct correlation between CD73 and HIV latency in CD4+ T cells thereby linking its expression regulation and enzymatic functionality to the establishment and persistence of viral reservoirs.

**Transcriptomics of the CD73+ CD4+ compartment.** As mentioned before, the CD73+ CD4+ T cell compartment is hitherto only poorly characterized. To address this knowledge gap, I assessed the transcriptional landscape of CD73+ CD4+ T cells and CD73- CD4+ T cells by RNA sequencing. 'Immune responses', 'complement activation' and 'receptor-mediated signaling cascades' significantly differed between these subsets, indicating diverging immunoregulatory programs in CD73+ and CD73- cells (Figure 26). In addition, 'positive regulation of angiogenesis', 'regulation of apoptotic processes' and 'tyrosine kinase signaling cascades' were all signaling pathways within the realm of adenosine production and signaling, thus emphasizing the relevance of CD73 expression in immunosuppression and implying potential survival mechanisms specific for CD73+ cells.

The intrinsic protein interaction network contained a tight cluster of upregulated cell surface proteins (Figure 27), which represented exciting new targets to test as markers for

latent infection. The combination of several markers would improve enrichment of the latent reservoir and thus specify targeting and elimination of latently-infected cells *in vivo.* The potential of the identified surface proteins to function as markers for latent infection requires further examination. Importantly, the network contained two significantly downregulated genes, transcription factor *GATA2*, and DNA topoisomerase *TOP2A*, known to support HIV transcription and replication[239,240], thus providing evidence for a cellular environment in CD73 expressing cells that favors latent infection.

Interestingly, a lot of the significantly differentially expressed genes are broadly expressed in B cells. This somewhat surprising finding is supported by another recent transcriptional profiling study, in which a novel IL-8 producing CR2+ T cell subset was identified. This subset exhibits similar expression signatures to CD73+ CD4+ T cells[241]. Thus, it will be crucial in follow-up studies to evaluate CR2+ T cells in context of HIV infection and measure the enrichment of HIV viral reservoirs in this newly identified T cell subset.

Of note, several of the significantly differentially expressed genes (*CD8A*, *CD8B, GZMB*) between CD73+ and CD73- CD4+ cells are typically limited to CTLs. As CD4+ T cells were isolated from fresh PBMCs upon negative selection with up to 97% purity, it cannot be excluded that this unexpected expression pattern is the result of minor contaminations with CD8+ T cells. Thus, the biological relevance of these targets needs to be considered with caution. Moreover, future sort experiments should include CD4 and CD8 lineage markers in order to completely exclude CD4 negative cells from downstream analysis.

**The relevance of hypoxia for HIV persistence.** A particularly interesting finding of this work is that CD73 is significantly upregulated under hypoxic conditions. This finding is important for two reasons: First, oxygen tension levels are highly variable throughout the body.

In well oxygenated tissues, as the upper airways, oxygen levels reach up to 19%[242]. In the gastrointestinal tract, oxygen ranges between 0-7%[243], while lymphoid organs exhibit ranges from 0.5-4.5% oxygen[244,245]. As a consequence, immune cells including CD4+ T cells encounter and operate at varying oxygen concentrations as they traffic through the body[245]. Lymphoid organs represent crucial viral sanctuary sites and as these are characterized by low oxygen levels, it seems intriguing to draw a natural link between HIV persistence and hypoxia.

Second, it is well known that environmental factors such as oxygen supply shape the cellular microenvironment and thus influence viral propagation. Low oxygen levels thereby have opposing effects on different human viruses[246]. The replication of influenza virus[247] and adenovirus[248] were found to be repressed under hypoxia, while Epstein-Barr virus[249] and Herpesvirus[250] replication is induced. A recent study about the retrovirus HTLV-1, a close relative of HIV, has reported enhanced viral transcription and latency reversal at physiological hypoxic conditions (1% oxygen)[251].

The role of oxygen levels and hypoxia in HIV infections remains elusive. Charles et al. (2009)[252] reported decreased HIV-1 RNA levels at 3% oxygen, while S. Deshmane and colleagues showed increased HIV transcription mediated by the interaction between HIV accessory protein Vpr and HIF-1α[253,254]. HIV-1 replication was also shown to be promoted by HIF-1α which in turn was stabilized not by hypoxia but reactive oxygen species (ROS)[255]. However, a study published last year demonstrated that hypoxia limited viral transcription and promoted HIV latency with HIF-2α as direct inhibitor of viral transcription[256].

**CD73 is the central mediator between hypoxia and HIV latency.** My data provided new insights into the connection between HIV latency and hypoxia with CD73 emerging as key facilitator. Firstly, I found that CD73 expression in CD4+ T cells was strongly upregulated under

hypoxic conditions (Figure 22A and B), thus proving that CD73 expression in CD4+ T cells is governed by the same, well-characterized mechanisms previously discovered in other cell lineages as well as solid tumors. Secondly, hypoxic conditioning led to a significant increase in the frequency of latently-infected cells (Figure 22C and D), supporting the hypothesis that low oxygenation in tissue sites may facilitate HIV persistence. Lastly, my flow cytometry data also showed that the CD73+ T cell compartment enriches for the latent reservoir; however, this enrichment did not further increase under hypoxia. Therefore, increasing latency upon hypoxia-inducing treatment can be solely attributed to the increased frequency of CD73+ cells. In other words, while hypoxia induction clearly modulated CD73 expression, the central determinant promoting the establishment and/or maintenance of HIV latency seemed to be the expression of CD73 itself.

**CD73 enzymatic reaction products promote latency.** The coherent association between CD73 expression and HIV latency suggested a mechanistical involvement of CD73 via its enzymatic function in the adenosine signaling cascade. CD73 occupies a pivotal role in generating extracellular adenosine, which functions as auto- and paracrine immunosuppressive metabolite triggering broadly immunosuppressive pathways upon binding to adenosine receptors (ARs): A1R, A2AR, A2BR, and A3R[227]. Adenosine signaling through A2AR potently suppresses effector functions of different immune cells and dampens inflammatory responses, counterbalancing ATP-induced hyperactivation of the immune system upon inflammation, hypoxia or nutrient starvation[223]. In the context of HIV infection however, this immunosuppressive microenvironment may constitute a perfect immunological niche for infected cells to evade host immune clearance. In addition, adenosine signaling leads to a suppression of cellular transcription factors that are critical for active viral

transcription[257,258]. Since high levels of CD73 expression marked latent infection, I hypothesized that modulating the CD73/adenosine axis may impact HIV latency. In fact, pharmacological blockade of A2AR in an HIV latency cell culture system clearly facilitated HIV latency reversal without impairing cell viability (Figure 30). Thus, my data demonstrated for the first time the potential of targeting the adenosinergic system as immunotherapy approach in context of HIV infection and provided first evidence that enzymatic activity of CD73 is directly involved in HIV persistence.

**A comprehensive model of the reservoir enrichment in CD73+ CD4+ T cells.** Based on my data, the existing literature about CD73, and previous publications on HIV latency and persistence, I was able to develop a preliminary model revolving around CD73, as well as its regulation and function, in context of latent infection (Figure 31): (A) During initial infection, uncontrolled viral spread disseminates integrated proviral DNA throughout the entire host, including circulation and lymphatic tissues. The latter are unique anatomical niches that feature low oxygen levels and consequently activated HIFs, which in turn upregulate CD73 expression. (B) High CD73 expressing CD4+ T cells generate adenosine-rich, immunosuppressive microenvironments, which promote the establishment of latent reservoirs and begin to enrich for latently-infected cells. Mechanistically, elevated CD73 expression levels result in accumulation of extracellular adenosine which creates optimal conditions for HIV persistence in two ways: (C) On one hand, adenosine, produced by HIV-infected, CD73+ cells, activates autocrine signaling pathways that result in suppression of crucial host transcription factors such as NF-κB and NFAT upon activation of PKA. Other factors may be involved in the suppression of viral replication in CD73+ cells, including some of the differentially expressed genes discovered by RNA sequencing. As a result, HIV transcription is diminished, and the

provirus is or becomes dormant. (D) On the other hand, adenosine signaling cascades impair effective host immune responses thus facilitating immune escape of HIV-infected cells and promoting survival of the latent reservoir.

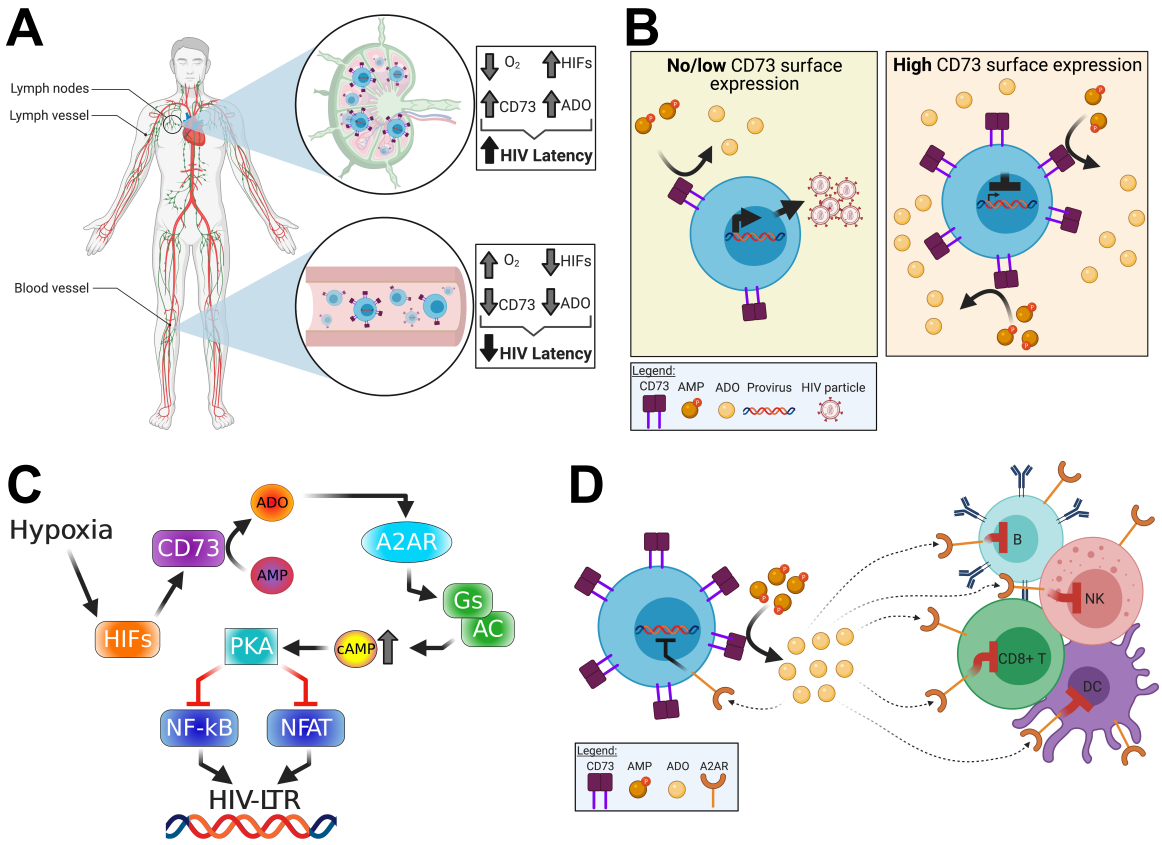


**Figure 31: CD73 plays a vital role in the maintenance of HIV persistence in ART-suppressed individuals.** (A) Under long-term ART, HIV persists *in vivo* preferentially in anatomical sanctuary sites like lymph nodes. Oxygen levels are known to be significantly lower in lymphoid tissues (0.5-4.5%) compared to the periphery (about 13%). Low oxygen supply or hypoxia lead to stabilization of hypoxia inducible factors (HIFs) which control the expression of CD73. (B) Upregulation of CD73 leads to the accumulation of adenosine (ADO) in the extracellular space. These factors favor the establishment of viral reservoirs and promote HIV persistence specifically in tissue compartments in presence of ART. (C) Adenosine production and downstream signaling may further contribute to transcriptional silencing of the provirus. CD73 converts AMP to ADO in the extracellular space, which functions as signaling molecule upon binding to the G-protein coupled adenosine receptor A2AR. Engagement of A2AR leads to the intracellular stimulation of G-proteins (Gs) and adenylate cyclase (AC) and thus upregulation of cyclic AMP (cAMP). cAMP binds and activates PKA, which inhibits transcription factors NF-κB and NFAT, both of utmost importance for transcriptional activity of the integrated provirus. (D) High concentrations of adenosine contribute extensively to the creation of an immunosuppressive microenvironment by inhibiting a variety of immune cells including cytotoxic T, NK, and dendritic cells (DCs). In this way, HIV latently-infected cells are protected from host immune clearance by overexpressing CD73 and the induction of adenosine signaling, creating a niche for long-term survival.

## 5.3 Limitations, Conclusions and Future Perspectives

In the final chapter, I reflect upon technical and biological limitations of the study and provide an outlook for follow-up projects and future studies of HIV persistence. It needs to be stressed that the presented work was solely focused on CD4+ T cells. The interaction of HIV-infected cells with other immune cells or the relevance of other viral sanctuaries such as for instance myeloid cells were not within the scope of this project.

**Limitations of $HIV_{DFII}$.** The dual reporter virus system is a reliable and well-established experimental tool to investigate HIV latency *in vitro* and by now, several different versions are available[172,173,187,259]. However, all dual reporters have in common that the frequency of latently-infected CD4+ T cells is extremely low, making it very difficult to collect the amounts of cells required for an in-depth characterization of viral reservoirs. To some extent, this fact truthfully reflects the inherent nature of HIV persistence, considering the rareness of latently-infected cells *in vivo*. However, some limitations of the viral construct may additionally exacerbate this problem. Several modifications in the reporter construct could lead to an improvement of its properties and facilitate purification of latently-infected cells. One concern is the high stability of eGFP with a half-life of ~26 h[260], which may lead to a distorted representation of active viral transcription as the reporter would still be detected even when the viral promoter has been silenced after a previous burst of LTR activity. I addressed this issue in the course of a side project (not presented here) and exchanged eGFP with the destabilized version d2eGFP that has an *in vivo* half-life of ~2h[261]. Theoretically, this strategy should allow for much more appropriate snapshots of the actual LTR-driven transcription and thus allow for a more accurate monitoring of ongoing viral transcription and latent infection. The EF1α promoter

that controls the expression of the latent reporter leaves room for optimization as well. Unfortunately, this promotor does not exhibit maximal activity in T cells, especially in quiescent T cells and thus may be inadequate to report latent infection. However, finding a reliable alternative that exerts sufficient activity in T cells at different maturation and activation stages is not trivial. To overcome this problem, I initiated a small-scale screen of select promoters and tested their activity in T cells. Follow up evaluation and analysis of this screen will be informative to select an optimal promoter for the HIV dual reporter system.

**Limitations of FACS purification of latent cells.** One experimental consequence of the low frequencies of latently-infected cells is that sorting efficiencies and purities are typically lower for this population than for the highly abundant uninfected and productively-infected cells (Figure 15C). Given the fact that therefore, latent samples were often 'diluted' with uninfected cells, it is even more remarkable that distinct expression signatures were found for latently-infected cells compared to both other sorted samples (Figure 18C and Figure 19). It stands to reason that upon ideal separation of all cell populations, differential gene expression would have been significantly more pronounced and more subtle differences would have been detected. Of note, some of the aforementioned improvements of the reporter virus may help to increase the frequency of latent cells and alleviate this impurity issue.

**Limitations of *in vitro* infection experiments.** Another limitation of the applied *in vitro* model system is that it focuses on a rather narrow time window of HIV latency, thus recapitulating the establishment and persistence of viral reservoirs within a few days after infection. In infected individuals however, HIV persists even after decades of successful ART. The question whether my *in vitro* findings emulate such long-term phenomena was addressed

in collaboration with Dr. Eugenin. His *in situ* imaging of lymph node tissues showed, for the first time, a significant association between CD73 expression in T cells and HIV-DNA specifically in ART-suppressed individuals. While these *in vivo* data corroborated my *in vitro* findings, a further validation of CD73 as biomarker for HIV persistence is necessary. In subsequent studies, I will thus scrutinize the enrichment of viral reservoirs in CD73+ CD4+ T cells from peripheral blood and other anatomical sites, including the spleen and gut-associated lymphoid tissue, obtained from ART-suppressed individuals. The measurement of viral reservoirs in different compartments will be performed with the recently established IPDA (intact proviral DNA) assay, a quantitative, multiplexed PCR[262], which allows for the quantification of integrated HIV-DNA while discriminating defective and replication-competent provirus. I will exploit this method to compare the enrichment of provirus in CD73+ vs CD73- cells. Simultaneously, I will be able to assess the contribution of the respective cell compartments to a functional reservoir *in vivo*, which could confirm and further strengthen the *in vitro* results of the current study.

**Environmental control of hypoxic pathways.** Throughout this study, hypoxic responses were induced by chemical inhibition of HIF-1α degradation. While it is widely accepted that DMOG mimics the natural stabilization of HIFs during hypoxia, it cannot be excluded that pleiotropic effects are exerted. It will be therefore important to contrast and compare latency at different oxygenation levels to provide a deeper understanding of T cell biology and HIV infection in these more physiological culture settings. In addition, I aim to investigate what role different HIFs (HIF-1, HIF-2, HIF-3) are playing in HIV persistence. Do different HIFs have different effects on viral replication? Are the various HIFs active at different time points of infection? Is there a competition between HIFs for binding to the HRE in the viral LTR, which

may lead to variable activity of the viral promotor? These and other open questions need to be addressed to fully understand how hypoxia impacts HIV transcription and latency.

**Exploitation of CD73 as therapeutic target.** The question may be raised whether CD73 could serve as therapeutic target, either to prevent latency establishment or to directly attack latent reservoirs. However, such attempts have to take into account that CD73 is widely expressed on other immune cells as well which renders an exclusive targeting of CD73+ cells to eliminate latent infection problematic. However, the emergence of bispecific therapeutic antibodies could ameliorate this issue when combining CD73 with the lineage marker CD4 or other putative markers for latent infection including CD30 and CD32a. In addition, if the enzymatic activity of CD73 is crucial for HIV persistence as hypothesized, targeting adenosine production and downstream signaling may provide an alternative way to improve host immune clearance of HIV-infected cells without the necessity to directly target specific cell compartments. Interestingly, manipulation of the CD73-adenosine axis has been intensively investigated in context of tumor biology[198,223,263–267]. Solid tumors hijack the adenosinergic signaling pathway creating an immunosuppressive tumor microenvironment (TME) thus fostering tumor progression and immune escape. Consequently, the adenosinergic system in particular in combination with other immune-modulating agents has received increasing attention as treatment option in oncology[264,266,268]. Several immunotherapeutic CD73 antibodies and pharmacological agents targeting the adenosine pathway have been developed and are currently tested in clinical trials for their potential to enhance antitumor responses and boost clearance of tumor cells[227,269]. Based on my data, it seems reasonable that HIV-infected cells exploit similar mechanisms as solid tumor cells to ensure long-term persistence. Such similarities between HIV infection and cancer have been discussed

before[270,271] and are currently actively explored as therapeutic targets for HIV cure attempts[272]. The prospects of a CD73-centered repurposing of anti-cancer drugs for HIV treatment therefore look promising. This will involve CD73 blockage and inhibition of adenosine signaling cascades, which may boost immune responses and elimination of viral reservoirs.

It will be critical to meticulously unravel the mechanism of adenosine signaling in the context of latent infection. Blockage of A2AR provided first insights into a potential suppression of viral replication due to the adenosinergic system (Figure 30). But these observations need to be verified in primary cell-based HIV latency systems and *in vivo* models. It further remains to be proven that CD73 enzymatic activity is directly involved in the maintenance of latent infection through the accumulation of suppressive adenosine. A pharmaceutical blockage or knockout/knockdown of CD73 should provide this missing link. Our recently established humanized mouse model of latent HIV infection (μ-Lat model) in combination with the highly CD73 expressing J-Lat 5A8 clone would be an ideal system to scrutinize the interplay between modulation of CD73 expression, adenosine signaling and HIV persistence *in vivo*[210].

**Final remarks.** Taken together, my results provide multiple complementary pieces of evidence, indicating that CD73 is phenotypically and mechanistically involved in HIV latency. My project therefore adds to our understanding of HIV latency and uncovers novel targets for therapeutic intervention. Additional, in-depth studies will be necessary to further dismantle the complexity of viral reservoirs and achieve our ultimate goal – a scalable and effective cure for HIV infection.

# 6 Bibliography


1. UNAIDS.org. http://aidsinfo.unaids.org/.
2. Avert.org. https://www.avert.org/global-hiv-and-aids-statistics#footnote9_8n2o0x5.
3. Brennan, R. O. & Durack, D. T. GAY COMPROMISE SYNDROME. *The Lancet* vol. 318 1338–1339 (1981).
4. Centers for Disease Control (CDC). Kaposi's sarcoma and Pneumocystis pneumonia among homosexual men-New York City and California. *MMWR. Morb. Mortal. Wkly. Rep.* **30**, 305–8 (1981).
5. Hymes, K. B. *et al.* Kaposi's sarcoma in homosexual men. A report of eight cases. *Lancet* **318**, 598–600 (1981).
6. A Timeline of HIV and AIDS. https://www.hiv.gov/hiv-basics/overview/history/hiv-and-aids-timeline.
7. Barre-Sinoussi, F. *et al.* Isolation of a T-lymphotropic retrovirus from a patient at risk for acquired immune deficiency syndrome (AIDS). *Science (80-. ).* **220**, 868–871 (1983).
8. PubMed. https://pubmed.ncbi.nlm.nih.gov/.
9. Rodger, A. J. *et al.* Sexual activity without condoms and risk of HIV transmission in serodifferent couples when the HIV-positive partner is using suppressive antiretroviral therapy. *JAMA - J. Am. Med. Assoc.* **316**, 171–181 (2016).
10. Rodger, A. J. *et al.* Risk of HIV transmission through condomless sex in serodifferent gay couples with the HIV-positive partner taking suppressive antiretroviral therapy (PARTNER): final results of a multicentre, prospective, observational study. *Lancet* **393**, 2428–2438 (2019).
11. Bavinton, B. R. *et al.* Viral suppression and HIV transmission in serodiscordant male couples: an international, prospective, observational, cohort study. *Lancet HIV* **5**, e438–e447 (2018).
12. Cohen, M. S. *et al.* Antiretroviral Therapy for the Prevention of HIV-1 Transmission. *N. Engl. J. Med.* **375**, 830–839 (2016).
13. Gilbert, P. B. *et al.* Comparison of HIV-1 and HIV-2 infectivity from a prospective cohort study in Senegal. *Stat. Med.* **22**, 573–593 (2003).
14. Zagury, J. F. *et al.* Genetic variability between isolates of human immunodeficiency virus (HIV) type 2 is comparable to the variability among HIV type 1. *Proc. Natl. Acad. Sci.* **85**, 5941–5945 (1988).
15. Fischer, H. E. & Reuben, J. M. Human Immunodeficiency Virus Type 2: Implications for Blood Donors. *Current Issues in Transfusion Medicine* vol. 2 http://www3.mdanderson.org/~citm/H-93-10.html (1993).
16. Reicin, A. S., Ohagen, A., Yin, L., Hoglund, S. & Goff, S. P. The role of Gag in human immunodeficiency virus type 1 virion morphogenesis and early steps of the viral life cycle. *J. Virol.*

**70**, 8645–8652 (1996).

17. Fuller, S. D., Wilk, T., Gowen, B. E., Kräusslich, H. G. & Vogt, V. M. Cryo-electron microscopy reveals ordered domains in the immature HIV-1 particle. *Curr. Biol.* **7**, 729–738 (1997).
18. Greene, W. C. & Peterlin, B. M. Charting HIV's remarkable voyage through the cell: Basic science as a passport to future therapy. *Nat. Med.* **8**, 673–680 (2002).
19. NIAID.NIH.org. https://www.niaid.nih.gov/diseases-conditions/hiv-replication-cycle.
20. Chan, D. C. & Kim, P. S. HIV entry and its inhibition. *Cell* vol. 93 681–684 (1998).
21. Wyatt, R. The HIV-1 Envelope Glycoproteins: Fusogens, Antigens, and Immunogens. *Science (80-. ).* **280**, 1884–1888 (1998).
22. Fassati, A. Multiple roles of the capsid protein in the early steps of HIV-1 infection. *Virus Research* vol. 170 15–24 (2012).
23. Yeo, J. Y., Goh, G. R., Tran-To Su, C. & Ken-En Gan, S. The determination of HIV-1 RT mutation rate, its possible allosteric effects, and its implications on drug resistance. *Viruses* vol. 12 297 (2020).
24. Chinen, J. & Shearer, W. T. Molecular virology and immunology of HIV infection. *J. Allergy Clin. Immunol.* **110**, 189–198 (2002).
25. Zheng, Y. H., Lovsin, N. & Peterlin, B. M. Newly identified host factors modulate HIV replication. in *Immunology Letters* vol. 97 225–234 (Elsevier, 2005).
26. Simmons, A., Aluvihare, V. & McMichael, A. Nef triggers a transcriptional program in T cells imitating single-signal T cell activation and inducing HIV virulence mediators. *Immunity* **14**, 763–777 (2001).
27. Glushakova, S. *et al.* CD4 Down-Modulation by Human Immunodeficiency Virus Type 1 Nef Correlates with the Efficiency of Viral Replication and with CD4+ T-Cell Depletion in Human Lymphoid Tissue Ex Vivo. *J. Virol.* **75**, 10113–10117 (2001).
28. Lama, J., Mangasarian, A. & Trono, D. Cell-surface expression of CD4 reduces HIV-1 infectivity by blocking Env incorporation in a Nef- and Vpu-inhibitable manner. *Curr. Biol.* **9**, 622–631 (1999).
29. Zheng, Y. H., Plemenitas, A., Linnemann, T., Fackler, O. T. & Peterlin, B. M. Nef increases infectivity of HIV via lipid rafts. *Curr. Biol.* **11**, 875–879 (2001).
30. Xu, X. N. *et al.* Induction of Fas ligand expression by HIV involves the interaction of Nef with the T cell receptor ζ chain. *J. Exp. Med.* **189**, 1489–1496 (1999).
31. Collins, K. L., Chen, B. K., Kalams, S. A., Walker, B. D. & Baltimore, D. HIV-1 Nef protein protects infected primary cells against killing by cytotoxic T lymphocytes. *Nature* **391**, 397–401 (1998).
32. Perkins, A., Cochrane, A. W., Ruben, S. M. & Rosen, C. A. Structural and functional characterization of the human immunodeficiency virus rev protein. *J. Acquir. Immune Defic. Syndr.* **2**, 256–263 (1989).
33. Wei, P., Garber, M. E., Fang, S. M., Fischer, W. H. & Jones, K. A. A novel CDK9-associated C-type cyclin interacts directly with HIV-1 Tat and mediates its high-affinity, loop-specific binding to

TAR RNA. *Cell* **92**, 451–462 (1998).

34. Zapp, M. L. & Green, M. R. Sequence-specific RNA binding by the HIV-1 Rev protein. *Nature* **342**, 714–716 (1989).
35. Cullen, B. R. Retroviruses as model systems for the study of nuclear RNA export pathways. *Virology* **249**, 203–210 (1998).
36. Kim, S. Y., Byrn, R., Groopman, J. & Baltimore, D. Temporal aspects of DNA and RNA synthesis during human immunodeficiency virus infection: evidence for differential gene expression. *J. Virol.* **63**, 3708–3713 (1989).
37. Hallenberger, S. *et al.* Inhibition of furin-mediated cleavage activation of HIV-1 glycoprotein gpl60. *Nature* **360**, 358–361 (1992).
38. Gottlinger, H. G., Sodroski, J. G. & Haseltine, W. A. Role of capsid precursor processing and myristoylation in morphogenesis and infectivity of human immunodeficiency virus type 1. *Proc. Natl. Acad. Sci. U. S. A.* **86**, 5781–5785 (1989).
39. WHO. *HIV/AIDS: confronting a killer. World Health Report 2003.* (2003).
40. Fauci, A. S. Immunopathogenic Mechanisms of HIV Infection. *Ann. Intern. Med.* **124**, 654 (1996).
41. Deeks, S. G. & Walker, B. D. Human Immunodeficiency Virus Controllers: Mechanisms of Durable Virus Control in the Absence of Antiretroviral Therapy. *Immunity* vol. 27 406–416 (2007).
42. Maenza, J. *et al.* How often does treatment of primary HIV lead to post-treatment control? *Antivir. Ther.* **20**, 855–863 (2015).
43. Namazi, G. *et al.* The Control of HIV After Antiretroviral Medication Pause (CHAMP) Study: Posttreatment Controllers Identified From 14 Clinical Studies. *J. Infect. Dis.* **218**, 1954–1963 (2018).
44. Fischl, M. A. *et al.* The Efficacy of Azidothymidine (AZT) in the Treatment of Patients with AIDS and AIDS-Related Complex. *N. Engl. J. Med.* **317**, 185–191 (1987).
45. Greene, W. C. A history of AIDS: Looking back to see ahead. *Eur. J. Immunol.* **37**, S94–S102 (2007).
46. James, J. S. Saquinavir (Invirase): first protease inhibitor approved--reimbursement, information hotline numbers. *AIDS Treat. News* 1–2 (1995).
47. Cully, M. Protease inhibitors give wings to combination therapy. *Nat. Milestones* **14**, 16 (2018).
48. Cooper, David A.; Merigan, T. C. Clinical treatment. *AIDS* **10**, S133-134 (1996).
49. Palmisano, L. & Vella, S. A brief history of antiretroviral therapy of HIV infection: Success and challenges. *Ann. Ist. Super. Sanita* **47**, 44–48 (2011).
50. Deeks, S. G., Lewin, S. R. & Havlir, D. V. The end of AIDS: HIV infection as a chronic disease. *The Lancet* vol. 382 1525–1533 (2013).
51. Truong, W. R., Schafer, J. J. & Short, W. R. Once-Daily, Single-Tablet Regimens For the Treatment of HIV-1 Infection. *P T* **40**, 44–55 (2015).
52. Deeks, S. G. HIV infection, inflammation, immunosenescence, and aging. *Annu. Rev. Med.* **62**, 141–155 (2011).

53. UNAIDS. Launch of a global partnership to eliminate HIV-related stigma and discrimination. (2018).
54. Pantelic, M., Steinert, J. I., Park, J., Mellors, S. & Murau, F. 'Management of a spoiled identity': Systematic review of interventions to address self-stigma among people living with and affected by HIV. *BMJ Glob. Heal.* **4**, (2019).
55. UNAIDS. *Confronting discrimination*. (2017).
56. Turan, B. *et al.* How Does Stigma Affect People Living with HIV? The Mediating Roles of Internalized and Anticipated HIV Stigma in the Effects of Perceived Community Stigma on Health and Psychosocial Outcomes. *AIDS Behav.* **21**, 283–291 (2017).
57. Clifford, D. B. & Ances, B. M. HIV-associated neurocognitive disorder. *The Lancet Infectious Diseases* vol. 13 976–986 (2013).
58. Lake, J. E. & Currier, J. S. Metabolic disease in HIV infection. *The Lancet Infectious Diseases* vol. 13 964–975 (2013).
59. UN. General Assembly (70th sess.: 2015-2016). Political Declaration on HIV and AIDS : On the Fast-Track to Accelerating the Fight against HIV and to Ending the AIDS Epidemic by 2030 : resolution / adopted by the General Assembly. *A/RES/70/266* (2016).
60. Ho, Y.-C. *et al.* Replication-Competent Noninduced Proviruses in the Latent Reservoir Increase Barrier to HIV-1 Cure. *Cell* **155**, 540–551 (2013).
61. Davey, R. T. *et al.* HIV-1 and T cell dynamics after interruption of highly active antiretroviral therapy (HAART) in patients with a history of sustained viral suppression. *Proc. Natl. Acad. Sci. U. S. A.* **96**, 15109–15114 (1999).
62. Finzi, D. *et al.* Latent infection of CD4+ T cells provides a mechanism for lifelong persistence of HIV-1, even in patients on effective combination therapy. *Nat. Med.* **5**, 512–517 (1999).
63. Siliciano, J. D. & Siliciano, R. F. *Latency and viral persistence in HIV-1 infection*. *The Journal of Clinical Investigation* vol. 106 (2000).
64. Chun, T.-W. W. *et al.* Quantification of latent tissue reservoirs and total body viral load in HIV-1 infection. *Nature* **387**, 183–188 (1997).
65. Finzi, D. *et al.* Identification of a reservoir for HIV-1 in patients on highly active antiretroviral therapy. *Science (80-. ).* **278**, 1295–1300 (1997).
66. Wong, J. K. *et al.* Recovery of replication-competent HIV despite prolonged suppression of plasma viremia. *Science (80-. ).* **278**, 1291–1295 (1997).
67. WM, E.-S. *et al.* CD4+ Count–Guided Interruption of Antiretroviral Treatment. *N. Engl. J. Med.* **355**, 2283–2296 (2006).
68. Henderson, L. J., Reoma, L. B., Kovacs, J. A. & Nath, A. Advances toward Curing HIV-1 Infection in Tissue Reservoirs. *J. Virol.* **94**, (2019).
69. Tabler, C. O. *et al.* CD4+ Memory Stem Cells Are Infected by HIV-1 in a Manner Regulated in Part by SAMHD1 Expression. *J. Virol.* **88**, 4976–4986 (2014).

70. Tran, T.-A. *et al.* Resting Regulatory CD4 T Cells: A Site of HIV Persistence in Patients on Long-Term Effective Antiretroviral Therapy. *PLoS One* **3**, e3305 (2008).
71. Perreau, M. *et al.* Follicular helper T cells serve as the major CD4 T cell compartment for HIV-1 infection, replication, and production. *J. Exp. Med.* **210**, 143–156 (2013).
72. Kulpa, D. A. & Chomont, N. HIV persistence in the setting of antiretroviral therapy: when, where and how does HIV hide? *J. Virus Erad.* **1**, 59–66 (2015).
73. Campbell, J. H., Hearps, A. C., Martin, G. E., Williams, K. C. & Crowe, S. M. The importance of monocytes and macrophages in HIV pathogenesis,treatment,and cure. *AIDS* vol. 28 2175–2187 (2014).
74. Calcagno, A., Di Perri, G. & Bonora, S. Treating HIV Infection in the Central Nervous System. *Drugs* **77**, 145–157 (2017).
75. Fois, A. F. & Brew, B. J. The Potential of the CNS as a Reservoir for HIV-1 Infection: Implications for HIV Eradication. *Curr. HIV/AIDS Rep.* **12**, 299–303 (2015).
76. Henrich, T. J., Deeks, S. G. & Pillai, S. K. Measuring the size of the latent human immunodeficiency virus reservoir: The present and future of evaluating eradication strategies. *J. Infect. Dis.* **215**, S134–S141 (2017).
77. Yukl, S. A. *et al.* Differences in HIV burden and immune activation within the gut of HIV-positive patients receiving suppressive antiretroviral therapy. *J. Infect. Dis.* **202**, 1553–1561 (2010).
78. Chun, T. W. *et al.* Persistence of HIV in gut-associated lymphoid tissue despite long-term antiretroviral therapy. *J. Infect. Dis.* **197**, 714–720 (2008).
79. Hellmuth, J., Valcour, V. & Spudich, S. CNS reservoirs for HIV: implications for eradication. *J. virus Erad.* **1**, 67–71 (2015).
80. Lamers, S. L. *et al.* HIV DNA Is Frequently Present within Pathologic Tissues Evaluated at Autopsy from Combined Antiretroviral Therapy-Treated Patients with Undetectable Viral Loads. *J. Virol.* **90**, 8968–8983 (2016).
81. Whitney, J. B. *et al.* Rapid seeding of the viral reservoir prior to SIV viraemia in rhesus monkeys. *Nature* **512**, 74–77 (2014).
82. Chun, T. W. *et al.* Early establishment of a pool of latently infected, resting CD4+ T cells during primary HIV-1 infection. *Proc. Natl. Acad. Sci. U. S. A.* **95**, 8869–8873 (1998).
83. Chavez, L., Calvanese, V. & Verdin, E. HIV Latency Is Established Directly and Early in Both Resting and Activated Primary CD4 T Cells. *PLOS Pathog.* **11**, e1004955 (2015).
84. Persaud, D. *et al.* Absence of Detectable HIV-1 Viremia after Treatment Cessation in an Infant. *N. Engl. J. Med.* **369**, 1828–1835 (2013).
85. Luzuriaga, K. *et al.* Viremic Relapse after HIV-1 Remission in a Perinatally Infected Child. *N. Engl. J. Med.* **372**, 786–788 (2015).
86. Sáez-Cirión, A. *et al.* Post-Treatment HIV-1 Controllers with a Long-Term Virological Remission after the Interruption of Early Initiated Antiretroviral Therapy ANRS VISCONTI Study. *PLoS*

*Pathog.* **9**, (2013).

87. Hocqueloux, L. *et al.* Long-term immunovirologic control following antiretroviral therapy interruption in patients treated at the time of primary HIV-1 infection. *AIDS* **24**, 1598–1601 (2010).
88. Palmer, S. *et al.* Low-level viremia persists for at least 7 years in patients on suppressive antiretroviral therapy. *Proc. Natl. Acad. Sci. U. S. A.* **105**, 3879–3884 (2008).
89. Palmer, S. *et al.* New real-time reverse transcriptase-initiated PCR assay with single-copy sensitivity for human immunodeficiency virus type 1 RNA in plasma. *J. Clin. Microbiol.* **41**, 4531–4536 (2003).
90. Wagner, T. A. *et al.* An Increasing Proportion of Monotypic HIV-1 DNA Sequences during Antiretroviral Treatment Suggests Proliferation of HIV-Infected Cells. *J. Virol.* **87**, 1770–1778 (2013).
91. Von Stockenstrom, S. *et al.* Longitudinal Genetic Characterization Reveals That Cell Proliferation Maintains a Persistent HIV Type 1 DNA Pool during Effective HIV Therapy. *J. Infect. Dis.* **212**, 596–607 (2015).
92. Cohn, L. B. *et al.* HIV-1 integration landscape during latent and active infection. *Cell* **160**, 420–432 (2015).
93. Jordan, A., Defechereux, P. & Verdin, E. The site of HIV-1 integration in the human genome determines basal transcriptional activity and response to Tat transactivation. *EMBO J.* **20**, 1726–1738 (2001).
94. Wagner, T. A. *et al.* Proliferation of cells with HIV integrated into cancer genes contributes to persistent infection. *Science (80-. ).* **345**, 570–573 (2014).
95. Hughes, S. H. & Coffin, J. M. What Integration Sites Tell Us about HIV Persistence. *Cell Host and Microbe* vol. 19 588–598 (2016).
96. Symons, J., Cameron, P. U. & Lewin, S. R. HIV integration sites and implications for maintenance of the reservoir. *Curr. Opin. HIV AIDS* **13**, 152–159 (2018).
97. Maldarelli, F. *et al.* Specific HIV integration sites are linked to clonal expansion and persistence of infected cells. *Science (80-. ).* **345**, 179–183 (2014).
98. Lenasi, T., Contreras, X. & Peterlin, B. M. Transcriptional Interference Antagonizes Proviral Gene Expression to Promote HIV Latency. *Cell Host Microbe* **4**, 123–133 (2008).
99. Nabel, G. & Baltimore, D. An inducible transcription factor activates expression of human immunodeficiency virus in T cells. *Nature* **326**, 711–713 (1987).
100. Kinoshita, S. *et al.* The T cell activation factor NF-ATc positively regulates HIV-1 replication and gene expression in T cells. *Immunity* **6**, 235–244 (1997).
101. Ruelas, D. S. & Greene, W. C. An Integrated Overview of HIV-1 Latency. *Cell* **155**, 519–529 (2013).
102. Pearson, R. *et al.* Epigenetic Silencing of Human Immunodeficiency Virus (HIV) Transcription by Formation of Restrictive Chromatin Structures at the Viral Long Terminal Repeat Drives the

Progressive Entry of HIV into Latency. *J. Virol.* **82**, 12291–12303 (2008).

103. Tyagi, M. & Karn, J. CBF-1 promotes transcriptional silencing during the establishment of HIV-1 latency. *EMBO J.* **26**, 4985–4995 (2007).
104. Tyagi, M., Pearson, R. J. & Karn, J. Establishment of HIV Latency in Primary CD4+ Cells Is due to Epigenetic Transcriptional Silencing and P-TEFb Restriction. *J. Virol.* **84**, 6425–6437 (2010).
105. Tacheny, A. *et al.* Unbiased proteomic analysis of proteins interacting with the HIV-1 5′LTR sequence: Role of the transcription factor Meis. *Nucleic Acids Res.* **40**, (2012).
106. Nguyen, K., Das, B., Dobrowolski, C. & Karn, J. Multiple histone lysine methyltransferases are required for the establishment and maintenance of HIV-1 latency. *MBio* **8**, (2017).
107. He, G. & Margolis, D. M. Counterregulation of Chromatin Deacetylation and Histone Deacetylase Occupancy at the Integrated Promoter of Human Immunodeficiency Virus Type 1 (HIV-1) by the HIV-1 Repressor YY1 and HIV-1 Activator Tat. *Mol. Cell. Biol.* **22**, 2965–2973 (2002).
108. Dlamini, Z. & Hull, R. Can the HIV-1 splicing machinery be targeted for drug discovery? *HIV/AIDS - Research and Palliative Care* vol. 9 63–75 (2017).
109. Khoury, G. *et al.* The molecular biology of HIV latency. in *Advances in Experimental Medicine and Biology* vol. 1075 187–212 (Springer New York LLC, 2018).
110. Karn, J. & Stoltzfus, C. M. Transcriptional and Posttranscriptional Regulation of HIV-1 Gene Expression. *Cold Spring Harb. Perspect. Med.* **2**, a006916–a006916 (2012).
111. Hütter, G. *et al.* Long-Term Control of HIV by CCR5 Delta32/Delta32 Stem-Cell Transplantation. *N. Engl. J. Med.* **360**, 692–698 (2009).
112. Jensen, B. Stammzelltransplantation – Der Düsseldorfer Patient. https://www.hivandmore.de/archiv/2020-1/stammzelltransplantation-der-duesseldorfer-patient.shtml (2020).
113. Jensen, B. *et al.* Analytic treatment interruption (ATI) after allogeneic CCR5-D32 HSCT for AML in 2013. in *Conference on Retroviruses and Opportunistic Infections (CROI)* CROI Abstract #394 (2019).
114. Knops, E. *et al.* Treatment of HIV and acute myeloid leukemia by allogeneic CCR5-d32 blood stem cell transplantation. in *Journal of Clinical Virology* vol. 82 S86 (2016).
115. Gupta, R. K. *et al.* HIV-1 remission following CCR5Δ32/Δ32 haematopoietic stem-cell transplantation. *Nature* **568**, 244–248 (2019).
116. Gupta, R. K. *et al.* Evidence for HIV-1 cure after CCR5Δ32/Δ32 allogeneic haemopoietic stem-cell transplantation 30 months post analytical treatment interruption: a case report. *Lancet HIV* **7**, e340–e347 (2020).
117. HIV cure of the 'London Patient' is confirmed and a third case of long-term viral remission is presented: the 'Düsseldorf Patient'. https://www.irsicaixa.es/en/news/hiv-cure-london-patient-confirmed-and-third-case-long-term-viral-remission-presented-dusseldorf (2020).
118. Namazi, G. *et al.* The Control of HIV After Antiretroviral Medication Pause (CHAMP) Study:

Posttreatment Controllers Identified From 14 Clinical Studies. *J. Infect. Dis.* **218**, 1954–1963 (2018).

119. Gebara, N. Y., El Kamari, V. & Rizk, N. HIV-1 elite controllers: an immunovirological review and clinical perspectives. *J. virus Erad.* **5**, 163–166 (2019).
120. Van Lint, C., Bouchat, S. & Marcello, A. HIV-1 transcription and latency: An update. *Retrovirology* vol. 10 67 (2013).
121. Schwarzer, R., Gramatica, A. & Greene, W. C. Reduce and control: A combinatorial strategy for achieving sustained HIV remissions in the absence of antiretroviral therapy. *Viruses* vol. 12 188 (2020).
122. Deeks, S. G. HIV: Shock and kill. *Nature* vol. 487 439–440 (2012).
123. Abner, E. & Jordan, A. HIV "shock and kill" therapy: In need of revision. *Antiviral Research* vol. 166 19–34 (2019).
124. Pache, L. *et al.* BIRC2/cIAP1 is a Negative Regulator of HIV-1 Transcription and Can Be Targeted by Smac Mimetics to Promote Reversal of Viral Latency. *Cell Host Microbe* **18**, 345–353 (2015).
125. Nixon, C. C. *et al.* Systemic HIV and SIV latency reversal via non-canonical NF-κB signalling in vivo. *Nature* **578**, 160–165 (2020).
126. Campbell, G. R., To, R. K., Zhang, G. & Spector, S. A. SMAC mimetics induce autophagy-dependent apoptosis of HIV-1-infected macrophages. *Cell Death Dis.* **11**, 1–14 (2020).
127. Gramatica, A. *et al.* Evaluating a New Class of AKT/mTOR Activators for HIV Latency Reversing Activity Ex Vivo and In Vivo. *J. Virol.* (2021) doi:10.1128/JVI.02393-20.
128. Singh, V., Dashti, A., Mavigner, M. & Chahroudi, A. Latency Reversal 2.0: Giving the Immune System a Seat at the Table. *Current HIV/AIDS Reports* 1–11 (2021) doi:10.1007/s11904-020-00540-z.
129. Spivak, A. M. & Planelles, V. Novel Latency Reversal Agents for HIV-1 Cure. *Annu. Rev. Med.* **69**, 421–436 (2018).
130. Vargas, B. *et al.* Inhibitors of signaling pathways that block reversal of HIV-1 latency. *Antimicrob. Agents Chemother.* **63**, (2019).
131. Maeder, M. L. & Gersbach, C. A. Genome-editing technologies for gene and cell therapy. *Molecular Therapy* vol. 24 430–446 (2016).
132. Rogers, G. L. & Cannon, P. M. Gene Therapy Approaches to Human Immunodeficiency Virus and Other Infectious Diseases. *Hematology/Oncology Clinics of North America* vol. 31 883–895 (2017).
133. Chavez, L. R. *et al.* Durable Control of HIV-1 Using a Staphylococcus aureus Cas9-Expressing Lentivirus Co-Targeting Viral Latency and Host Susceptibility. *bioRxiv* 2020.08.10.243329 (2020) doi:https://doi.org/10.1101/2020.08.10.243329.
134. Ebina, H., Misawa, N., Kanemura, Y. & Koyanagi, Y. Harnessing the CRISPR/Cas9 system to disrupt latent HIV-1 provirus. *Sci. Rep.* **3**, 1–7 (2013).

135. Mock, U. *et al.* mRNA transfection of a novel TAL effector nuclease (TALEN) facilitates efficient knockout of HIV co-receptor CCR5. *Nucleic Acids Res.* **43**, 5560–5571 (2015).
136. Shi, B. *et al.* TALEN-Mediated Knockout of CCR5 Confers Protection Against Infection of Human Immunodeficiency Virus. *JAIDS J. Acquir. Immune Defic. Syndr.* **74**, 229–241 (2017).
137. Hu, W. *et al.* RNA-directed gene editing specifically eradicates latent and prevents new HIV-1 infection. *Proc. Natl. Acad. Sci. U. S. A.* **111**, 11461–11466 (2014).
138. Lebbink, R. J. *et al.* A combinational CRISPR/Cas9 gene-editing approach can halt HIV replication and prevent viral escape. *Sci. Rep.* **7**, 1–10 (2017).
139. Ophinni, Y., Inoue, M., Kotaki, T. & Kameoka, M. CRISPR/Cas9 system targeting regulatory genes of HIV-1 inhibits viral replication in infected T-cell cultures. *Sci. Rep.* **8**, 7784 (2018).
140. Liao, H. K. *et al.* Use of the CRISPR/Cas9 system as an intracellular defense against HIV-1 infection in human cells. *Nat. Commun.* **6**, 1–10 (2015).
141. Kaminski, R. *et al.* Elimination of HIV-1 Genomes from Human T-lymphoid Cells by CRISPR/Cas9 Gene Editing. *Sci. Rep.* **6**, 1–15 (2016).
142. Dash, P. K. *et al.* Sequential LASER ART and CRISPR Treatments Eliminate HIV-1 in a Subset of Infected Humanized Mice. *Nat. Commun.* **10**, 1–20 (2019).
143. Kaminski, R. *et al.* Excision of HIV-1 DNA by gene editing: A proof-of-concept in vivo study. *Gene Ther.* **23**, 690–695 (2016).
144. Bella, R. *et al.* Removal of HIV DNA by CRISPR from Patient Blood Engrafts in Humanized Mice. *Mol. Ther. - Nucleic Acids* **12**, 275–282 (2018).
145. Yin, C. *et al.* In Vivo Excision of HIV-1 Provirus by saCas9 and Multiplex Single-Guide RNAs in Animal Models. *Mol. Ther.* **25**, 1168–1186 (2017).
146. Ward, A. R., Mota, T. M. & Jones, R. B. Immunological approaches to HIV cure. *Seminars in Immunology* 101412 (2020) doi:10.1016/j.smim.2020.101412.
147. Herzig, E. *et al.* Attacking Latent HIV with convertibleCAR-T Cells, a Highly Adaptable Killing Platform. *Cell* **179**, 880-894.e10 (2019).
148. Wagner, T. A. Quarter Century of Anti-HIV CAR T Cells. *Curr. HIV/AIDS Rep.* **15**, 147–154 (2018).
149. Kim, G. B., Hege, K. & Riley, J. L. Car talk: How cancer-specific car t cells can instruct how to build car T cells to cure HIV. *Frontiers in Immunology* vol. 10 2310 (2019).
150. Zhen, A. *et al.* HIV-specific Immunity Derived from Chimeric Antigen Receptor-engineered Stem Cells. *Mol. Ther.* **23**, 1358–1367 (2015).
151. Wightman, F. *et al.* Effect of ipilimumab on the HIV reservoir in an HIV-infected individual with metastatic melanoma. *AIDS* **29**, 504–506 (2015).
152. Velu, V. *et al.* Enhancing SIV-specific immunity in vivo by PD-1 blockade. *Nature* **458**, 206–210 (2009).
153. Mylvaganam, G. H. *et al.* Combination anti-PD-1 and antiretroviral therapy provides therapeutic benefit against SIV. *JCI insight* **3**, (2018).

154. Alrubayyi, A., Ogbe, A., Moreno Cubero, E. & Peppa, D. Harnessing Natural Killer Cell Innate and Adaptive Traits in HIV Infection. *Frontiers in cellular and infection microbiology* vol. 10 395 (2020).
155. Margolis, D. M., Koup, R. A. & Ferrari, G. HIV antibodies for treatment of HIV infection. *Immunol. Rev.* **275**, 313–323 (2017).
156. Caskey, M. Broadly neutralizing antibodies for the treatment and prevention of HIV infection. *Curr. Opin. HIV AIDS* **15**, 49–55 (2020).
157. Caskey, M. Delivery of anti-HIV bNAbs by viral vectors. *The Lancet HIV* vol. 6 e207–e208 (2019).
158. Bruel, T. *et al.* Elimination of HIV-1-infected cells by broadly neutralizing antibodies. *Nat. Commun.* **7**, 1–12 (2016).
159. Darcis, G., Berkhout, B. & Pasternak, A. O. The quest for cellular markers of HIV reservoirs: Any color you like. *Frontiers in Immunology* vol. 10 2251 (2019).
160. Fromentin, R. *et al.* CD4+ T Cells Expressing PD-1, TIGIT and LAG-3 Contribute to HIV Persistence during ART. *PLoS Pathog.* **12**, (2016).
161. McGary, C. S. *et al.* CTLA-4+PD-1− Memory CD4+ T Cells Critically Contribute to Viral Persistence in Antiretroviral Therapy-Suppressed, SIV-Infected Rhesus Macaques. *Immunity* **47**, 776-788.e5 (2017).
162. Iglesias-Ussel, M., Vandergeeten, C., Marchionni, L., Chomont, N. & Romerio, F. High levels of CD2 expression identify HIV-1 latently infected resting memory CD4+ T cells in virally suppressed subjects. *J. Virol.* **87**, 9148–58 (2013).
163. Serra-Peinado, C. *et al.* Expression of CD20 after viral reactivation renders HIV-reservoir cells susceptible to Rituximab. *Nat. Commun.* **10**, 1–15 (2019).
164. Hogan, L. E. *et al.* Increased HIV-1 transcriptional activity and infectious burden in peripheral blood and gut-associated CD4+ T cells expressing CD30. *PLOS Pathog.* **14**, e1006856 (2018).
165. Descours, B. *et al.* CD32a is a marker of a CD4 T-cell HIV reservoir harbouring replication-competent proviruses. *Nature* **543**, 564–567 (2017).
166. Pérez, L. *et al.* Conflicting evidence for HIV enrichment in CD32+ CD4 T cells. *Nature* **561**, E9–E16 (2018).
167. Osuna, C. E. *et al.* Evidence that CD32a does not mark the HIV-1 latent reservoir. *Nature* **561**, E20–E28 (2018).
168. Martin, G. E. *et al.* CD32-expressing CD4 T cells are phenotypically diverse and can contain proviral HIV DNA. *Front. Immunol.* **9**, 1 (2018).
169. Thornhill, J. P. *et al.* CD32 expressing doublets in HIV-infected gut-associated lymphoid tissue are associated with a T follicular helper cell phenotype. *Mucosal Immunol.* **12**, 1212–1219 (2019).
170. Noto, A. *et al.* CD32 + and PD-1 + Lymph Node CD4 T Cells Support Persistent HIV-1 Transcription in Treated Aviremic Individuals . *J. Virol.* **92**, 901–919 (2018).
171. Vasquez, J. J. *et al.* CD32-RNA Co-localizes with HIV-RNA in CD3+ Cells Found within Gut Tissues

from Viremic and ART-Suppressed Individuals. *Pathog. Immun.* **4**, 147 (2019).

172. Calvanese, V., Chavez, L., Laurent, T., Ding, S. & Verdin, E. Dual-color HIV reporters trace a population of latently infected cells and enable their purification. *Virology* **446**, 283–292 (2013).
173. Dahabieh, M. S., Ooms, M., Simon, V. & Sadowski, I. A Doubly Fluorescent HIV-1 Reporter Shows that the Majority of Integrated HIV-1 Is Latent Shortly after Infection. *J. Virol.* **87**, 4716–4727 (2013).
174. Lassen, K. G., Hebbeler, A. M., Bhattacharyya, D., Lobritz, M. A. & Greene, W. C. A Flexible Model of HIV-1 Latency Permitting Evaluation of Many Primary CD4 T-Cell Reservoirs. *PLoS One* **7**, e30176 (2012).
175. Gent, U. of. Draw Venn Diagram. *Bioinformatics and Evolutionary Genetics* http://bioinformatics.psb.ugent.be/webtools/Venn/.
176. NanoString Technologies. nCounter Advanced Analysis 2.0 - User Manual. https://www.nanostring.com/application/files/2715/1789/8043/MAN-10030-03_nCounter_Advanced_Analysis_2.0_User_Manual.pdf (2018).
177. Ganor, Y. *et al.* HIV-1 reservoirs in urethral macrophages of patients under suppressive antiretroviral therapy. *Nat. Microbiol.* **4**, 633–644 (2019).
178. Prevedel, L. *et al.* Identification, Localization, and Quantification of HIV Reservoirs Using Microscopy. *Curr. Protoc. Cell Biol.* **82**, 64 (2019).
179. Real, F. *et al. Platelets from HIV-infected individuals on antiretroviral drug therapy with poor CD4 + T cell recovery can harbor replication-competent HIV despite viral suppression*. *Sci. Transl. Med* vol. 12 https://hal.archives-ouvertes.fr/hal-03000932 (2020).
180. Dunn, K. W., Kamocka, M. M. & McDonald, J. H. A practical guide to evaluating colocalization in biological microscopy. *Am. J. Physiol. Cell Physiol.* **300**, C723–C742 (2011).
181. Brooks, D. G. & Zack, J. A. Effect of Latent Human Immunodeficiency Virus Infection on Cell Surface Phenotype. *J. Virol.* **76**, 1673–1681 (2002).
182. Lambert, T. J. FPbase: a community-editable fluorescent protein database. *Nat. Methods* **16**, 277–278 (2019).
183. Laurent-Crawford, A. G. *et al.* Membrane Expression of HIV Envelope Glycoproteins Triggers Apoptosis in CD4 Cells. *AIDS Res. Hum. Retroviruses* **9**, 761–773 (1993).
184. Pan, X., Baldauf, H. M., Keppler, O. T. & Fackler, O. T. Restrictions to HIV-1 replication in resting CD4 + T lymphocytes. *Cell Research* vol. 23 876–885 (2013).
185. Siliciano, R. F. & Greene, W. C. HIV latency. *Cold Spring Harb. Perspect. Med.* **1**, (2011).
186. Vanhamel, J., Bruggemans, A. & Debyser, Z. Establishment of latent HIV-1 reservoirs: What do we really know? *Journal of Virus Eradication* vol. 5 3–9 (2019).
187. Battivelli, E. *et al.* Distinct chromatin functional states correlate with HIV latency reactivation in infected primary CD4+ T cells. *Elife* **7**, 40 (2018).
188. Fujii, Y., Okumura, M., Inada, K., Nakahara, K. & Matsuda, H. CD45 isoform expression during T

cell development in the thymus. *Eur. J. Immunol.* **22**, 1843–1850 (1992).

189. Ruiz, A., Guatelli, J. C. & Stephens, E. B. The Vpu Protein: New Concepts in Virus Release and CD4 Down-Modulation. *Curr. HIV Res.* **8**, 240–252 (2010).
190. Willey, R. L., Maldarelli, F., Martin, M. A. & Strebel, K. Human immunodeficiency virus type 1 Vpu protein induces rapid degradation of CD4. *J. Virol.* **66**, 7193–7200 (1992).
191. Lundquist, C. A., Tobiume, M., Zhou, J., Unutmaz, D. & Aiken, C. Nef-Mediated Downregulation of CD4 Enhances Human Immunodeficiency Virus Type 1 Replication in Primary T Lymphocytes. *J. Virol.* **76**, 4625–4633 (2002).
192. Crise, B., Buonocore, L. & Rose, J. K. CD4 is retained in the endoplasmic reticulum by the human immunodeficiency virus type 1 glycoprotein precursor. *J. Virol.* **64**, 5585–5593 (1990).
193. Jabbar, M. A. & Nayak, D. P. Intracellular interaction of human immunodeficiency virus type 1 (ARV-2) envelope glycoprotein gp160 with CD4 blocks the movement and maturation of CD4 to the plasma membrane. *J. Virol.* **64**, 6297–6304 (1990).
194. Hansen, K. R., Resta, R., Webb, C. F. & Thompson, L. F. Isolation and characterization of the promoter of the human 5′-nucleotidase (CD73)-encoding gene. *Gene* **167**, 307–312 (1995).
195. Fausther, M., Sheung, N., Saiman, Y., Bansal, M. B. & Dranoff, J. A. Activated hepatic stellate cells upregulate transcription of ecto-5=-nucleotidase/ CD73 via specific SP1 and SMAD promoter elements. *Am J Physiol Gastrointest Liver Physiol* **303**, 904–914 (2012).
196. Synnestvedt, K. *et al.* Ecto-5′-nucleotidase (CD73) regulation by hypoxia-inducible factor-1 mediates permeability changes in intestinal epithelia. *J. Clin. Invest.* **110**, 993–1002 (2002).
197. Kordaß, T., Osen, W. & Eichmüller, S. B. Controlling the immune suppressor: Transcription factors and MicroRNAs regulating CD73/NT5E. *Frontiers in Immunology* vol. 9 813 (2018).
198. Di Virgilio, F. & Adinolfi, E. Extracellular purines, purinergic receptors and tumor growth. *Oncogene* vol. 36 293–303 (2017).
199. Jordan, A. HIV reproducibly establishes a latent infection after acute infection of T cells in vitro. *EMBO J.* **22**, 1868–1877 (2003).
200. Chan, J. K., Bhattacharyya, D., Lassen, K. G., Ruelas, D. & Greene, W. C. Calcium/Calcineurin Synergizes with Prostratin to Promote NF-κB Dependent Activation of Latent HIV. *PLoS One* **8**, e77749 (2013).
201. Jordan, A., Bisgrove, D. & Verdin, E. HIV reproducibly establishes a latent infection after acute infection of T cells in vitro. *EMBO J.* **22**, 1868–1877 (2003).
202. Hurst, J. *et al.* Immunological biomarkers predict HIV-1 viral rebound after treatment interruption. *Nat. Commun.* **6**, 1–9 (2015).
203. Banga, R. *et al.* PD-1+ and follicular helper T cells are responsible for persistent HIV-1 transcription in treated aviremic individuals. *Nat. Med.* **22**, 754–761 (2016).
204. Beier, K. C. C. *et al.* Induction, binding specificity and function of human ICOS. *Eur. J. Immunol.* **30**, 3707–3717 (2000).

205. Hutloff, A. Regulation of T follicular helper cells by ICOS. *Oncotarget* vol. 6 21785–21786 (2015).
206. Baxter, A. E. *et al.* Single-Cell Characterization of Viral Translation-Competent Reservoirs in HIV-Infected Individuals. *Cell Host Microbe* **20**, 368–380 (2016).
207. Lu, J. *et al.* Expansion of circulating T follicular helper cells is associated with disease progression in HIV-infected individuals. *J. Infect. Public Health* **11**, 685–690 (2018).
208. Porichis, F. & Kaufmann, D. E. Role of PD-1 in HIV pathogenesis and as target for therapy. *Current HIV/AIDS Reports* vol. 9 81–90 (2012).
209. Shi, J. *et al.* PD-1 Controls Follicular T Helper Cell Positioning and Function Article PD-1 Controls Follicular T Helper Cell Positioning and Function. *Immunity* **49**, 264–274 (2018).
210. Sperber, H. S. *et al.* μ-Lat: A mouse model to evaluate human immunodeficiency virus eradication strategies. *FASEB J.* **34**, 14615–14630 (2020).
211. Kerkau, T., Gernert, S., Kneitz, C. & Schimpl, A. Mechanism of MHC Class I Downregulation in HIV Infected Cells. *Immunobiology* **184**, 402–409 (1992).
212. Cohen, G. B. *et al.* The selective downregulation of class I major histocompatibility complex proteins by HIV-1 protects HIV-infected cells from NK cells. *Immunity* **10**, 661–671 (1999).
213. Jacobs, M. D. & Harrison, S. C. Structure of an IκBα/NF-κB complex. *Cell* **95**, 749–758 (1998).
214. Doitsh, G. *et al.* Cell death by pyroptosis drives CD4 T-cell depletion in HIV-1 infection. *Nature* **505**, 509–514 (2014).
215. Hamilton, J. A. Colony-stimulating factors in inflammation and autoimmunity. *Nature Reviews Immunology* vol. 8 533–544 (2008).
216. Hamilton, J. A. GM-CSF as a target in inflammatory/autoimmune disease: Current evidence and future therapeutic potential. *Expert Review of Clinical Immunology* vol. 11 457–465 (2015).
217. Sheng, W., Png, C. W., Reynolds, J. M. & Zhang, Y. T Cell-Derived GM-CSF, Regulation of Expression and Function. (2015) doi:10.4172/1745-7580.1000098.
218. Brown, P. A. & Angel, J. B. Granulocyte-macrophage colony-stimulating factor as an immune-based therapy in HIV infection. *Journal of Immune Based Therapies and Vaccines* vol. 3 3 (2005).
219. Lane, B. R. *et al.* Interleukin-8 Stimulates Human Immunodeficiency Virus Type 1 Replication and Is a Potential New Target for Antiretroviral Therapy. *J. Virol.* **75**, 8195–8202 (2001).
220. Ellwanger, J. H. *et al.* Increased IL-8 levels in HIV-infected individuals who initiated ART with CD4+ T cell counts <350 cells/mm3 – A potential hallmark of chronic inflammation. *Microbes Infect.* **22**, 474–480 (2020).
221. Gargan, S. *et al.* HIV-1 Promotes the Degradation of Components of the Type 1 IFN JAK/STAT Pathway and Blocks Anti-viral ISG Induction. *EBioMedicine* **30**, 203–216 (2018).
222. Nguyen, N. V., Tran, J. T. & Sanchez, D. J. HIV blocks Type I IFN signaling through disruption of STAT1 phosphorylation. *Innate Immun.* **24**, 490–500 (2018).
223. Allard, B., Allard, D., Buisseret, L. & Stagg, J. The adenosine pathway in immuno-oncology. *Nat. Rev. Clin. Oncol.* **17**, 611–629 (2020).

224. Yegutkin, G. G., Henttinen, T., Samburski, S. S., Spychala, J. & Jalkanen, S. *The evidence for two opposite, ATP-generating and ATP-consuming, extracellular pathways on endothelial and lymphoid cells*. *Biochem. J* vol. 367 (2002).
225. Antonioli, L., Pacher, P., Vizi, E. S. & Haskó, G. CD39 and CD73 in immunity and inflammation. *Trends Mol. Med.* **19**, 355–367 (2013).
226. Robson, S. C., Sévigny, J. & Zimmermann, H. The E-NTPDase family of ectonucleotidases: Structure function relationships and pathophysiological significance. *Purinergic Signal.* **2**, 409–430 (2006).
227. Kazemi, M. H. *et al.* Adenosine and adenosine receptors in the immunopathogenesis and treatment of cancer. *J. Cell. Physiol.* **233**, 2032–2057 (2018).
228. Deaglio, S. *et al.* Adenosine generation catalyzed by CD39 and CD73 expressed on regulatory T cells mediates immune suppression. *J. Exp. Med.* **204**, 1257–1265 (2007).
229. Schuler, P. J. *et al.* Human CD4+CD39+ regulatory T cells produce adenosine upon co-expression of surface CD73 or contact with CD73+ exosomes or CD73+ cells. *Clin. Exp. Immunol.* **177**, 531–543 (2014).
230. Dwyer, K. M. *et al.* Expression of CD39 by human peripheral blood CD4+CD25 + T cells denotes a regulatory memory phenotype. *Am. J. Transplant.* **10**, 2410–2420 (2010).
231. Schuler, P. J. *et al.* CD4+CD73+ T cells are associated with lower T-cell activation and C reactive protein levels and are depleted in HIV-1 infection regardless of viral suppression. *AIDS* **27**, 1545–1555 (2013).
232. Nikolova, M. *et al.* CD39/Adenosine Pathway Is Involved in AIDS Progression. *PLoS Pathog.* **7**, e1002110 (2011).
233. Jenabian, M.-A. A. *et al.* Regulatory T Cells Negatively Affect IL-2 Production of Effector T Cells through CD39/Adenosine Pathway in HIV Infection. *PLoS Pathog.* **9**, e1003319 (2013).
234. Burton, C. T. *et al.* Altered phenotype of regulatory T cells associated with lack of human immunodeficiency virus (HIV)-1-specific suppressive function. *Clin. Exp. Immunol.* **166**, 191–200 (2011).
235. Ambada, G. N. *et al.* Phenotypic characterization of regulatory T cells from antiretroviral- naive HIV-1-infected people. 405–416 (2017) doi:10.1111/imm.12738.
236. Moreno-Fernandez, M. E., Rueda, C. M., Rusie, L. K. & Chougnet, C. A. Regulatory T cells control HIV replication in activated T cells through a cAMP-dependent mechanism. *Blood* **117**, 5372–5380 (2011).
237. Tóth, I. *et al.* Decreased frequency of CD73 + CD8 + T cells of HIV-infected patients correlates with immune activation and T cell exhaustion. *J. Leukoc. Biol.* **94**, 551–561 (2013).
238. He, T. *et al.* Critical Role for the Adenosine Pathway in Controlling Simian Immunodeficiency Virus-Related Immune Activation and Inflammation in Gut Mucosal Tissues. *J. Virol.* **89**, 9616–9630 (2015).

239. Towatari, M., Kanei, Y., Saito, H. & Hamaguchi, M. Hematopoietic transcription factor GATA-2 activates transcription from HIV-1 long terminal repeat. *AIDS* **12**, 253–259 (1998).
240. Balakrishna, S. L., Satyanarayana, N. & Kondapi, A. K. Involvement of human topoisomerase II isoforms in HIV-1 reverse transcription. *Arch. Biochem. Biophys.* **532**, 91–102 (2013).
241. Pekalski, M. L. *et al.* Neonatal and adult recent thymic emigrants produce IL-8 and express complement receptors CR1 and CR2. *JCI insight* **2**, (2017).
242. Carreau, A., Hafny-Rahbi, B. El, Matejuk, A., Grillon, C. & Kieda, C. Why is the partial oxygen pressure of human tissues a crucial parameter? Small molecules and hypoxia. *J. Cell. Mol. Med.* **15**, 1239–1253 (2011).
243. Zenewicz, L. A. Oxygen Levels and Immunological Studies. *Front. Immunol.* **8**, 8–11 (2017).
244. Caldwell, C. C. *et al.* Differential Effects of Physiologically Relevant Hypoxic Conditions on T Lymphocyte Development and Effector Functions. *J. Immunol.* **167**, 6140–6149 (2001).
245. Ohta, A. *et al.* In vivo T cell activation in lymphoid tissues is inhibited in the oxygen-poor microenvironment. *Front. Immunol.* **2**, (2011).
246. Morinet, F., Casetti, L., François, J.-H. H., Capron, C. & Pillet, S. Oxygen tension level and human viral infections. *Virology* **444**, 31–36 (2013).
247. Zhao, C. *et al.* Deficiency of HIF-1α enhances influenza A virus replication by promoting autophagy in alveolar type II epithelial cells. *Emerg. Microbes Infect.* **9**, 691–706 (2020).
248. Shen, B. H., Bauzon, M. & Hermiston, T. W. The effect of hypoxia on the uptake, replication and lytic potential of group B adenovirus type 3 (Ad3) and type 11p (Ad11p). *Gene Ther.* **13**, 986–990 (2006).
249. Jiang, J. H. *et al.* Hypoxia can contribute to the induction of the Epstein-Barr virus (EBV) lytic cycle. *J. Clin. Virol.* **37**, 98–103 (2006).
250. Davis, D. A. *et al.* Hypoxia induces lytic replication of Kaposi sarcoma-associated herpesvirus. *Blood* **97**, 3244–3250 (2001).
251. Kulkarni, A. *et al.* Glucose Metabolism and Oxygen Availability Govern Reactivation of the Latent Human Retrovirus HTLV-1. *Cell Chem. Biol.* **24**, 1377-1387.e3 (2017).
252. Charles, S. *et al.* Regulation of HIV-1 transcription at 3% versus 21% oxygen concentration. *J. Cell. Physiol.* **221**, 469–479 (2009).
253. Deshmane, S. L., Amini, S., Sen, S., Khalili, K. & Sawaya, B. E. Regulation of the HIV-1 promoter by HIF-1 and Vpr proteins. *Virol. J.* **8**, 1–7 (2011).
254. Deshmane, S. L. *et al.* Activation of the Oxidative Stress Pathway by HIV-1 Vpr Leads to Induction of Hypoxia-inducible Factor 1α Expression. *J. Biol. Chem.* **284**, 11364–11373 (2009).
255. Duette, G. *et al.* Induction of HIF-1α by HIV-1 Infection in CD4 + T Cells Promotes Viral Replication and Drives Extracellular Vesicle-Mediated Inflammation. *MBio* **9**, 1–21 (2018).
256. Zhuang, X. *et al.* Hypoxic microenvironment shapes HIV-1 replication and latency. *Commun. Biol.* **3**, (2020).

257. Romio, M. *et al.* Extracellular purine metabolism and signaling of CD73-derived adenosine in murine Treg and Teff cells. *Am. J. Physiol. Physiol.* **301**, C530–C539 (2011).
258. Sheridan, C. M., Heist, E. K., Beals, C. R., Crabtree, G. R. & Gardner, P. Protein kinase A negatively modulates the nuclear accumulation of NF-ATc1 by priming for subsequent phosphorylation by glycogen synthase kinase-3. *J. Biol. Chem.* **277**, 48664–48676 (2002).
259. Kim, Y., Cameron, P. U., Lewin, S. R. & Anderson, J. L. Limitations of dual-fluorescent HIV reporter viruses in a model of pre-activation latency. *J. Int. AIDS Soc.* **22**, e25425 (2019).
260. Corish, P. & Tyler-Smith, C. *Attenuation of green fluorescent protein half-life in mammalian cells*. *Protein Engineering vol* vol. 12 (1999).
261. Li, X. *et al.* Generation of destabilized green fluorescent protein as a transcription reporter. *J. Biol. Chem.* **273**, 34970–34975 (1998).
262. Bruner, K. M. *et al.* A quantitative approach for measuring the reservoir of latent HIV-1 proviruses. *Nature* **566**, 120–125 (2019).
263. Zhang, B. CD73: A Novel Target for Cancer Immunotherapy. *Cancer Res.* **70**, 6407–6411 (2010).
264. Leone, R. D. & Emens, L. A. Targeting adenosine for cancer immunotherapy. *J. Immunother. Cancer* **6**, 57 (2018).
265. Antonioli, L., Yegutkin, G. G., Pacher, P., Blandizzi, C. & Haskó, G. Anti-CD73 in Cancer Immunotherapy: Awakening New Opportunities. *Trends in Cancer* **2**, 95–109 (2016).
266. Chen, S. *et al.* CD73: an emerging checkpoint for cancer immunotherapy. *Immunotherapy* **11**, 983–997 (2019).
267. Allard, D., Chrobak, P., Allard, B., Messaoudi, N. & Stagg, J. Targeting the CD73-adenosine axis in immuno-oncology. *Immunol. Lett.* 1–9 (2018) doi:10.1016/j.imlet.2018.05.001.
268. Sek, K. *et al.* Targeting Adenosine Receptor Signaling in Cancer Immunotherapy. *Int. J. Mol. Sci.* **19**, 3837 (2018).
269. Antonioli, L., Blandizzi, C., Malavasi, F., Ferrari, D. & Haskó, G. Anti-CD73 immunotherapy: A viable way to reprogram the tumor microenvironment. *OncoImmunology* vol. 5 e1216292 (2016).
270. Mylvaganam, G., Yanez, A. G., Maus, M. & Walker, B. D. Toward T Cell-Mediated Control or Elimination of HIV Reservoirs: Lessons From Cancer Immunology. *Front. Immunol.* **10**, 1–15 (2019).
271. Paiardini, M., Dhodapkar, K., Harper, J., Deeks, S. G. & Ahmed, R. Editorial: HIV and Cancer Immunotherapy: Similar Challenges and Converging Approaches. *Frontiers in Immunology* vol. 11 (2020).
272. I. Munoz-Arias, E. Gibson, E. Hanhauser, G. Wu, C. Thanh, M.A. Mohsen, L. Hogan, K. Hobbs, B. Howell, S. Pillai, S. Deeks, T. H. FDA-approved chemotherapeutic drugs that inhibit VEGF, RAF-1, B-RAF and the proteosome reverse HIV latency without global T cell activation. in (2018).

# 7 Acknowledgements

My dear reader, thank you for your attention and time to read my dissertation. This work is the result of 3 ½ years of research in Satish Pillai's Laboratory at Vitalant Research Institute in San Francisco, CA, USA. During this time, I have learned so much, in- and outside of science, collected priceless memories and experienced countless unique moments (besides features of latent infection). Along my journey as doctoral student, I was accompanied by so many different people, and everyone contributed to my work and to my development as a scientist but also as a person in their own way. I would like to take the time now to tell you about a few of them and express my appreciation and thanks to them all.

First of all, there is my 'Doktorvater', Satish. Satish is definitely a one-of-a-kind scientist, and if you haven't met him yet, you should. There are many options to get to know him, for example in numerous videos and interviews online where he loves to talk about science. But you will also find him playing his piano, singing his songs, following his passion for music. I am grateful for my time in his lab and for the exceptional opportunity to perform my dissertation work as external student. His intoxicating joy and enthusiasm make the daily science lighter and turns the 10% success rate into 90% excitement and drive to push forward. Thank you, Satish, for support and guidance at all times.

I also want to mention and thank my supervisor, Prof. Florian Heyd from the Free University of Berlin. Without him, I wouldn't have been able to conduct my graduate studies the way I did. I very much appreciate your agreement and availability in pursuing my endeavor, Prof. Heyd, and I am looking forward to future intersections in the scientific world.

Science is most fruitful when conducted collectively. On that note, great thanks belong to Dr. Eliseo (Cheo) Eugenin and the members of his laboratory. Their great effort in our collaboration considerably moved our project forward and I am excited to see where we are going next.

Of course, I cannot forget to mention my lab members and colleagues - a diverse mixture of unique characters. Kyle, Shivani, Leonard, Mohamed, Konstantinos, Zain, and Li. Leonard, our senior scientist and infamous lab grinch, shared his profound expertise and also a smile every once and a while over a beer. Shivani was my close bench partner and I think she finally understood before she moved on to her next adventure that Curry might not be the best NBA player. I'm glad we could settle that over many Amitis sammitches. Li, our most recent addition, never falls short to spread her happiness, and Zain takes googling skills to another level, as well as breakfast, lunch and afternoon snack session preparations. Mohamed and Kyle were just great supporting, reliable lab companions, working hard in the lab and turning midnight hours into fun. I'm also appreciative of our adoptive lab members and my friends, Erika, Renata, and Anushka. Anushka, I especially want to thank you for your care, your encouragement, but most importantly for strawberry milkshakes.

To me, my family is one of the most important elements in my life. I thank my closest ones, my siblings Francis, Niclas, Clara, Kaspar and Lena. They might not know but give me strength from far. My mom and Sarko. I contribute my work to all of them. I thank Katja and Rolf, always giving us a welcoming and loving home. I thank all the little ones; they never fail to make me smile. I'm thankful for Ansu and Andrea for giving a distant place a feeling of home. Hopefully, there are many more reunions to come very soon along with new Black Mirror episodes.

Now, I want to dedicate these final lines to my best friend and my partner Roland. He has been by my side for many years with endless support and encouragement, and I cannot envision anyone else taking this journey with me. His creativity and passion for science are truly inspiring. His extraordinary capability to consider science from different angles and perspectives has elevated my science and has opened doors when I was stuck. Thank you for being there. I can't wait to hit the ground running with our lab now and to see what the future holds for us.

Let me close by thanking voluntary blood donors, study participants and funding sources that enabled me to perform the work and conduct crucial experiments to complete my studies.

# 8 Publications

This chapter provides a brief overview of the manuscripts I was involved in during my doctoral studies. Presented is only research that has been accepted by peer-reviewed journals or is in the review process. The purpose and relevance of each publication are summarized below. Please not that three of the manuscripts are also attached as separate file.

1. Gramatica A, Schwarzer R, Brantley W, Varco-Merth B, **Sperber HS**, Hull PA, Montano M, Migueles SA, Rosenthal D, Hogan LE, Johnson JR, Packard TA, Grimmett ZW, Herzig E, Besnard E, Nekorchuk M, Hsiao F, Deeks SG, Snape M, Kiernan B, Roan NR, Lifson JD, Estes JD, Picker LJ, Verdin E, Krogan NJ, Henrich TJ, Connors M, Ott M, Pillai SK, Okoye AA, Greene WC. Evaluating a New Class of AKT/mTOR Activators for HIV Latency Reversing Activity *Ex Vivo* and *In Vivo*. J Virol. 2021 Feb 3:JVI.02393-20. doi: 10.1128/JVI.02393-20. PMID: 33536176.

Our recently published study in the Journal of Virology describes a new pharmacological strategy to reverse HIV latency in context of an HIV cure approach. We have discovered that a hitherto untapped cellular protein, glycogen synthase kinase-3 (GSK3), can be targeted to achieve efficient reactivation of dormant HIV infections in blood samples from aviremic individuals on ART. Importantly, in contrast to many previously described latency reversing agents, GSK3 inhibitors do not induce T cell activation, release of inflammatory cytokines, cell toxicity, or impair effector functions of cytotoxic T lymphocytes or NK cells. Unfortunately, unfavorable pharmacodynamics of the tested compound hampered *in vivo* latency reversal in SIV-infected rhesus macaques on suppressive ART. Our data nonetheless clearly demonstrate

that GSK3 is a viable and promising cellular target for efficient and safe latency reversal and that GSK3-centered drugs should be further explored as HIV therapeutics.

2. Khanna K, Raymond W, Charbit AR, Jin J, Gitlin I, Tang M, **Sperber HS**, Franz S, Pillai S, Simmons G, Fahy JV. Binding of SARS-CoV-2 spike protein to ACE2 is disabled by thiol-based drugs; evidence from *in vitro* SARS-CoV-2 infection studies. bioRxiv [Preprint]. 2020 Dec 8:2020.12.08.415505. doi: 10.1101/2020.12.08.415505. PMID: 33330868; PMCID: PMC7743076.

The studies described in this preprint deal with the development of unique SARS-CoV-2 entry inhibitors that exploit the vulnerability of viruses to manipulation of the thiol/disulfide balance in their surface glycoprotein complexes. A panel of thiol-based drugs was thoroughly tested, revealing that the compounds cysteamine and WR-1065 decrease binding of the viral spike to its receptor, as well as overall virus infection levels, both in pseudo virus and live virus assays. These compounds represent first-in-class entry inhibitors and should be further explored for their clinical potential to treat Coronavirus infections, but also as broad-band antivirals which may block other virus infection and alleviate disease progression.

3. **Sperber HS**, Togarrati PP, Raymond KA, Bouzidi MS, Gilfanova R, Gutierrez AG, Muench MO, Pillai SK. μ-Lat: A mouse model to evaluate human immunodeficiency virus eradication strategies. FASEB J. 2020 Nov;34(11):14615-14630. doi: 10.1096/fj.202001612RR. Epub 2020 Sep 9. PMID: 32901981.

The goal of this paper was to establish and characterize a new, straightforward and scalable humanized mouse model of latent HIV infections. To this aim, we have tested and optimized transplantation of J-Lat cells (Jurkat cells harboring a latent HIV provirus) into NSG mice,

ultimately achieving successful engraftment in several tissues including spleen, bone barrow, peripheral blood, and lung. We show that viral latency can be pharmacologically reversed in transplanted mice demonstrating the potential of our system to be used for *in vivo* studies of latency reversing agents. Our model therefore enables rapid determination of how effectively HIV eradication drugs, including latency reversal agents, penetrate, and function in diverse anatomical sites that harbor HIV *in vivo* and could therefore significantly foster the development of future HIV cure strategies.

4. Chavez LR, Reddy NR, Raymond KA, Bouzidi MS, Desai S, Dossani ZY, **Sperber HS**, Theiler J, Korber B, Pillai SK. Durable Control of HIV-1 Using a Staphylococcus aureus Cas9-Expressing Lentivirus Co-Targeting Viral Latency and Host Susceptibility. bioRxiv [Preprint]. 2020 Aug 10 [cited 2021 Feb 23];2020.08.10.243329. Available from: https://doi.org/10.1101/2020.08.10.243329

In this work, we have explored a novel CRISPR/Cas9-based strategy to target and neutralize proviral DNA and concomitantly block host permissivity factors. A single lentiviral vector that simultaneously targets multiple highly-conserved regions of the provirus and the host coreceptor CXCR4 was developed and tested in a unique coculture system, enabling real-time monitoring of latent infection, viral reactivation, and infection of new target cells. Our data demonstrate that dual-targeting depleted HIV-1-infected cells with significantly greater efficacy than vectors targeting either virus or host independently, highlighting the prospects of our new approach as a potent HIV cure strategy.

# 9 Curriculum Vitae

For reasons of data protection, the curriculum vitae is not included in the online version.

# 10 Appendix

In addition to this monography, three manuscripts for the referees were included. These manuscripts that I co-authored are relevant for my dissertation because they illustrate current advances in the HIV persistence field. The full references can be found above (8 Publications):

1. Gramatica, A. et al. (2021)
2. Sperber, H.S. et al. (2020)
3. Chavez, L.R. et al. (2020)